

THE PULSE RADIOLYSIS OF SODIUM TETRAPHENYLBORATE AND  
SODIUM HEXACHLOROIRIDATE IN AQUEOUS SOLUTION

BY  
CHARLES L. CRAWFORD

A DISSERTATION PRESENTED TO THE GRADUATE SCHOOL  
OF THE UNIVERSITY OF FLORIDA IN PARTIAL FULFILLMENT  
OF THE REQUIREMENTS FOR THE DEGREE OF  
DOCTOR OF PHILOSOPHY

UNIVERSITY OF FLORIDA

1991

Dedicated to  
my parents, Nathan and Doris

## ACKNOWLEDGMENTS

The author expresses his sincere appreciation to his research director, Prof. Robert J. Hanrahan, and to Prof. M. Luis Muga for their advice, encouragement, and friendship throughout this work.

Special thanks are given to Avinash Gupta and Zuoqian Li for their friendship and assistance.

Appreciation is given to Ravi Bhawe for his efforts in initiating the experimental setup. Mohammad Gholami and Sandra Roberts are also acknowledged for their contributions towards much of the data collection.

Thanks to Prof. D. N. Silverman of the J. Hillis Miller Health Science Center for the use of the stopped-flow apparatus. Experimental assistance with this instrument, provided by Dr. Chingkuan Tu, is also gratefully acknowledged.

The author's deepest thanks are expressed to Kama Siegel for her unprecedented companionship and editorial prowess -- both of which have helped make this work possible.

Thanks to Dave Burnsed for his assistance with the electronics.

## TABLE OF CONTENTS

	<u>page</u>
ACKNOWLEDGEMENTS .....	iii
LIST OF TABLES .....	vi
LIST OF FIGURES .....	vii
ABSTRACT .....	x
1. INTRODUCTION .....	1
1.1 Foreword .....	1
1.2 Review of Previous Work .....	3
2. EXPERIMENTAL APPARATUS AND PROCEDURES .....	19
2.1 Pulse Radiolysis Setup .....	19
2.2 Absorption Spectrophotometry .....	22
2.3 Light Source Systems .....	30
2.4 Reaction Cells and Cellholder .....	37
2.5 Monochromators .....	47
2.6 Febetron 706 System .....	50
2.7 Transient Recorder and Computer System ...	59
2.8 Computer Program .....	63
2.9 Reagents and Their Purification .....	65
2.10 Sample Irradiation .....	67
3. PULSE RADIOLYSIS OF SODIUM TETRAPHENYLBORATE IN AQUEOUS SOLUTION .....	69
3.1 Experimental Results .....	69
3.2 Discussion .....	83
3.3 Conclusions .....	91
4. PULSE RADIOLYSIS OF SODIUM HEXACHLOROIRIDATE IN AQUEOUS SOLUTION .....	93
4.1 Experimental Results .....	93
4.2 Discussion .....	101
4.3 Conclusions .....	114

	<u>page</u>
APPENDIX A      CHEMICAL DOSIMETRY FOR A PULSED RADIATION SOURCE .....	118
APPENDIX B      RELEVANT REACTION SYSTEMS .....	128
APPENDIX C      INPUT DATA FILES FOR COMPUTER INTEGRATION SIMULATIONS .....	132
APPENDIX D      PULSE RADIOLYSIS COMPUTER PROGRAM ...	138
REFERENCES .....	155
BIOGRAPHICAL SKETCH .....	169

## LIST OF TABLES

<u>Table</u>	<u>Page</u>
1 Radiation Chemical Yields for Water .....	9
2 Transient Decay Rate Constants .....	78
3 Physical Constants for Chemical Dosimetry Systems .....	120
4 Absorbed Dose for Chemical Dosimetry Systems ..	127
5 Chemical Reaction Systems for Computer Simulation Studies .....	129

## LIST OF FIGURES

<u>Figure</u>	<u>Page</u>
1 Scheme for the radiolysis of water .....	8
2 University of Florida pulse radiolysis system .	21
3 Experimental arrangement using the McPherson 218 monochromator .....	26
4 Experimental arrangement using the Jarrell-Ash monochromator .....	27
5 Photomultiplier tube-base schematic used with the EMI 9250 QB PMT in the model 3262 housing .	29
6 Lead shields for PMT photocathodes in the Pacific Precision Instruments PMT housings ....	31
7 Photomultiplier tube-base schematic used with the Hamamatsu R928 side window PMT and Model 3150 housing .....	32
8 Xenon-arc lamp spectrum .....	34
9 Xenon-arc lamp schematic diagram .....	35
10 Flow-reaction cell with modified UV-VIS cuvette .....	39
11 Non-flow-reaction cell from UV-VIS cuvette ....	41
12 Reaction cellholder with adjustable razor blades mounts and wire-mesh screens .....	42
13 Depth-dose curves for microscope coverslide experiment .....	45
14 Absorbance change with number of pulses delivered for microscope coverslide experiment	46
15 Entrance and exit slit system flange adaption to the Jarrell-Ash monochromator .....	51

<u>Figure</u>	<u>Page</u>
16 Febetron 706 system schematic .....	53
17 Refurbished electron beam tube with ion pump ..	56
18 Total beam calorimetric dosimetry arrangement .	58
19 Timing sequence for pulse radiolysis experiment	62
20 Graphical display of optical signal versus time following pulse radiolysis of a N <sub>2</sub> O-saturated solution containing 10 mM NaTPB .....	71
21 Transient absorption spectrum .....	72
22 Graphical display of optical signal versus time following pulse radiolysis of a N <sub>2</sub> O-saturated NaTPB and NaN <sub>3</sub> solution .....	74
23 Curve fit of data from Fig. 20 (a) .....	76
24 Curve fit of data from Fig. 20 (b) .....	77
25 Carbonate competition experiment for determining the OH + TPB <sup>-</sup> rate constant .....	80
26 Graphical display of optical signal versus time following pulse radiolysis of a N <sub>2</sub> -saturated solution containg NaTPB and t-butanol .....	82
27 Comparison of experimental and computer simulated concentration versus time plots .....	90
28 UV-VIS spectrum .....	94
29 Carbonate competition experiment for determining the OH + Ir(III) rate constant .....	96
30 Transient digitizer traces of Ir(IV) absorption recorded at 488 nm with N <sub>2</sub> O-saturation .....	98
31 Transient digitizer traces of Ir(IV) absorption recorded at 488 nm with N <sub>2</sub> and air saturation .	100
32 Change in first order decay of hydrated electron with Ir(III) concentration .....	102
33 Comparison of experimental and computer simulated Ir(IV) concentration verses time plots; N <sub>2</sub> O, alkaline .....	109



<u>Figure</u>	<u>Page</u>
34 Comparison of experimental and computer simulated Ir(IV) concentration verses time plots; nitrogen-saturated .....	111
35 Comparison of experimental and computer simulated Ir(IV) concentration verses time plots; aerated .....	112
36 Computer simulations of the transient Ir(IV) trace .....	113
37 Change in absorbance with accumulated irradiation pulses for the modified Fricke system .....	124
38 Thiocyanate dosimetry .....	125
39 Hydrated electron dosimetry .....	126

Abstract of Dissertation Presented to the Graduate School  
of the University of Florida in Partial Fulfillment of the  
Requirements for the Degree of Doctor of Philosophy

THE PULSE RADIOLYSIS OF SODIUM TETRAPHENYLBORATE AND  
SODIUM HEXACHLOROIRIDATE IN AQUEOUS SOLUTION

By

Charles L. Crawford

December, 1991

Chairman: Dr. R. J. Hanrahan  
Major Department: Chemistry

A pulse radiolysis facility for the study of fast chemical kinetics in aqueous solution, based on a Febetron 706 electron beam accelerator, has been established at the University of Florida Radiation Chemistry Laboratory.

In previous work on the radiolysis of tetraphenylborate (TPB) solutions carried out in this laboratory, it was found that several organic products, including benzene, phenol, and biphenyl, are produced with substantial yield. However, the reaction mechanism has not been determined. Since the tetraphenylborate anion,  $\text{TPB}^-$ , is a reducing species, it should be more readily subject to attack by  $\text{OH}\cdot$  than by  $e_{\text{aq}}^-$  or by  $\text{H}\cdot$ . The lack of reactivity between TPB and  $e_{\text{aq}}^-$  has been confirmed by directly monitoring the transient signal due to  $e_{\text{aq}}^-$ . Concerning the reaction with  $\text{OH}\cdot$ , two schemes were investigated: (1) a rapid electron transfer from

$B(C_6H_5)_4^-$  to  $OH\cdot$ ; (2)  $OH\cdot$  addition to  $B(C_6H_5)_4^-$ . Comparison of transient absorption spectra resulting from the two different schemes above suggests that the  $OH\cdot$  addition is the dominant reaction under conditions of  $N_2O$  saturation, with an experimentally determined second-order rate constant of  $6.2 \times 10^9 \text{ M}^{-1}\text{s}^{-1}$ . A mechanism based on an initial first-order self-decomposition of the  $OH\cdot$  adduct,  $(C_6H_5)_3BC_6H_5OH^\cdot$ , is proposed.

Reactions initiated by  $OH\cdot$  radicals or  $e_{aq}^-$  in aqueous  $IrCl_6^{3-}$  solutions were studied. The rate constant for the respective reactions were found to be  $4.9 \times 10^9 \text{ M}^{-1}\text{s}^{-1}$  and  $6.1 \times 10^9 \text{ M}^{-1}\text{s}^{-1}$ . The oxidation product,  $IrCl_6^{2-}$  disappears rapidly in  $N_2O$ -saturated basic solution or in either neutral  $N_2$ -saturated or aerated solution, but is nearly inert in neutral solution with  $N_2O$  present. The complex  $IrCl_6^{2-}$  reacts rapidly with hydrogen peroxide in basic media, as confirmed on the benchtop and by stopped-flow kinetics. It is therefore inferred that reaction with  $HO_2^-$  may account for the loss of  $IrCl_6^{2-}$  under basic conditions. Loss of  $Ir(IV)$  in neutral  $N_2$ -saturated solution without added  $N_2O$  may involve electron transfer from  $Ir(II)$ , and loss of  $Ir(IV)$  in aerated solution is attributed to reduction by superoxide ion,  $O_2^-$ .

Kinetic modeling on the respective mechanistic schemes of the above systems gives good agreement with our experimental results.

## CHAPTER I INTRODUCTION

### 1.1 Foreword

The pulse radiolysis technique offers a convenient way of generating a variety of unstable or transient species under well-defined conditions. This technique involves the initiation of a chemical reaction process via a short pulse of ionizing radiation. Of major interest is the kinetics of, as well as both the qualitative and quantitative measurement of these transient species involved in the fast elementary steps of the reaction process.

The modification of a gas-phase pulse radiolysis system to a liquid-phase pulse radiolysis system was undertaken to expand the chemical kinetics facility of the University of Florida Radiation Chemistry Laboratory. Efforts to obtain kinetic information related to various aqueous solution systems were made in order to supplement existing aqueous-solution-based studies carried out in this laboratory involving techniques such as steady-state Co-60  $\gamma$ -radiolysis and solar-assisted photoelectrochemistry.

To study fast chemical reaction systems, two necessary requirements are the initiation of the process on a time-scale that is shorter than or comparable to the process being observed, and the detection of a physicochemical

change associated with the process. Our liquid-phase pulse radiolysis system was developed around a Febetron 706 electron beam (e-beam) accelerator capable of delivering a short, 3 nanosecond full width at half-max (FWHM) pulse of 600 KeV electrons with a peak current of  $8 \times 10^3$  amps. The monitoring technique employed was time-resolved absorption spectroscopy.

A microcomputer-based data acquisition system was integrated into the pulse radiolysis system to acquire, analyze, and store data obtained from the study of fast chemical processes.

The kinetic studies involving aqueous solutions of sodium tetrphenylborate (NaTPB) were undertaken to aid in developing a plausible mechanism concerning the radiolytic degradation of the  $\text{TPB}^-$  ion. Examination of the iridium chloride system was carried out to expand the solution conditions under which this system had been previously studied by pulse radiolysis. Due to the similarities of flash photolysis and pulse radiolysis, specifically in the case of radiation-induced redox reactions, previous photolysis work on the iridium chlorides served as a reference to the pulse radiolysis data collected in this study.

Various chemical dosimeter methods applicable to pulsed electron sources were studied to establish the proper dose delivered to the liquid sample in the Febetron 706 system, as modified for liquid-phase work.

## 1.2 Review of Previous Work

### 1.2.1 Pulse Radiolysis

At the University of Florida Radiation Chemistry Laboratory, Febetron 706 studies have been completed on the gas phase reaction kinetics and mechanisms of various chemical systems such as the alkyl and perfluoroalkyl iodides,<sup>1</sup> oxygen/ozone,<sup>2</sup> and OH reaction dynamics with small molecules.<sup>3-5</sup> The identity and reactivity of important transient species generated in the pulse radiolysis of gaseous systems, at atmospheric pressures or less, was of previous interest in these studies.

Historically, pulse radiolysis was developed to elucidate postulated transient behavior in radiation-induced chemical reaction systems, and apparatus was first brought into operation in about 1960.<sup>6,7</sup> Early pulse radiolysis systems used visible absorption spectroscopy to monitor intermediates produced from intense single electron accelerator pulses lasting typically around one microsecond or less, and much of the developmental work on pulse radiolysis involved liquid phase systems.<sup>8-10</sup> Development of the pulse radiolysis technique has since brought about variations of the method to include stroboscopic techniques capable of picosecond resolution<sup>11</sup> and multiple time-resolved observation techniques such as electron spin resonance (ESR),<sup>12-14</sup>

conductivity,<sup>15-17</sup> emission spectroscopy,<sup>18</sup> and resonance Raman spectroscopy,<sup>19-21</sup> to monitor reaction intermediates.

The pulse radiolysis method is the radiation chemistry analog of flash photolysis, in that the photoflash and photodissociation of molecules is replaced by a short, high-energy pulse of electrons, causing excitation and ionization of molecules by electron impact.<sup>22</sup> The technique of pulse radiolysis, used to study fast reactions, has been applied in areas of aqueous inorganic, organic, and biochemistry. Other fast reaction techniques such as flash photolysis, stopped-flow techniques, and temperature jump or pressure jump relaxation methods have been designed to monitor concentrations and to measure rate coefficients.<sup>23</sup> However, the pulse radiolysis technique was the first method capable of studying processes occurring at or below  $10^{-9}$  seconds.<sup>24</sup>

The characteristics of the electron pulse used in electron beam pulse radiolysis are its time profile, peak current and energy, cross-sectional homogeneity, and divergence. For adequate time resolution of the observed transient signal, the time profile of the pulse should be very short compared to the relaxation of the intermediates. The pulse current determines the number of interactions between the chemical system and the e-beam which, in turn, determines the concentration or amount of species formed. The maximum electron energy determines the penetration depth of the e-beam into the reaction cell and should be high enough to adequately irradiate the volume of the chemical system

being monitored. The cross-sectional homogeneity and divergence of the beam determine how uniformly irradiated the optically-sampled reaction region is.

Transformations over the years of the standard pulse radiolysis installation have led to increasingly sophisticated experimental setups.<sup>25-28</sup> Spectrographic methods involving oscilloscopes and Polaroid cameras have been largely replaced by digital signal processors, or transient digitizers that have an interface for computer control.<sup>11</sup> Signal processing has been aided by the use of backing-off circuits which can measure small transients on top of the analyzing light.<sup>29</sup> Lasers and the capability of commercial xenon-arc lamps to supply pulse current on top of DC current have provided intense analyzing light sources.<sup>30-32</sup> Lastly, on-line computer systems have been developed which not only greatly reduce the time required for data analysis but also improve both quantity and quality of the data processed.<sup>29,33-35</sup>

### 1.2.2 Radiolysis of Water and Aqueous Solutions

Early investigations on the radiolysis of water have played a significant role in the development of radiation chemistry.<sup>36-39</sup> In addition, sophisticated pulse radiolysis techniques achieving the time resolution of radiation induced chemical events have been applied more often in the radiolysis of water than in any other liquid.<sup>40</sup> As a



result, most of the aspects of the radiation chemistry of water and aqueous solutions are now reasonably well understood.

A few practical purposes for water irradiation studies arise from 1) the importance of understanding the effect of radiation on biological systems in which water is the main substrate, and 2) various aspects of nuclear reactor technology concerning water's use as both a coolant and moderator.<sup>41,42</sup> Water and aqueous solutions have been studied, in particular, for three reasons: (1) their role as solvents is central to chemistry in general and to radiochemistry in particular; (2) they are readily available and easy to work with; (3) water is a polar liquid that responds in characteristic ways to radiation.

Important features of the radiation chemistry of water are: (1) a description of the primary radical and molecular products and how they evolve in both time and space; (2) the effect of pH on the radiation chemical yields of primary products; (3) the track structure and related phenomena associated with the passage of a charged particle through a liquid; and (4) a detailed account of all the radical reactions involving the primary radicals and radiolysis products.<sup>43</sup>

Upon initial ionization of a water molecule by a fast primary charged particle such as an electron, the liberated electron from the ionization event will typically have sufficient energy to further ionize several adjacent water

molecules, which leads to the creation of clusters of ions along the track of the ionizing particle. These clusters are called spurs; detailed descriptions of their structure and distribution along the particle tracks can be found in the literature.<sup>44</sup> Once the dry electrons have been slowed to thermal energy, they undergo a hydration (or solvation) process which involves the water molecules becoming oriented about the charged species. This process occurs on the order of  $10^{-11}$  seconds, which is the relaxation time for dipoles in water. Alternatively, some water molecules are excited to upper electronic states from which they can autoionize, dissociate, or fall back to the ground electronic state. Figure 1 from Buxton<sup>43</sup> shows the time scale of events initiated by the absorption of energy by water from an incident ionizing radiation, such as an energetic photon or charged particle. Also shown are the various routes to formation of the primary radical and molecular products.

At approximately  $10^{-10}$  seconds after the ionizing event, all the physicochemical processes are complete and the chemical stage begins. Initially, this process involves diffusion of the radiolysis products out of the spurs where they either react together to form molecular and secondary radical products, or they escape to the bulk solution, becoming homogeneously distributed. Appendix B lists the elementary reaction steps in the radiolysis of liquid water, along with their appropriate rate constants.

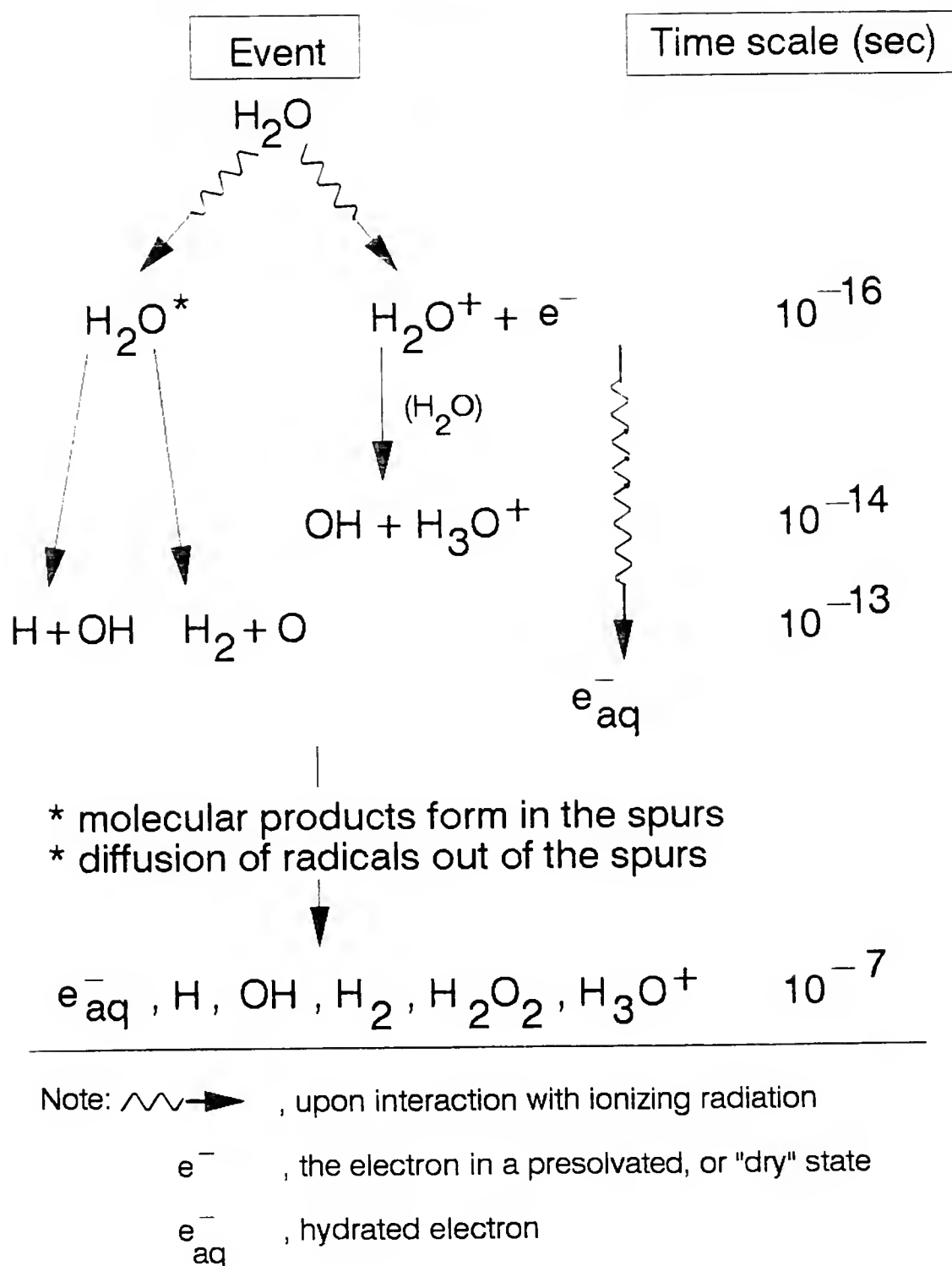


Fig. 1. Scheme for the radiolysis of water.

At approximately  $10^{-7}$  seconds, the spur expansion is complete, resulting in the so-called "primary yield" of the radiolysis products  $e_{aq}^-$ ,  $H_3O^+$ , OH, H,  $H_2$ ,  $H_2O_2$ , and  $HO_2$ . Radiation chemical yields are expressed as G-values, as shown in Table 1,<sup>38</sup> where G is the number of species (represented by X) created or destroyed per 100 eV of absorbed dose, and are written as G(X).

Table 1

## Radical and Molecular Product Yields in Irradiated Water

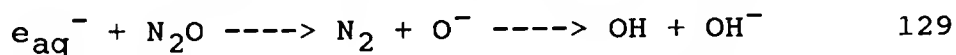
Primary yield	$e_{aq}^-$	$H^+$	OH	H	$H_2$	$H_2O_2$	$HO_2$
G( $\frac{\text{molecules}}{100 \text{ eV}}$ )	2.63	2.63	2.72	.55	.45	.68	0.026

The yields are essentially independent of pH except for extreme acidic conditions ( $pH < 3$ ). The G-values are also dependent on the quality of the ionizing radiation, or the mean linear energy transfer (LET). Under extremely intense irradiations, at dose rates so high that the spurs overlap, yields may also depend on the dose rate.<sup>40</sup> In the case of high-LET radiation<sup>45</sup> such as  $\alpha$  particles, heavy ions or fission fragments, or very high dose rates ( $> 10^9$  rad/sec),<sup>46-49</sup> lower radical and larger molecular yields result.

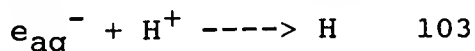
In the radiolysis of dilute solutions, most of the energy is absorbed by the solvent, and effects due to energy

deposited directly in the solute are unimportant for solute concentrations less than about 0.01 M. Thus all the observed chemical changes in irradiated dilute aqueous solutions are brought about indirectly by the molecular and radical products of the water radiolysis; this phenomenon is referred to as the "indirect effect."<sup>40</sup> In the presence of a solute, transient species and final products result from attack of H,  $e_{aq}^-$ , OH, and  $H_2O_2$  on the added substrate. Radicals derived from the substrate may also react to form final products. As evinced by the G-values of the primary radicals, the radiolysis of water produces approximately equal numbers of powerful oxidizing and reducing radicals. The standard reduction potentials for the hydroxyl radical, OH, and the hydrated electron,  $e_{aq}^-$ , are 2.72 V and -2.9 V, respectively.<sup>40</sup>

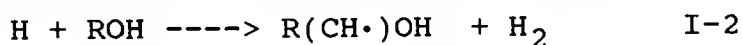
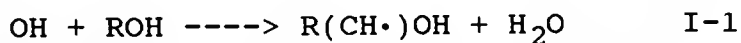
For pulse radiolysis chemical applications, well-defined conditions, i.e. either totally oxidizing or totally reducing, are desirable, and these conditions can be achieved by interconversion of the primary radicals.<sup>50</sup> Briefly, for a convenient way of obtaining almost totally oxidizing conditions,  $N_2O$ -saturated ( $N_2O = 2.5 \times 10^{-2}$  M) solutions are used.  $N_2O$  converts  $e_{aq}^-$  to OH, or



Acidic conditions of  $pH \leq 3$  should be avoided due to the interconversion of  $e_{aq}^-$  to the hydrogen atom, which is a major reducing species in acidic media,



For the creation of almost totally reducing conditions, addition of an organic solute to an inert gas-saturated solution leaves  $e_{aq}^-$  as the predominant reducing primary species. Reactions involved are



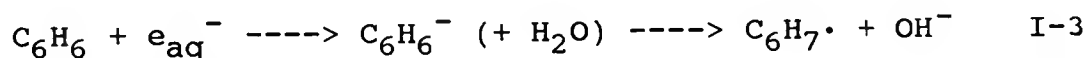
In general, the organic radicals formed,  $R(CH\cdot)OH$ , are less powerful reductants than  $e_{aq}^-$  and are rather unreactive. In particular,  $N_2$ -saturated solutions with added tertiary butanol were used in our work.

### 1.2.3 Aqueous Solution Studies of Aromatic Systems

In aqueous systems containing organic solutes, reactions occurring between solute and the primary products of water radiolysis are predominately abstraction, addition, and one-electron reduction. Organic radicals produced by these processes can further react before being converted to stable products, thus leading to complex radiolysis mechanisms, which have been reviewed.<sup>51-53</sup>

Mechanisms can be somewhat generalized within families of organic compounds containing the same functional group due to the tendency of the primary products,  $e_{aq}^-$ , H and OH, to react with these functional groups as opposed to the molecule as a whole.<sup>40</sup> Particularly, benzene can be utilized as an analogous system for many aromatic compounds,

with addition to the unsaturated bonds being the characteristic reaction path. Reaction of the primary radicals from water radiolysis with aromatic systems exhibit rate constants in the range of  $10^5$  to  $10^7 \text{ M}^{-1}\text{s}^{-1}$  for  $e_{\text{aq}}^-$ , and  $> 10^9 \text{ M}^{-1}\text{s}^{-1}$  for H and OH.<sup>40</sup>



Products of these addition reactions are cyclohexadiene systems containing an unpaired electron delocalized about the benzene ring. The dienyl radicals, namely cyclohexadiene,  $\text{C}_6\text{H}_7\cdot$ , and hydroxycyclohexadiene,  $\text{C}_6\text{H}_6\text{OH}\cdot$ , have been investigated by electron spin resonance techniques that indicate a positive electron density assignment to the ortho- and para-carbon atoms.<sup>54</sup>

Extensive pulse radiolysis work has shown these dienyls exhibit a reasonably strong absorption ( $\epsilon \approx 5 \times 10^3 \text{ M}^{-1}\text{cm}^{-1}$ ) in the 310-315 nm range.<sup>55,56</sup> Rate constants involving the primary radicals with benzene as well as the dimerization and disproportionation of the resulting cyclohexa- and hydroxycyclohexadienyls have also been reported.<sup>55-61</sup>

Steady-state  $\gamma$ -radiolysis studies involving liquid chromatography,<sup>62</sup> radio-liquid chromatography,<sup>63</sup> and gas chromatography,<sup>64,65</sup> as analyzing methods, indicate a complex mixture of products formed from the combination and disproportionation of the cyclohexa- and hydroxycyclohexa-

dienyl radicals. Phenol and biphenyl are the major products reported, in addition to mixed dienyls and regenerated benzene. All of the previous studies were carried out in  $N_2O$ -saturated or deoxygenated aqueous benzene solutions. In aerated aqueous benzene solutions,  $e_{aq}^-$  and  $H$  are scavenged by  $O_2$ . The hydroxycyclohexadiene radical reacts with  $O_2$  forming phenol and phenol-like products.<sup>66,67</sup>

#### 1.2.4 Sodium Tetrphenylborate System

Pulse radiolysis studies of the aqueous NaTPB solutions have been carried out in this laboratory to help establish a mechanism consistent with the end product yields obtained from Co-60  $\gamma$ -radiolysis on aqueous NaTPB solutions.<sup>68</sup> These steady-state radiolysis studies were done in conjunction with the United States Department of Energy operation at the Savannah River Plant in South Carolina and concerned the problem of cesium-137 separation and removal from nuclear waste obtained from spent fuel reprocessing.<sup>69</sup> Precipitation of the radiocesium as its insoluble tetrphenylborate salt is a method of separating it from the nonradioactive components and concentrating it to reduce the volume of the liquid radioactive waste. Other decontamination methods include ion exchange and evaporation techniques.<sup>70,71</sup> The radioactive precipitate will be stored in large underground steel tanks until it is sent to the Defense Waste Processing Facility (DWPF) for immobilization in glass.<sup>72,73</sup>



The TPB precipitate will undergo intense  $\beta$ - and  $\gamma$ -radiation from the cesium-137 during processing and storage that will partially decompose the tetraphenylborate, producing several organic compounds. Understanding the reaction scheme which leads to these various organic products as well as their impact on subsequent processing of the precipitate are important aspects concerning the design and operation of the DWPF.<sup>68</sup>

Since the tetraphenylborate anion,  $\text{TPB}^-$ , is rather different structurally from benzene or simple aromatics, it is not obvious that previous work on the mechanism of benzene radiolysis is relevant. However, several lines of evidence will be presented in this dissertation which indicate that there is a substantial connection. The preparation and properties of aqueous metal tetraphenylborate salts have been described by Flaschka and Barnard.<sup>74</sup>  $\text{LiTPB}$  and  $\text{NaTPB}$  are found to be the only TPB salts that are appreciably soluble in water; all TPB salts tend to be soluble in polar organic solvents.

Only a few mechanistic studies involving primary radiolysis radical reactions with the  $\text{TPB}^-$  anion have been found in the literature. Horii and Taniguchi, using pulse radiolysis, studied the oxidation intermediates of the  $\text{TPB}^-$  anion in aqueous solutions using the oxidizing radicals  $\text{N}_3^\cdot$ ,  $\text{Br}_2^\cdot$ , and  $\text{SCN}_2^\cdot$ .<sup>75</sup> Kinetic as well as spectral information was reported for the resulting intermediate,  $\text{B}(\text{C}_6\text{H}_5)_4^\cdot$ , which

was produced in all cases by an electron transfer from the  $\text{TPB}^-$  anion to the oxidizing radical. Liu *et al.* reported an absorbing species at  $\lambda = 300$  nm for the expected radical derived by  $\text{OH}^\bullet$  addition to the phenyl group of the  $\text{TPB}^-$  anion.<sup>76</sup> Another transient, derived from  $\text{H}^\bullet$  addition to the phenyl group was also discussed; however, no kinetic information was supplied regarding the fate of these resulting transient species.

Other pulse radiolysis investigations involving the NaTPB salt include ion association studies, in which the spectra of the diamagnetic species,  $\text{Na}^-$ , the solvated electron,  $e_{\text{aq}}^-$ , and the ion pair species ( $\text{Na}^+, e_{\text{aq}}^-$ ) are reported for alkali metal solutions in various non-aqueous solvents.<sup>77-82</sup>

The photochemistry literature of the metal tetraphenylborates was surveyed to find possible mechanisms concerning the reactions of the  $\text{TPB}^-$  anion and subsequent intermediates under UV-irradiation. Photolysis of aqueous solutions of NaTPB using UV light with a wavelength of 2537 Å generates biphenyl as the major product in oxygenated solutions and 1-phenyl-1,4-cyclohexadiene as the major product in the absence of  $\text{O}_2$ .<sup>83,84</sup> Other photochemical studies involve the photolysis of tetraphenylborates in non-aqueous organic solvents.<sup>85-87</sup>

Additional photochemical studies involving  $\text{TPB}^-$  report on photochemically-induced electron transfer from the  $\text{TPB}^-$

anion to oxygen,<sup>88</sup> and various intermolecular charge-transfer transitions of donor-acceptor ion pairs involving the TPB<sup>-</sup> anion.<sup>89-91</sup>

#### 1.2.5 Aqueous Solution Studies of Transition-metal Complexes

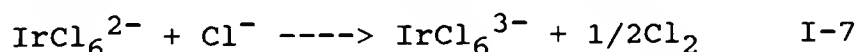
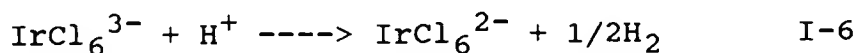
In aqueous systems containing transition metal complexes, the predominant reaction occurring between the solute and the primary products of water radiolysis is a one-electron transfer, either oxidation or reduction. This electron transfer can occur by an inner- or outer-sphere mechanism,<sup>92,93</sup> often leaving the complex ion in an unstable oxidation state. Aqueous solutions of both transition metals and their complexes, most notably bio-inorganic molecules, have been irradiated and the radiation chemical processes which occur have been extensively reviewed.<sup>94,95</sup>

In aqueous systems, aquation of the metal complex from ligand exchange with water molecules can occur, and has been reported in both pulse radiolysis studies<sup>96-99</sup> and photochemical studies.<sup>100,101</sup> Changes in the stereochemistry and coordination number of the transition metal complex upon pulse irradiation have also been investigated.<sup>102,103</sup>

#### 1.2.6 Hexachloroiridate System

The redox chemistry of the  $\text{IrCl}_6^{2-}$  and  $\text{IrCl}_6^{3-}$  complexes has been of recent interest due to the prospect of using the system to produce molecular hydrogen by the solar photochemical reduction of protons in acidic aqueous solu-

tions.<sup>104</sup> The solar chemistry of metal complexes has been reported by Gray and Maverick.<sup>105</sup> Solar chemistry is defined as that area of photochemistry in which the excitation energies fall within the spectrum of solar irradiation at the earth's surface. The proposed scheme involving aqueous HCl solutions of  $\text{IrCl}_6^{2-/3-}$  is



The net result is the conversion of HCl to hydrogen and chlorine using UV and visible light as the only energy sources. While Gray reports that the second reaction occurs with low efficiency at wavelengths higher than 430 nm, the first unfortunately occurs only with UV light, e.g. at 254 nm.

In this study we attempt to further elucidate the radiation chemistry of the chloroiridates under various aqueous solution conditions, namely in alkaline,  $\text{N}_2\text{O}$ -saturated solutions and in neutral, aerated solutions.

Dynamic processes occurring in the  $\text{IrCl}_6^{2-} / \text{IrCl}_6^{3-}$  system have been previously investigated by photochemical techniques.<sup>100,101,106,107</sup> Dainton and Rumfeldt made pertinent observations concerning the chemistry of the system, although their experimental procedure involved Co-60  $\gamma$ -radiolysis rather than direct studies of the transients.<sup>108</sup>

Mills and Henglein used steady-state gamma radiolysis of aqueous  $\text{IrCl}_6^{3-}$  to explore the formation of colloidal iridium and the catalytic properties of the colloid with respect to  $\text{H}_2$  formation.<sup>109,110</sup> Pulse radiolysis of  $\text{NaIrCl}_6$  aqueous solutions, carried out by Mills and Henglein, examined the reduction of  $\text{IrCl}_6^{3-}$  by  $e_{\text{aq}}^-$  and the  $(\text{CH}_3)_2\text{COH}^\cdot$  radical. A fundamental pulse radiolysis study on the aqueous solution redox reactions of hexachloroiridate complexes by Broszkiewicz addressed both the reduction and oxidation of aqueous  $\text{IrCl}_6^{3-}$ .<sup>111</sup> From his work, the author concluded that octahedral  $\text{IrCl}_6^{3-}$  is oxidized by a single electron transfer to octahedral  $\text{IrCl}_6^{2-}$  without changing its structure or ligand composition, i.e. aquation. Edwards also commented that the iridium chlorides are typical examples of complex ions that are relatively inert toward substitution, but which undergo rapid electron transfer reactions.<sup>112</sup>

Further pulse radiolysis studies on transition metal hexachloride complexes have been reported by Broszkiewicz.<sup>113-115</sup> Other pulse radiolysis studies involving aqueous  $\text{IrCl}_6^{3-}$  have examined its oxidation by the azidyl radical,  $\text{N}_3^\cdot$ ,<sup>116</sup> and the hydroxyl radical,  $\text{OH}^\cdot$ .<sup>93</sup>

## CHAPTER II EXPERIMENTAL APPARATUS AND PROCEDURES

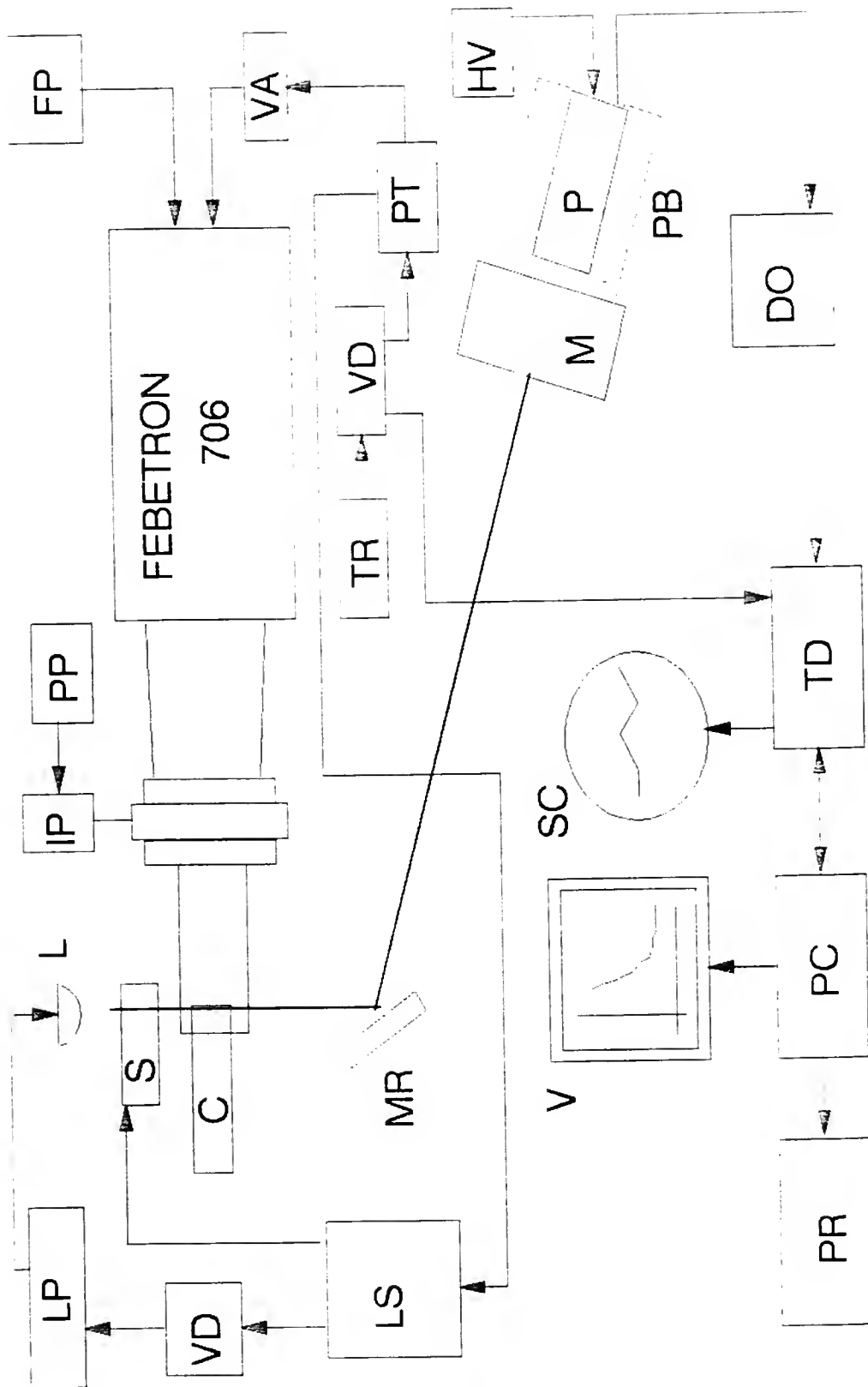
### 2.1 Pulse Radiolysis Instrumentation

Reactive intermediates generated in radiation-induced chemical processes are short-lived; thus the pulse radiolysis instrumentation must be able to monitor the transient behavior with a high degree of resolution over extremely short intervals. Since the concentration of such intermediates can influence both the mechanistic pathway and the final product yields, detection techniques that are sensitive to very low concentrations of radicals are necessary for a complete characterization of the transient behavior.

The University of Florida pulse radiolysis system configuration incorporating computer control is shown in Figure 2. The accelerator used is a Febetron (brand name for the impulse generator produced by Field Emission Corp.) 706, which operates on the principle of the Marx-bank circuit. Other accelerators used in time-resolved studies include the linear accelerator (linac), and the Van de Graaff generator. One may see that the other components shown comprise an absorption spectrophotometer. Absorption spectroscopy is the most widely used technique among others mentioned previously, for monitoring transient behavior in pulse radiolysis.

C: solution flow cell	PC: lab microcomputer
DO: dual op amp	PP: ion pump power supply
FP: Febetron power supply	PR: printer
HV: PMT power supply	PT: programmable time delay
IP: ion pump	S: shutter
L: xenon-arc lamp	SC: digitized recorder screen
LP: lamp power supply	TD: transient digitizer
LS: lamp, shutter drive	TR: trigger source
M: monochromator	V: video display
MR: mirror	VA: voltage amplifier
P: photomultiplier	VD: voltage divider
PB: lead cave	

Fig. 2. University of Florida pulse radiolysis system.





## 2.2 Absorption Spectrophotometry

Components involved in an absorption spectrophotometer are the light source, an optical train including all lenses, mirrors and absorption cell, the monochromator, the detector and a recorder. In flash photolysis and pulse radiolysis, the absorption cell also serves as the reaction region.

### 2.2.1 Light Source

The light source used should provide high monitoring light output to optimize the signal-to-noise ratio, S/N, which is directly related to the intensity of light striking the photocathode of a photomultiplier by the equation:

$$S/N = (I_S / \Delta f)^{1/2} \quad \text{II-1}$$

where  $I_S$  is the light intensity at the photocathode and  $\Delta f$  is the bandwidth of the recorder system.<sup>117,118</sup> This relationship is applicable when signal shot noise is the limiting S/N determining factor as is the case in fast ( $> 1$  kHz) kinetic spectrophotometry. Lasers provide high monitoring light intensities but are limited as to their wavelength of operation. Thus in order to utilize an absorption technique that is applicable to all transients or combination of transients throughout the ultraviolet and visible spectrum, a high power spectral lamp with a continuous distribution is preferred. Xenon-arc lamps filled with

xenon gas at above atmospheric pressures provide the following features: high arc stability and luminous flux, high reliability and long operating lifetimes up to 1000 hours. In addition, high-current pulses can be delivered to the arc lamp, which enable very high monitoring lamp outputs during transient measurement times of microseconds to milliseconds.

### 2.2.2 Absorption Path and Monochromators

The flow reaction cell previously mentioned allows for the production of transient species in the irradiated volume which can be directly monitored by absorption spectrophotometry. For example, using the Beer-Lambert relationship,

$$A = \epsilon b c \quad \text{II-2}$$

where  $\epsilon$  = molar extinction coefficient ( $\text{M}^{-1}\text{cm}^{-1}$ )

$b$  = pathlength (cm)

$c$  = concentration (M)

and assuming 1) a transient molar absorption coefficient,  $\epsilon$ , of approximately  $1000 \text{ mol}^{-1}\text{dm}^3\text{cm}^{-1}$ , 2) a transient population which produces a 10% deflection in the initial light intensity, and 3) a 1 cm absorption pathlength, one calculates the initial transient concentration formed in the irradiated volume immediately following the pulse to be approximately  $4.5 \times 10^{-5} \text{ M}$ .

Monochromators function to isolate a small wavelength band from a polychromatic source and consist of a dispersive element, either a prism or grating, and an image transfer

system of slits and mirrors. By using a monochromator with an adequate light flux throughput and a varying wavelength range, transient signals can be recorded as a function of wavelength to build a time-resolved transient spectrum.

The throughput factors which determine the radiant power passing out of the exit slit of a monochromator are the source spectral radiance,  $B_\lambda$  in units of  $\text{Wmm}^{-2} \text{sr}^{-1} \text{nm}^{-1}$ , and the monochromator throughput factor,  $Y$  in units of  $\text{mm}^2 \text{sr nm}$ . The product of these two factors gives the output spectral radiant power,  $Q$ , in watts.<sup>118</sup> For operating a monochromator with a broadband or continuum source the monochromator throughput factor,  $Y$ , is defined as

$$Y = w^2 h \frac{(\pi/4)}{(F/n)} T_{\text{op}} R_d \quad \text{II-3}$$

where  $w$  = slit width (mm)  
 $h$  = slit height (mm)  
 $F/n$  = f-number or effective aperture  
 $T_{\text{op}}$  = optical transmission factor (unitless)  
 $R_d$  = reciprocal linear dispersion (nm/mm)

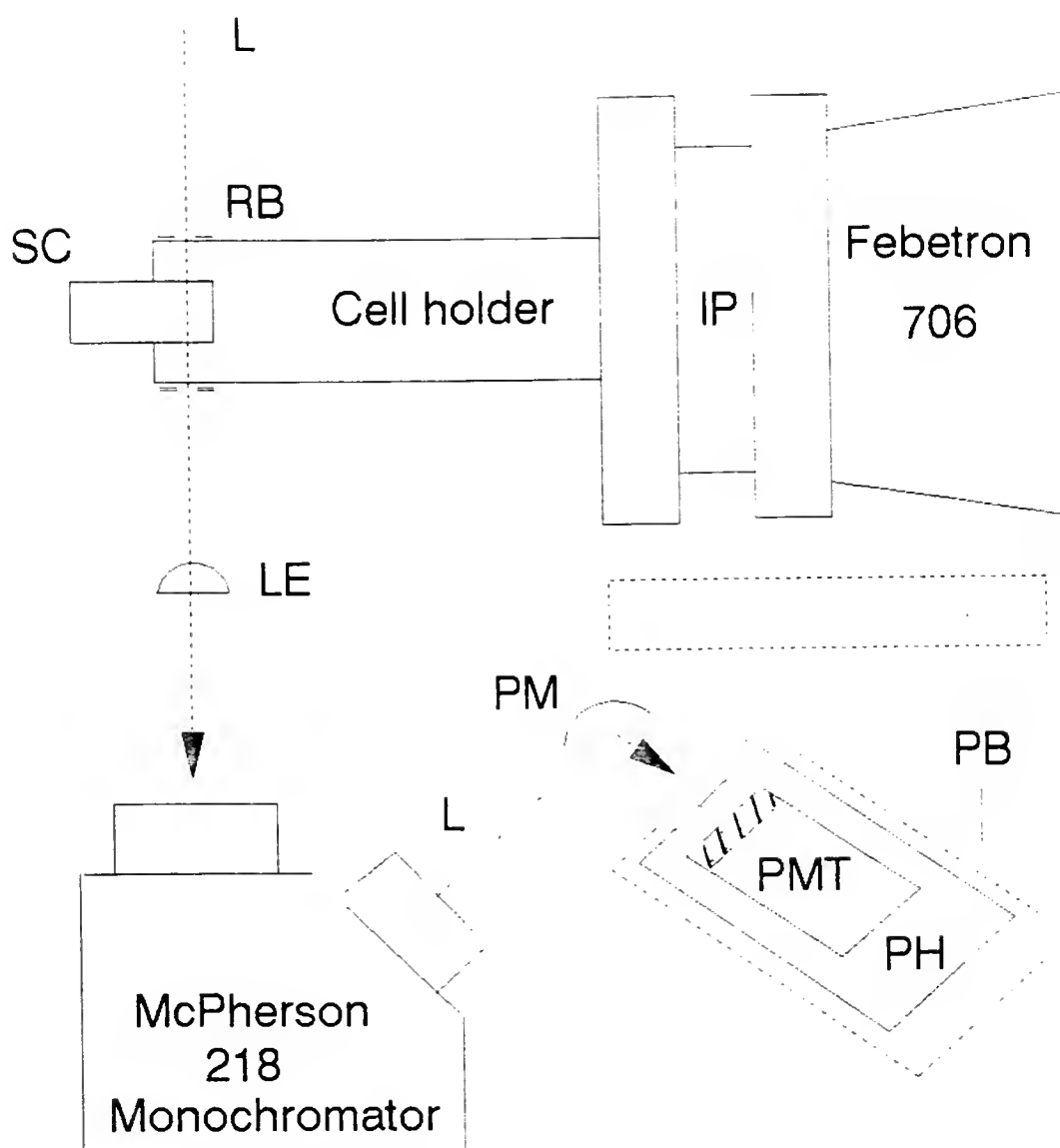
Since the light image is usually focused down on the entrance slits by a condensing lens, the slit width is the only experimental variable parameter in determining the light throughput at a particular wavelength for a monochromator with a fixed optical transmission factor, effective aperture and reciprocal linear dispersion.<sup>117</sup>

### 2.2.3 Photomultipliers

The advantages of using photomultiplier detectors to display transient absorption signals on transient recorders are high sensitivity due to secondary emission multiplication, fast response times relative to the half-life of the relaxation processes being monitored, and the ability to handle high light flux levels while maintaining a linear signal at high output photocurrents.<sup>119</sup> Two types of photomultipliers were used in this work which have different spectral response ranges. An EMI Model 9250 QB end-on 50 mm window PMT fitted in a Pacific Precision Instruments Model 3262 housing was used initially with the geometry shown in Figure 3. Because of its extended spectral response range above 600 nm, a Hamamatsu Model R928 side-on 30 mm window PMT fit into a Pacific Precision Instruments Model 3150 housing was eventually incorporated into the geometry shown in Figure 4.

The photomultipliers were powered by a John Fluke, Inc. Model 412A High Voltage DC power supply, which proved to be a well regulated and stable dc source. The overall gain on the PMT could be altered by changing the applied voltage, typically from 1000 Vdc to 1250 Vdc in increments of 10 or 100 volts, while maintaining maximum gain on the operational amplifier.

The EMI end-on tube has a bialkali photocathode, a Spectrosil quartz window, and an optical range of 165-650 nm



L - Xenon arc lamp

LE - Condensing lense

IP - Ion pump

PB - Lead cave / shield

PH - PMT housing

PM - Parabolic mirror

PMT - Photomultiplier tube

RB - Adjustable razor blades

SC - Solution cell

Fig. 3. Experimental arrangement using the McPherson 218 monochromator.

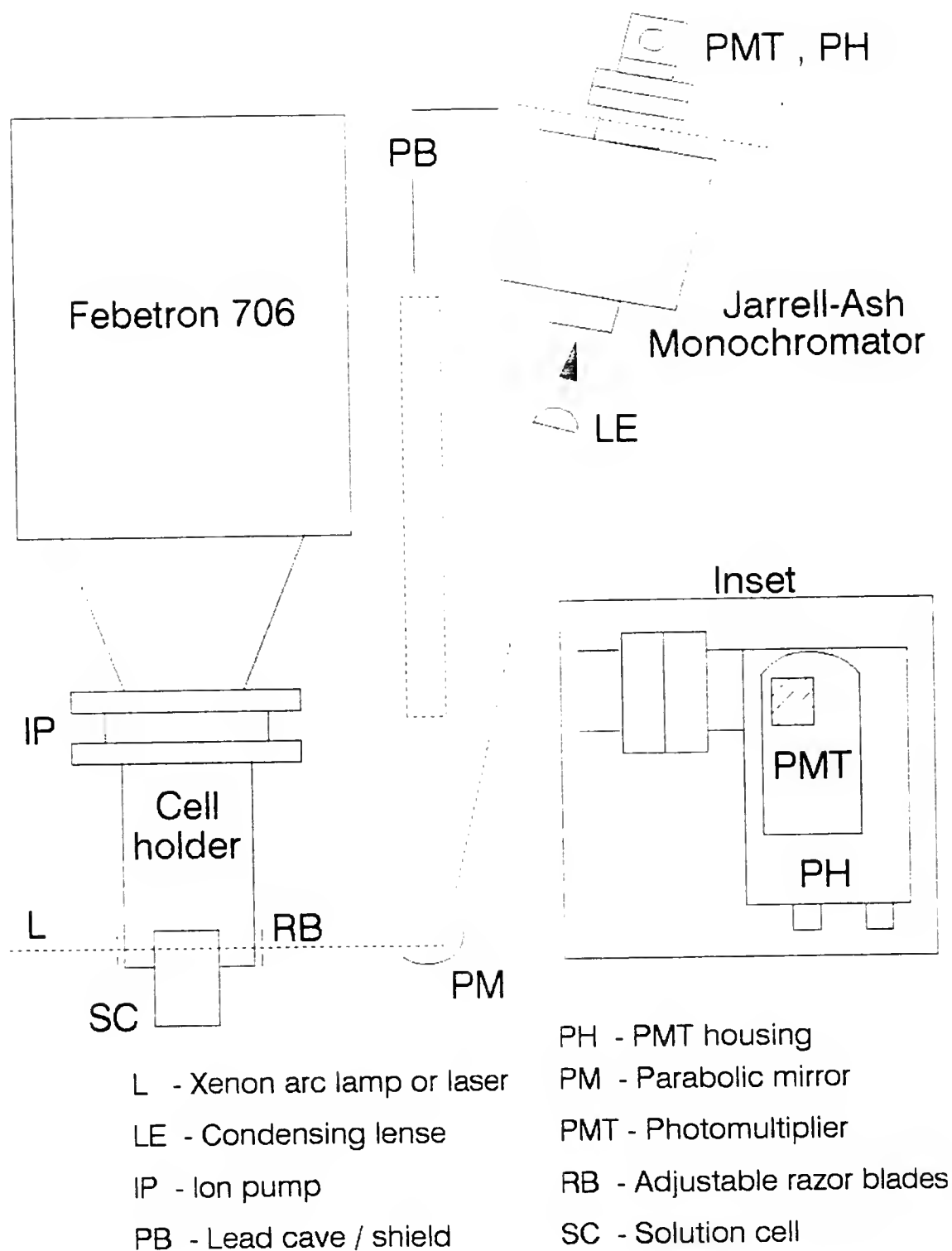


Fig. 4. Experimental arrangement using the Jarrell-Ash monochromator.

with a peak wavelength, or maximum radiant sensitivity (mA/W), at 420 nm. Figure 5 shows a diagram of the base components which were customized to achieve optimum rise times, gains and linearities for use in the pulse radiolysis system. The EMI Model GB 1001A fast electronic switching circuit connected through an optoisolator and switching transistor gates off the first dynode voltage of the PMT to eliminate overloading problems caused by short burst exposure to high light intensities. The gating circuit offers a precise way to regulate the PMT from a + 5 volt gate signal and has the specifications of an on-to-off fall-time of 0.5 microseconds and an off-to-on rise-time of 1.5 microseconds. This circuit which is normally applied in flashlamp or laser systems to protect from overloading conditions was originally employed to eliminate the overloading of the PMT by fluorescence of OH radicals which occurred in previous gas phase studies on the argon sensitized pulse radiolysis of water vapor.<sup>3</sup> In the present liquid phase work, such severe fluorescence problems derived from radiation interactions with either the aqueous chemical system or the quartz cell have not been encountered.

Gating of the PMT was applied to reduce the effect of high levels of electromagnetic interferences (EMI) associated with the high beam current Febetron 706 machine. Accounts of these electromagnetic fields and their effects on detection electronics are discussed in the literature.<sup>26,120</sup>

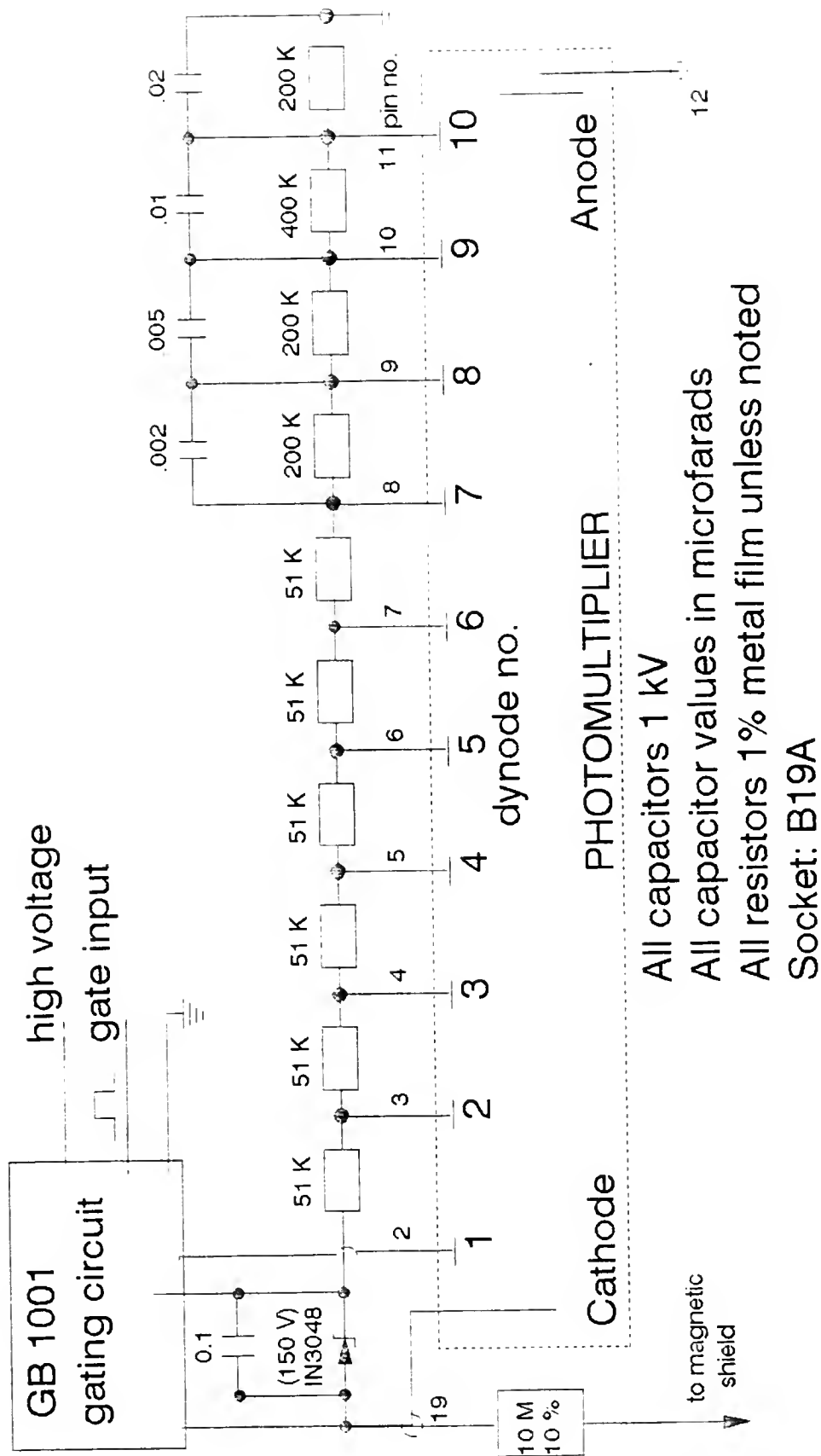


Fig. 5. Photomultiplier tube base schematic used with EMI 9250 QB in model 3262 housing.

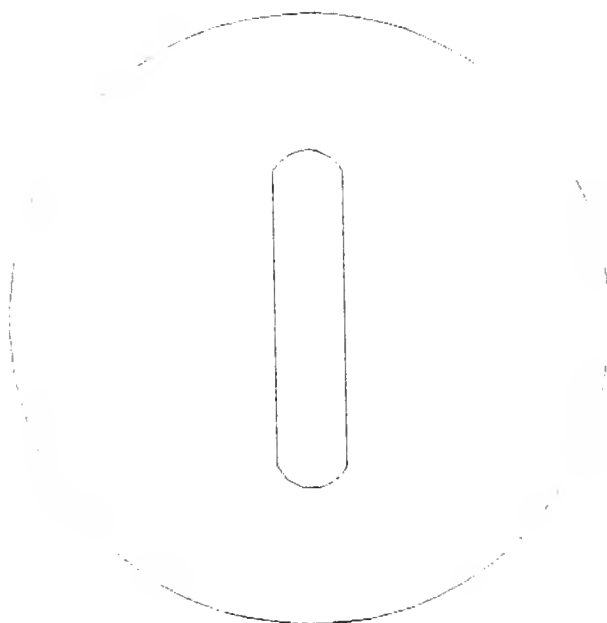


By gating off the initial dynode of the PMT during the radiation pulse, overloading of the photocathode by the X-ray (X-radiation) and the radio-frequency (RF) noise coincident with the electron pulse was significantly attenuated. Further attempts to reduce the EMI effects included the use of lead shields inserted into the entrance of the PMT housings, Figure 6, and extensive lead shielding around the outside of the PMT housing.

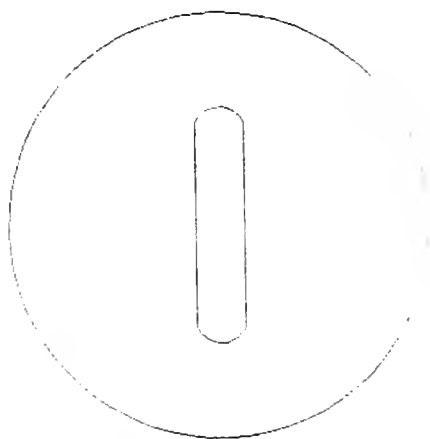
The Hamamatsu side-on PMT was obtained to expand the wavelength range to allow transient absorption measurements above 600 nm, and was used in all subsequent experiments after installation. This PMT has a multialkali photocathode, a UV-glass window, and an optical range of 195-900 nm with a peak wavelength at 400 nm. Figure 7 shows a diagram of the customized base components used with this PMT along with a gating circuit that is analogous to the one previously described.

### 2.3 Light Source Systems

For a versatile pulse radiolysis system with capabilities of nanosecond sampling times in the UV-VIS region of the spectrum, stable and high analyzing light intensities are needed in order to permit the observation of weak or long-lived absorption signals, to reduce shot noise, and to increase the signal to noise ratio.<sup>119</sup>



a) 2 1/16 inch diameter x 1/2 inch thick lead shield for end-on PMT housing, Model 3262.



b) 1 1/4 inch diameter x 1/2 inch thick lead shield for side window PMT housing, Model 3150.

Fig. 6. Lead shields for PMT photocathodes in the Pacific Precision Instruments PMT housings.



### 2.3.1 Xenon-Arc Lamp

The lamp system used in this work consisted of a xenon-arc high pressure discharge lamp contained in a water-cooled housing and powered by a water-cooled ignition device / DC power supply. Several different bulbs including an Advance Radiation Corporation XSA 350 and 500 watt and a Ushio UXL 302-O 300 watt were used throughout the work. The ARC bulbs were of the deep UV design, in which a metal vapor, such as mercury, is present in addition to the xenon gas providing a strong distribution in the deep UV region (190 to 250 nm). The Ushio bulb was not seeded with such a metal and its continuous spectrum is shown in Figure 8. This spectrum was generated by feeding the PMT output across a load resistor and into a Linear Instruments Corporation Model 591 chart recorder.

The bulb was contained in a PRA-Canada ALH 220 housing with dual water cooling loops and powered by a PRA-Canada Model M301 ignition-power supply. The power supply uses a continuous feedback, constant current mode of operation to give excellent current stability. Current programming with square, triangular, or sine wave modulation can be used in this unit to vary the optical output of the lamp. As shown in Figure 9, a 2-3 L/minute cooling line was in series with the power supply and top face plate portion of the housing which was oriented vertically. A separate 0.25 L/minute

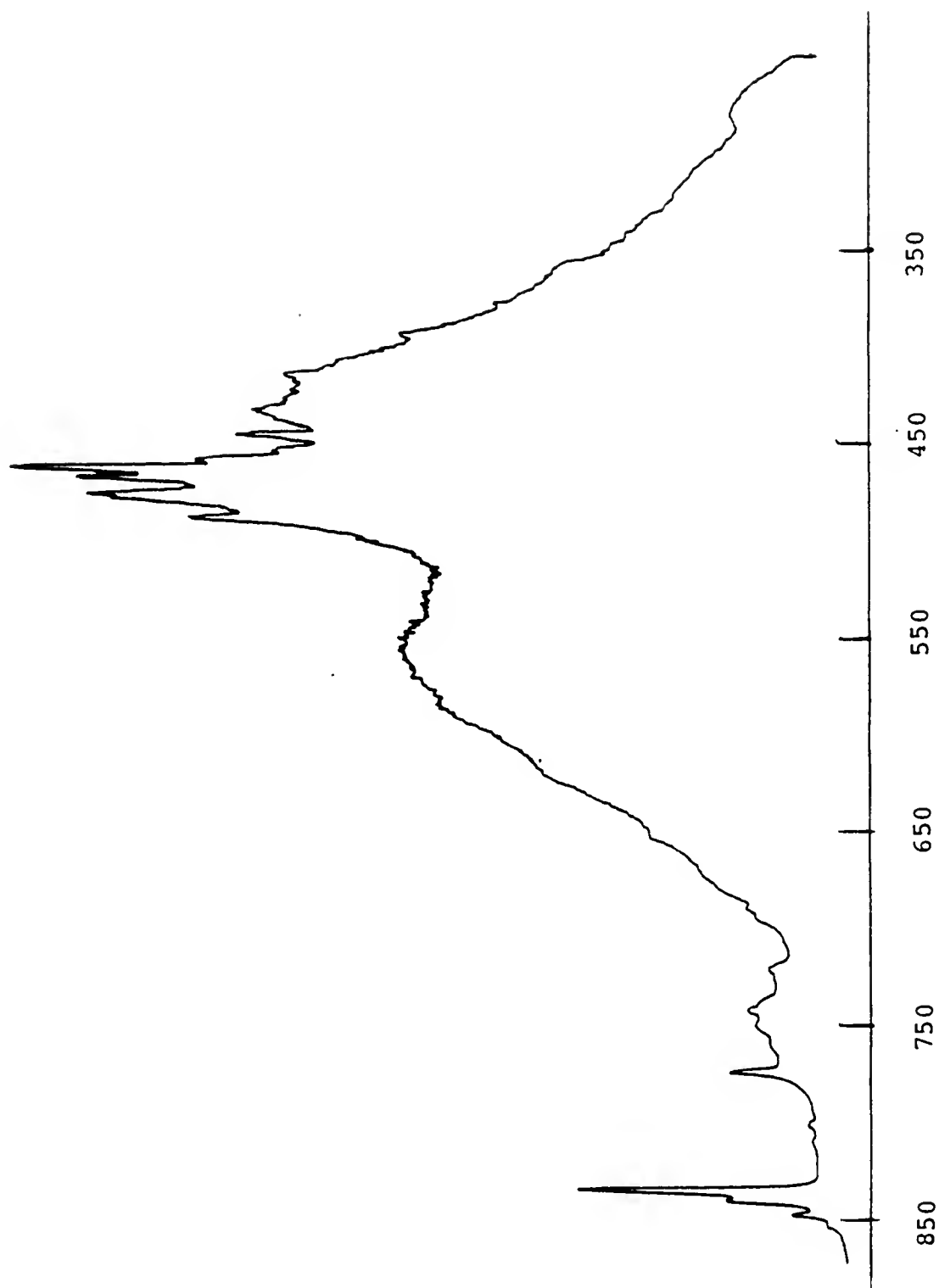


Fig. 8. Xenon-arc lamp spectrum. (nm)

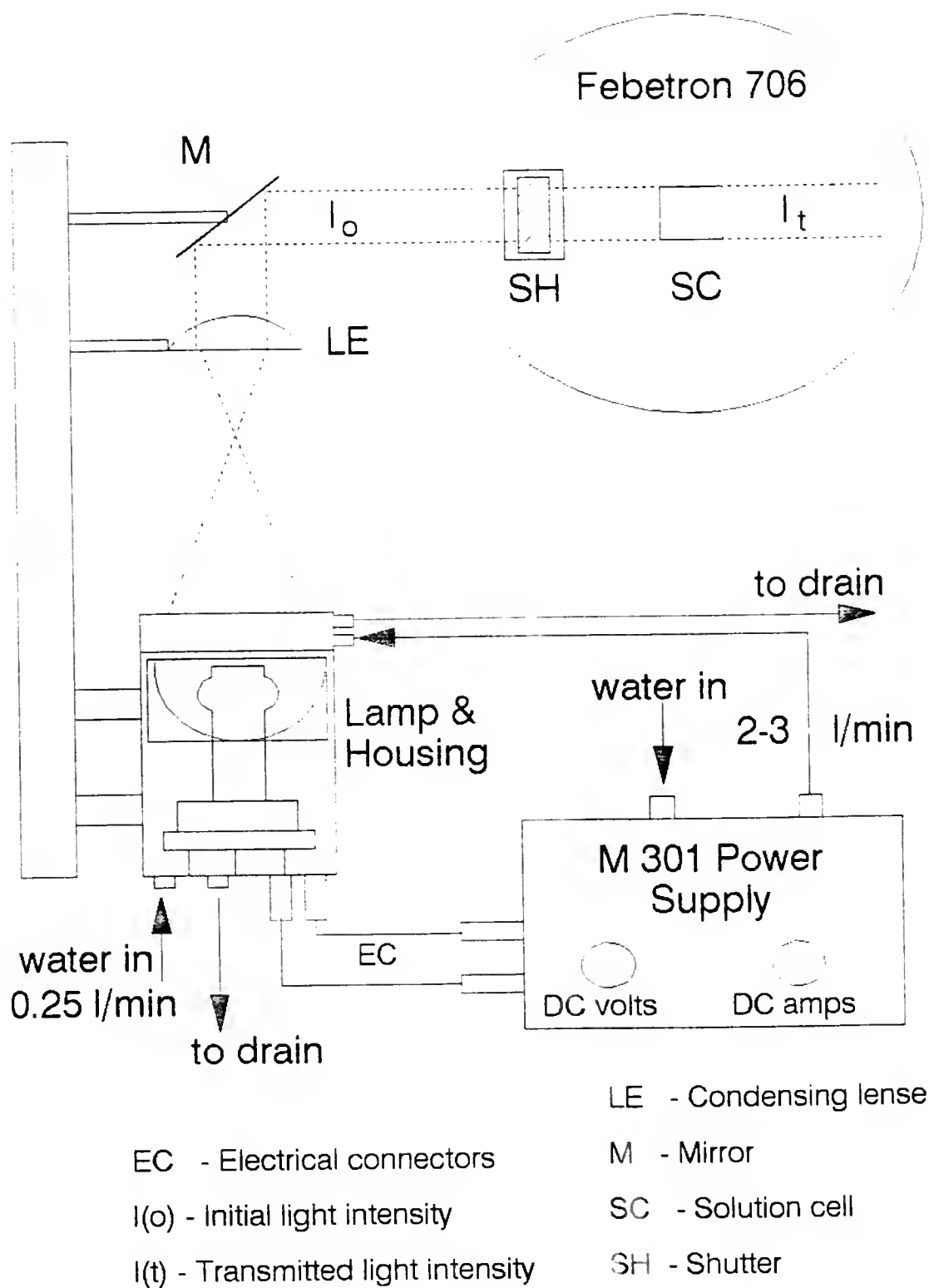


Fig. 9. Xenon-arc lamp schematic diagram.

cooling line was used for cooling of the lamp electrodes. The approximate dimensions of the different optical arrangements are also shown for the lamp housing which contains an f/2.4 exit lens.

For conditions of 1) low absorbance monitoring on the order of a 1% change in light intensity or less, or 2) lower relative light output (i.e. the lower and upper regions of the lamp output spectrum shown in Figure 8) a short duration, very high monitoring light output is desired. This was accomplished by using a conventional signal generator feeding a BNC connector in the rear panel of the M301 power supply. The timing and magnitude of the positive going square pulse was determined by the specifications given by the manufacturer.<sup>121</sup> The pulse width is required to be < 1 second to eliminate damage to the bulb. The pulse magnitude can be varied between 0 and 1 volt according to the following equation

$$I_{out} = I_{idle} + [V_{mod}/4) \times 50] \quad II-4$$

where

$I_{out}$  = M301 output current

$I_{idle}$  = idle current, typically 3-5 amps

$V_{mod}$  = output voltage of the signal generator

The upper limit of  $V_{mod}$ , 1 volt, is determined so that  $I_{out}$  does not exceed the listed nominal operating current of the lamp which for the Ushio UXL 300 W bulb is approximately 15 amps. To attenuate and fine control the 5-volt TTL type signal from the pulse generator, a potentiometer voltage

divider circuit was placed in series with the pulse generator and M301 power supply. Preliminary monitoring of the pulse parameters was done through a Tektronix Model 35A oscilloscope prior to actually pulsing the lamp.

### 2.3.2 He-Ne Laser

A Spectra Physics Model 155 helium-neon laser was used for alignment of the optical systems, calibration of the monochromator gratings, and as a light source for absorption spectrophotometry involving the kinetics of the hydrated electron,  $e_{aq}^-$ . Characteristics of the monochromatic 632.8 laser light such as high collimation, low divergence, and high intensity make this source ideally suited for  $e_{aq}^-$  studies.<sup>122</sup> Figure 4 shows the optical arrangement used for the He-Ne laser, the Jarrell-Ash monochromator and side-on PMT. Attempts to monitor the 632.8 nm light with the end-on EMI PMT were unsuccessful due to this tube's lack of sensitivity above 600 nm.

### 2.4 Reaction Cells and Cellholder

Two types of reaction cells, both consisting of modified quartz UV-VIS spectrophotometric cuvettes, were constructed for this study. Previous accounts of similar reaction cells for use in low energy electron beam radiolysis studies involving liquids indicated the importance of



using very thin electron entrance windows that would minimize the attenuation of the low energy electron beam in the liquid.<sup>123</sup> A cuvette fitted with a reservoir and flow exit for flushing purposes was used in all the on-line absorption detection work and a non-flow cell was used exclusively for the Fricke dosimetry experiments.<sup>40</sup> Both cells were fitted into an aluminum cell holder to provide reproducible positioning and to assure the delivery of equal doses.

#### 2.4.1 Flow Reaction Cell

The flow cell, Figure 10, was constructed from a 60 ml separatory funnel, a  $\frac{1}{2}$  stopcock, a  $\frac{5}{20}$  glass joint, a glass/quartz connector seal and a modified quartz UV-VIS cuvette. A thin mylar sheet  $\approx$  200 microns thick was held by epoxy glue to the quartz cell and served as the electron entrance window. In the initial construction of the cell, FISHER brand microscopic optical glass cover slides with a thickness of 0.13 to 0.17 mm were used.<sup>124</sup> However, the mylar sheet material was chosen as the electron entrance window due to its lesser thickness and the ease by which it could be mounted and trimmed on the cuvette. The optical pathlength was 1 cm, and with an electron penetration depth of ca. 1.5 mm for 600 KeV electrons in water,<sup>122</sup> the irradiated volume was 1 x 1 x 0.15 cm. This electron penetration depth, which is less than the extrapolated range of 1.9 mm, is taken as the depth over which a reasonably uniform dose

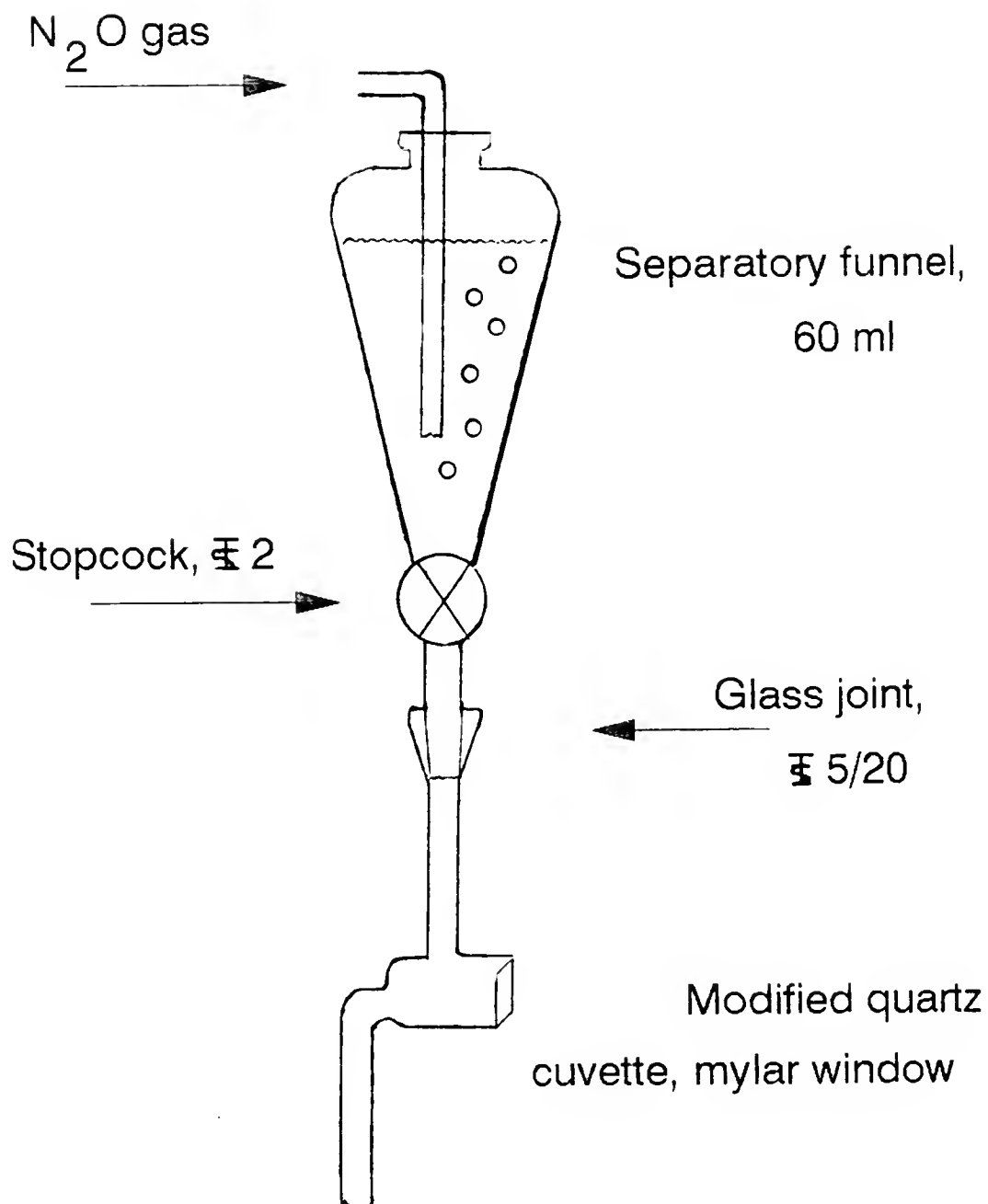


Fig. 10. Flow-reaction cell with modified UV-VIS cuvette.

deposition can be assumed.<sup>125</sup> For studies using purging gases, the gas was continuously bubbled into the upper reservoir for the duration of the experiment.

#### 2.4.2 Non-Flow Reaction Cell

This cell, Figure 11, was constructed from a UV-VIS cuvette to provide detection of 304 nm light associated with the maximum absorption of the ferric ion,  $\text{Fe}^{3+}$ , the oxidation product derived from the radiolysis of an acid solution of ferrous ion,  $\text{Fe}^{2+}$ , in the Fricke dosimetry system as discussed in Appendix B.<sup>40</sup> The electron entrance window was identical to that of the flow cell and a total volume of 1.4 ml was delivered by syringe to the cell prior to radiolysis. This cell could be readily removed from the aluminum cell holder in the pulse radiolysis system and transferred to a Beckman DU model 2400 spectrophotometer with Gilford solid-state electronics, allowing absorption measurements to be made as a function of the number of radiation pulses received. A dilution factor involving the actual irradiated volume of 0.15 ml and the total volume of 1.4 ml was used in all dose calculations.

#### 2.4.3 Cell Holder

An aluminum cell holder, Figure 12, was used to enable reproducible placement of the solution cell with respect to both the electron beam and analyzing light. The holder

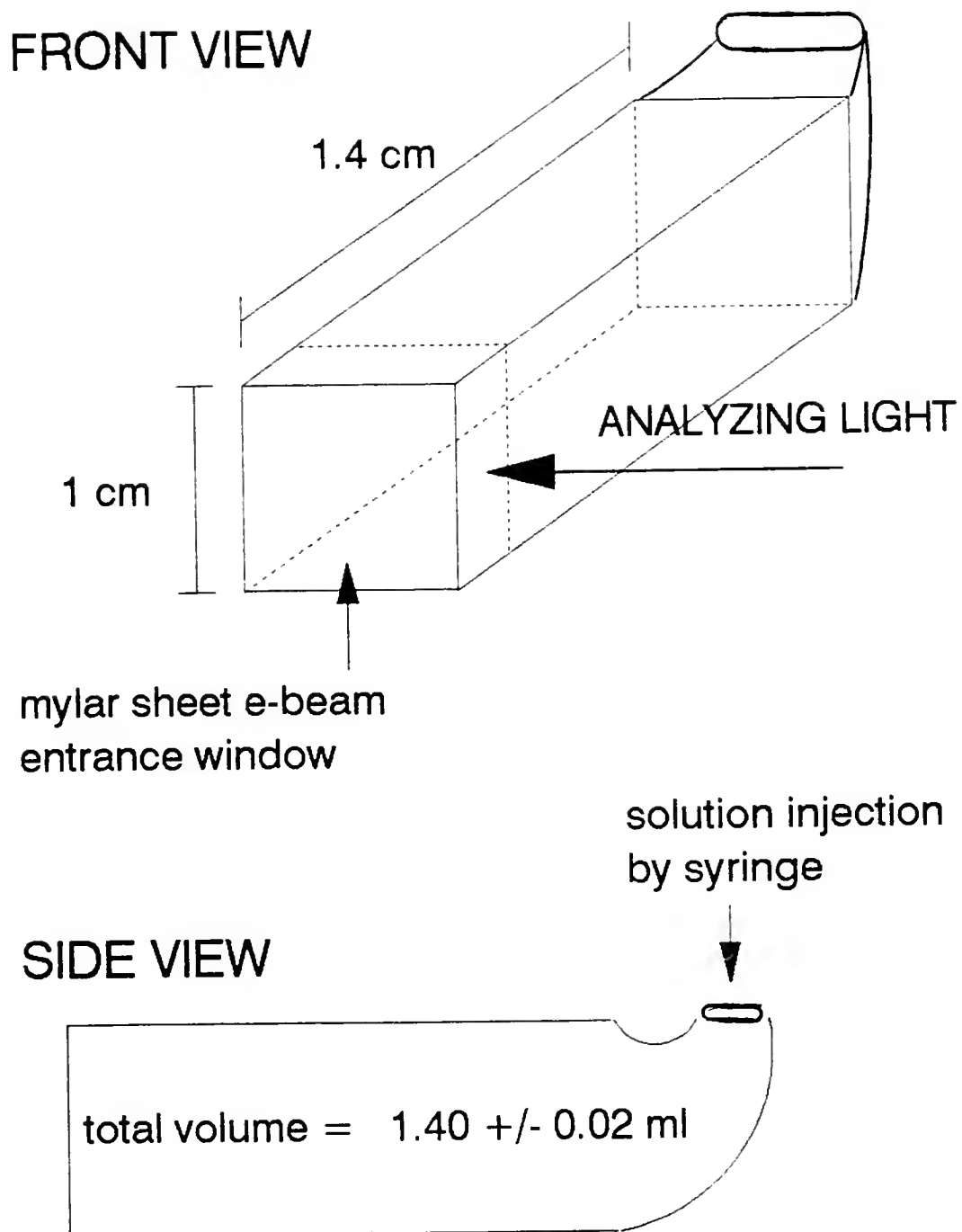


Fig. 11. Non-flow-reaction cell formed from UV-VIS cuvette. Reaction volume consists of  $1 \times 1 \times 0.15$  cm region immediately behind mylar entrance window.

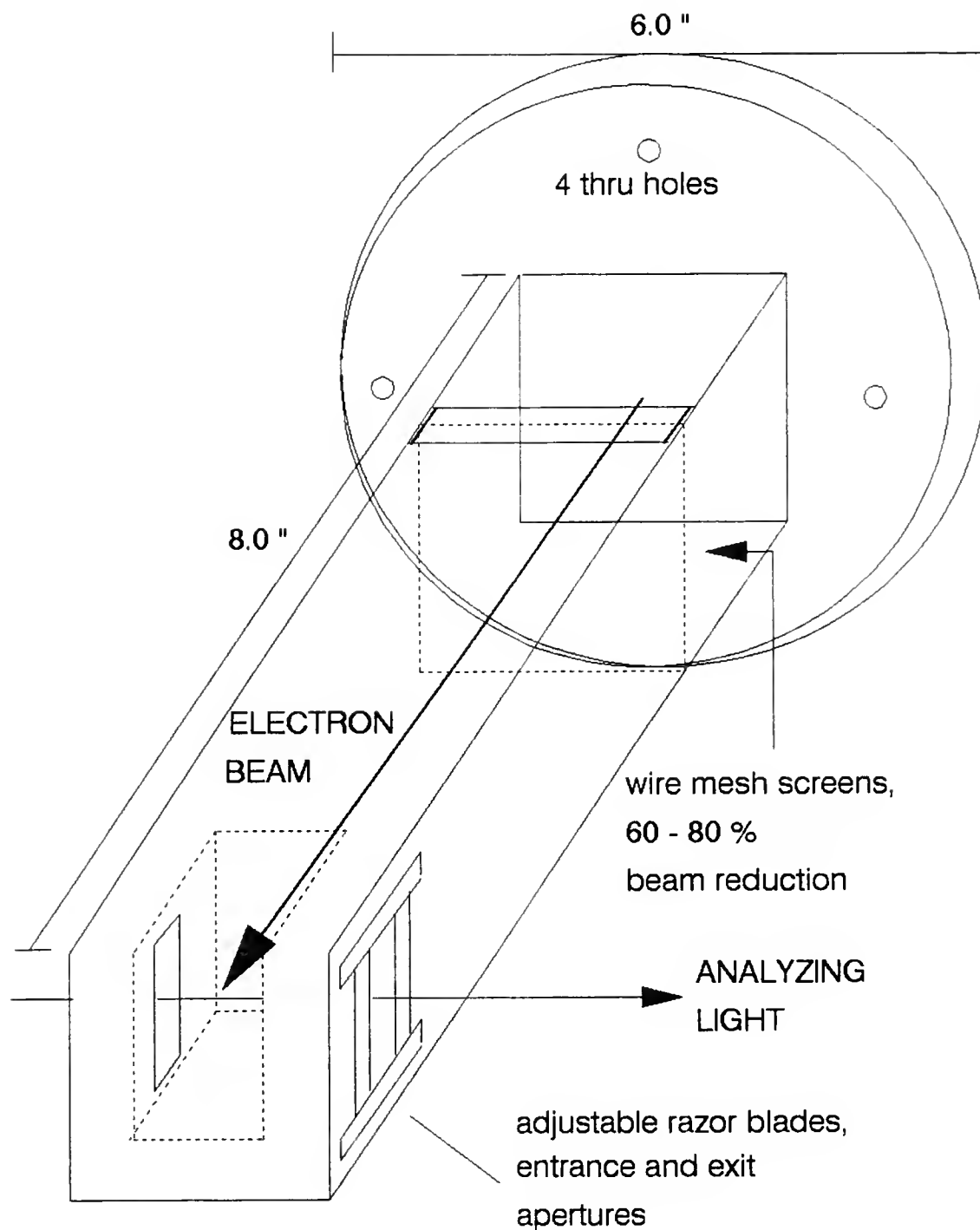


Fig. 12. Reaction cellholder with adjustable razor blade mounts and wire-mesh screens. Electron beam enters through rear flange and traverses 8.0 inches in air. Radiation-induced reaction region occurs in cell (not shown) located at intersection of e-beam and analyzing light.

consists of a 1 x 1 inch open rectangular aluminum column eight inches in length fitted to a six-inch diameter aluminum flange that is attached by four threaded screws to the outer edge of the short-pulse adapter chamber of the Febe-tron 706. Adjustable razor blades mounted at the entrance and exit apertures at right angles to the electron beam axis defined the width of the analyzing light beam. The use of a very narrow analyzing light-beam allowed for the study of the solution kinetics by monitoring only a narrow cross-section for which the dose could be reasonably defined.

Using this arrangement, the electron beam traversed ca. 8 inches of air between the field emission tube exit window and the thin mylar entrance window of the reaction cell. This distance creates a slight attenuation of the electron beam intensity which is primarily associated with a spreading of the effective beam diameter away from the tube face. For a distance of eight inches the beam will have an effective diameter of three centimeters as compared to a diameter of 1.5 centimeters as it exits the tube face. The loss of beam intensity due to absorption in air should be negligible due to the maximum penetration range of 80 inches for 600 KeV electrons in air.<sup>125,126</sup>

Experiments with FISHER brand optical glass microscopic coverslides placed in the cell holder at the solution cell position were performed to determine the depth distribution of the electron beam. Typical depth-dose curves are shown

in Figure 13 which includes data for two experimental conditions. Initially a stack of approximately 20 slides was exposed to a single Febetron shot with maximum charging of 30KeV. Absorption measurements were then made on each individual slide to detect the amount of discoloration in the glass due to the e-beam penetration. Secondly, a similar stack of coverslides was exposed to 10 cumulative shots at full charge, followed by individual absorption measurements. Both data sets indicate an extrapolated range for the 600 keV electrons in the glass to be approximately 7 slides. Using a slide thickness of 0.15 mm, the extrapolated depth in glass is found to be 1.0 mm. Assuming that glass is approximately twice as dense as water, these data indicate a maximum range for 600 Kev electrons in water to be approximately 2.0 mm, which agrees with the earlier reported value of 1.9 mm.<sup>125</sup>

Figure 14 shows the absorption due to the discoloration in a single slide as a function of the number of pulses delivered at maximum charging. The accumulated discoloration resulting from the e-beam passage through the glass slide was found to be non-linear, with the absorption falling off as a function of pulse-number.

Wire mesh screens capable of 60% to 80% electron beam reductions could be positioned in the cell holder two inches from the field emission tube window (Figure 12) to aid in

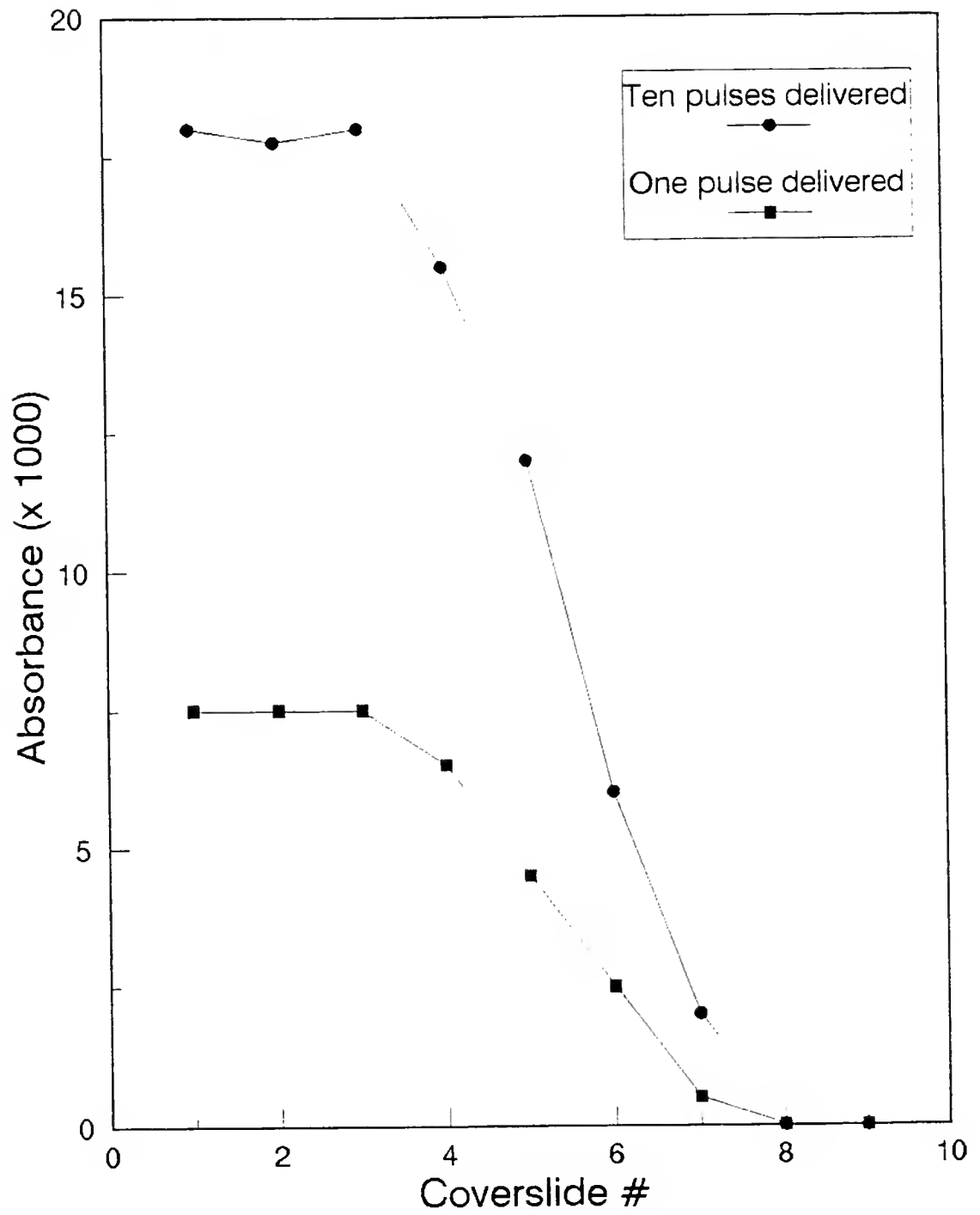


Fig. 13. Depth-dose curves for glass coverslide experiment.



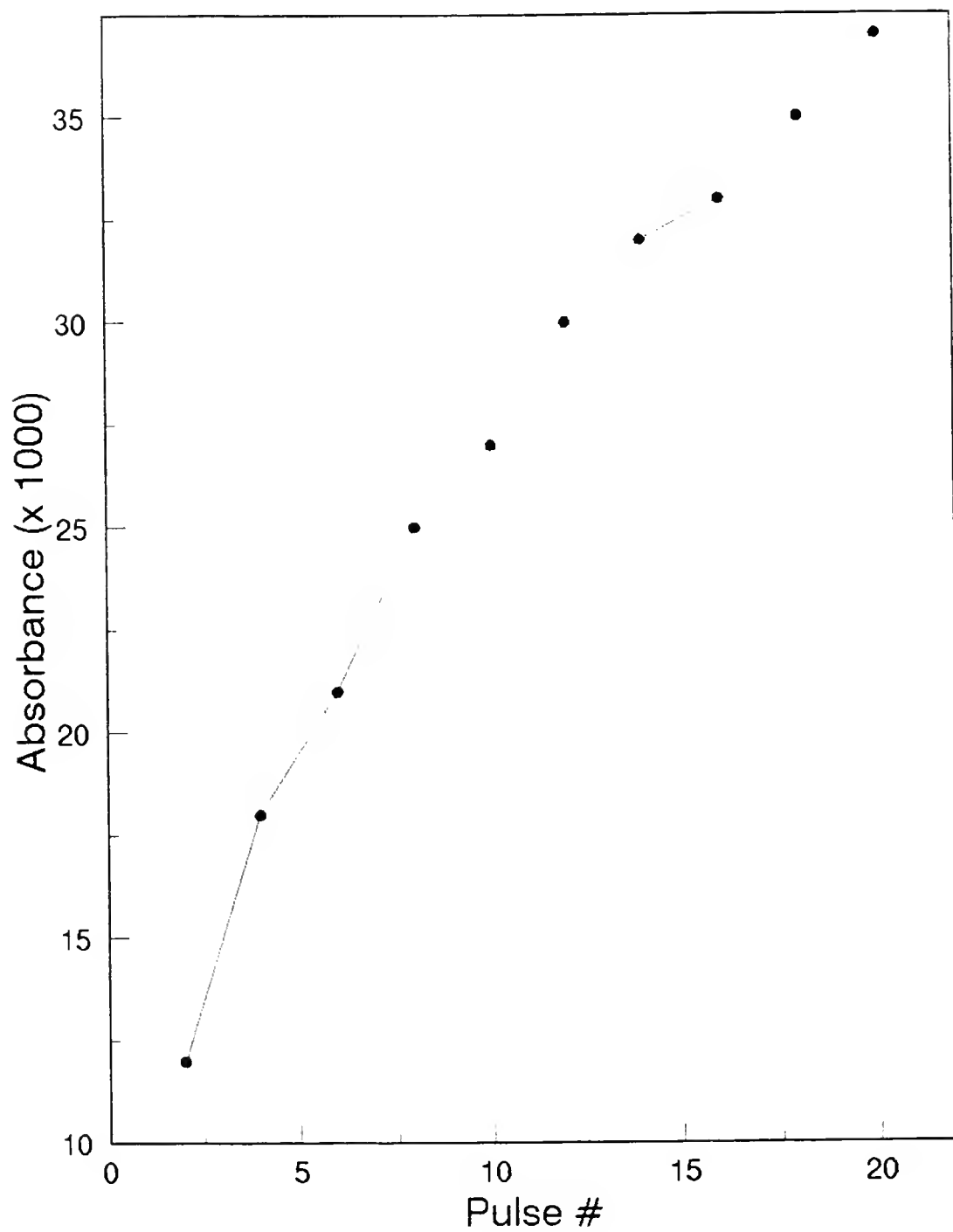


Fig. 14. Absorbance change with number of pulses delivered for glass coverslide experiment.

acquiring transient formation signals occurring during the first few microseconds immediately following the radiolysis pulse. These screens restrict the flux of the electron beam which was maintained at a maximum charging voltage of 30 KeV. With the wire mesh screens inserted, attenuation of the beam intensity decreases the total average population of initial radicals formed. This beam flux attenuation helps to prevent radical-radical interactions and provide favorable radical-solute interaction conditions. However, due to both a malfunction in the fastest data acquisition mode of the transient digitizer, and electromagnetic interferences associated with the Febetron 706 system that were discussed earlier, attempts to capture transient formation signals with enough resolution for kinetic analysis were not successful.

## 2.5 Monochromators

In the early stages of this work a 0.3 meter McPherson 218 monochromator was used. Later, efforts were made to reduce electronic interferences associated with the electron beam pulse by removing the monochromator and PMT couple away from and to the rear of the field emission tube. Due to the rather permanent fixture of the Mcpherson 218 and its associated vacuum pump assembly relative to the initial experimental geometry, a second 0.25 meter Jarrell-Ash 82-41550 monochromator was employed.

### 2.5.1 0.3 Meter Monochromator

Initial studies were carried out using a McPherson 218 vacuum/atmospheric monochromator which has an  $f/5.3$ , a 2400 G/mm plane grating and a 1.33 nm/mm linear dispersion. The vacuum capabilities were not employed for any of this work and the 2400 G/mm grating having a 0 - 5,000 angstrom wavelength range was eventually replaced with a 1200 G/mm grating capable of operating in the wavelength range from 0 - 10,000 angstroms. A synchronous motor-driven gear box supplies 12 scanning speeds from 0.5 angstroms/minute to 200 angstroms/minute and slit widths were adjustable from 10 microns to 2 millimeters. Slit widths of 1.5 millimeters and a fixed slit height of 8 millimeters were used. Figure 3 shows the optical configuration used with the McPherson monochromator. Light exiting the xenon arc lamp was passed through a condensing lens onto a first surface mirror and reflected through the solution cell. The beam was then focused on the entrance slit of the monochromator and after wavelength dispersion the exiting beam was reflected onto the photocathode of the PMT by a 2.5 cm focal length parabolic mirror.

### 2.5.2 0.25 Meter Monochromator

Initial testing of the Jarrell-Ash monochromator coupled to the end-on PMT with both components located approxi-

mately 2 meters away from the field emission tube showed a marked improvement in reducing the electromagnetic noise interferences. Using the McPherson monochromator in the previously shown geometry in conjunction with the gating circuit produced a net dead-time, caused by gross overloading of the PMT, of  $> 5$  microseconds in the detection system. When the detection system was relocated, as shown in Figure 4, net dead-times of 2 to 3 microseconds could be attained without the use of the gating circuit. All subsequent work was completed with this arrangement and eventually the end-on PMT was replaced by the side-on PMT. To attain further reduction of the EMI effects, the entire detection system and signal lines would have to be either completely removed from the room containing the Febetron 706 or extensively shielded.<sup>120,127</sup>

In this modified configuration the analyzing light, after passing through the solution, was reflected by a first surface mirror back to a plano-convex  $f/2.5$  condensing lens and focused onto the entrance slit of the Jarrell-Ash monochromator. This monochromator has an  $f/3.5$ , a 1180 G/mm grating and a 3.3 nm/mm linear dispersion. A wavelength motor drive of 100 nm/minute was coupled to a wavelength drive knob to enable scanning of the light source spectrum.

The slit arrangement provided with this monochromator was altered to accommodate the direct coupling of the Jarrell-Ash monochromator to both a previous gas phase aluminum

reaction cell, and the Pacific Precision Instruments PMT housing.<sup>128</sup> In this work only, the direct couple of the monochromator and PMT housing was utilized. This was accomplished by screwing the PMT housing containing the side-on Hamamatsu tube directly to the exit slit flange adapter. Figure 15 shows the entrance and exit system flange adapters. Brass slit bodies of fixed width and height, 0.71 mm and 15 mm respectively, were screwed into the aluminum flange by turning the two small holes in the slit body with a sharp tool.

## 2.6 Febetron 706 System

The principle of pulse radiolysis involves the delivery of ionizing radiation to a chemical system in the form of a short pulse that creates a non-equilibrium system with an adequate amount of transient species that are monitored in time. An accelerator is used as the source of the high kinetic energy ions and several related parameters are important in pulse radiolysis measurements. Primarily, the radiolytic pulse should be very short relative to relaxation of the transient system, and the pulse current should be large enough to produce an observable concentration of transients. Energy deposition, which depends on 1) the particle's mass, charge, and velocity, and 2) the medium density, is critical in determining the distribution (either homogeneous or non-homogeneous) of radical concentrations produced.

slit area = 0.71 mm x 15 mm

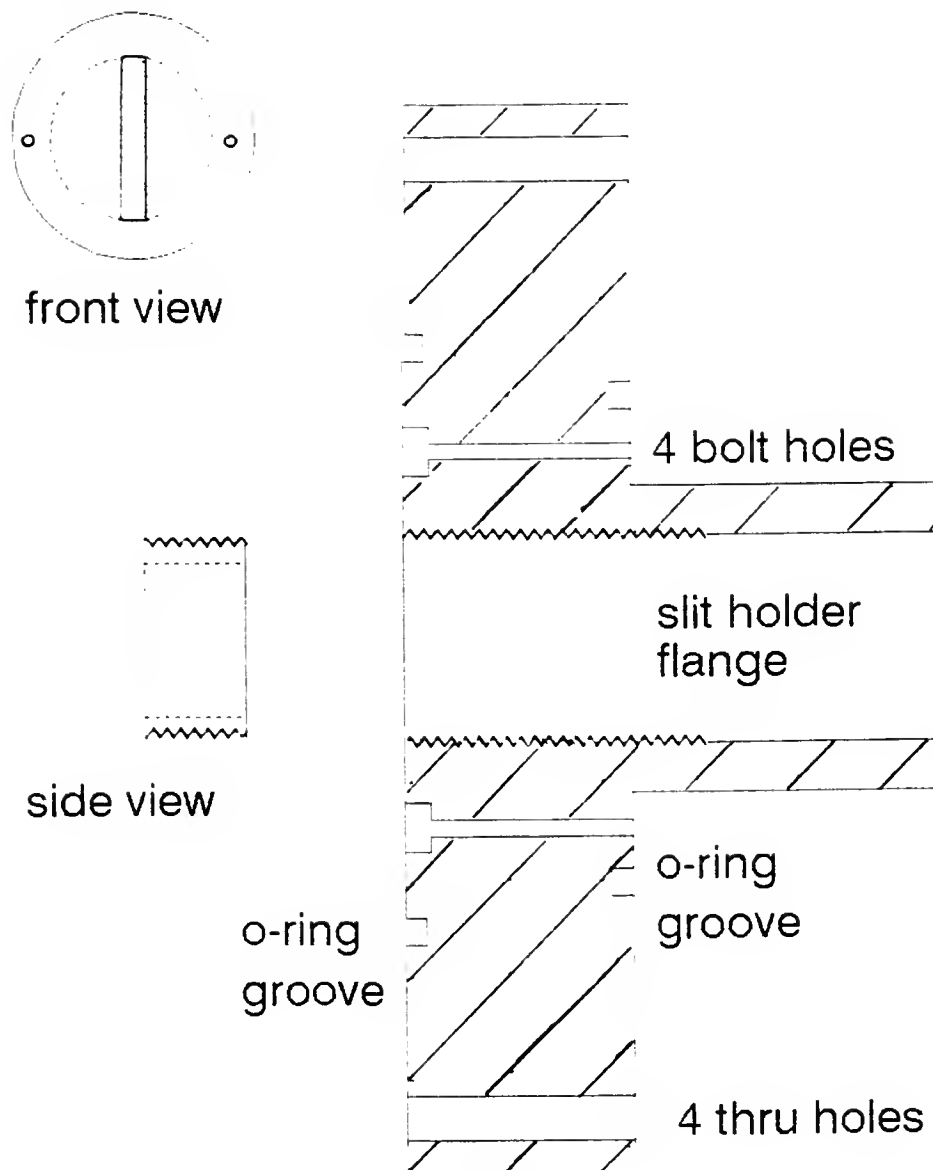


Fig. 15. Entrance and exit slit system flange adaption to the Jarrell-Ash monochromator.

The Febetron 706 electron accelerator used in this work is fitted with a Model 5515 high vacuum field emission electron tube and has the following specifications: 12 joules maximum pulse energy, 8,000 amperes of peak current, 3 nanosecond pulse duration (FWHM), 5% peak to peak repeatability, and a maximum electron energy of 600 KeV. The extremely high currents make this model particularly applicable to gas phase studies.

However, it was suspected that the high vacuum electron tube had become gaseous due to intermittent use in previous years and the extended lifetime of the electron tube beyond its suggested 3500 pulses. The e-beam tube had failed after ca. 8000 pulses; the beam had burned microscopic holes in the window which allowed the pressure in the tube to rise to atmospheric. It was expected that partial operation could be restored by replacing the window and reevacuating the tube. This attenuated beam feature would be beneficial to condensed phase studies by eliminating radical-radical interactions caused by the absorbance of enormous radiation doses. Encouraged by other somewhat analogous and confirming reports,<sup>122,129-132</sup> we pursued the application of the Febetron 706 accelerator to aqueous solution work.

Details of the Febetron 706 system can be found elsewhere.<sup>125,126,133</sup> Figure 16 shows a block diagram of the Model 706/2677 system. The Febetron 706 system was maintained by keeping the various chambers with their associated

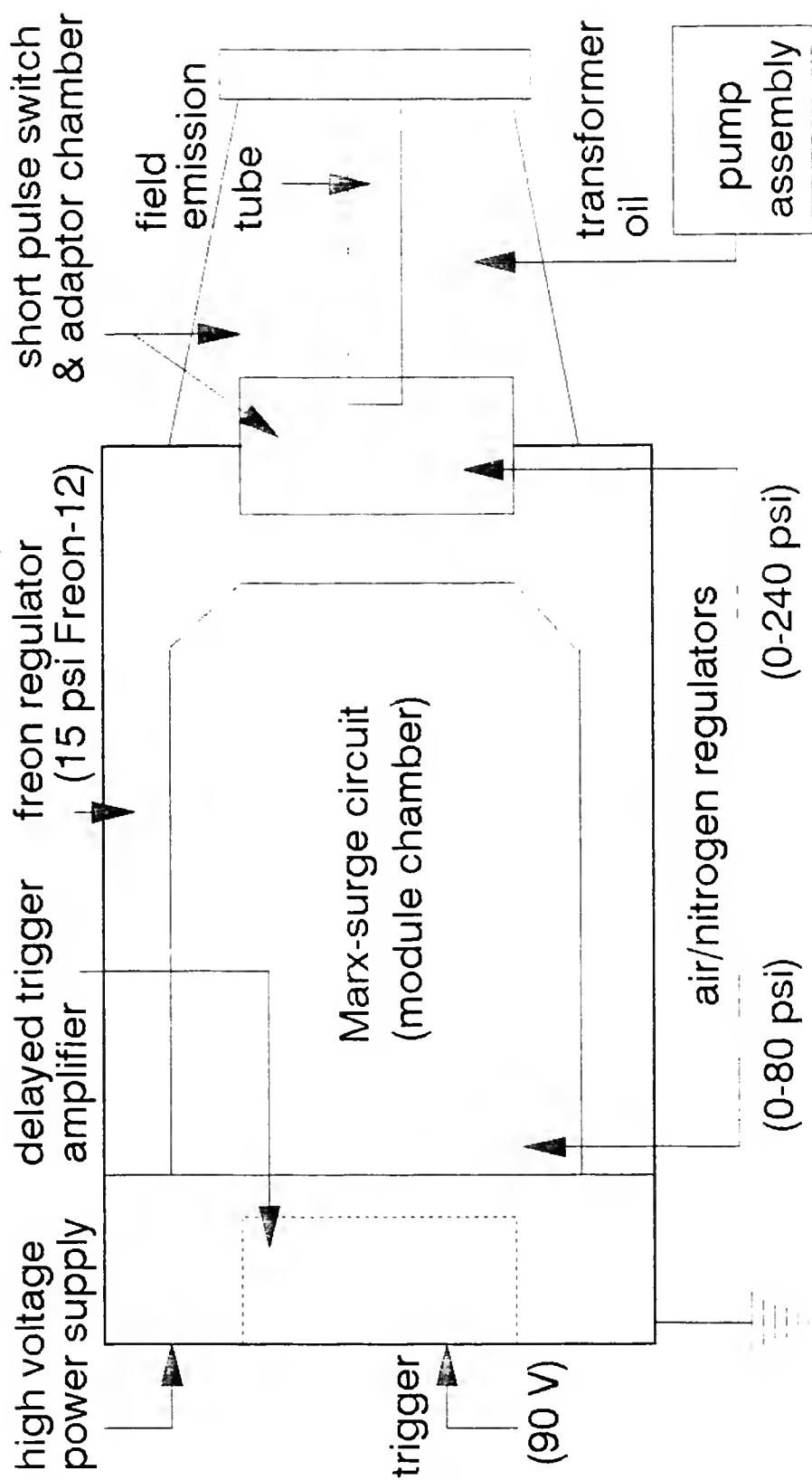


Fig. 16. Febetron 706 system schematic.



pressure regulators and gauges properly pressurized. A compressed air tank is used to pressurize the module chamber at a maximum of 80 psi and the short pulse adapter at a maximum of 240 psi. Freon-12 was maintained at 13 psi in the pulser case. The transformer oil in the short pulse adapter was circulated daily by an electric pump connected to a large oil reservoir.

The accelerator operates on the principle of the Marx-bank circuit which consists of a number of connected high voltage capacitors that are charged in parallel and subsequently rapidly switched to a series arrangement through spark gaps. This circuit, located in the Marx-surge stage of the pulser, produces a high voltage, extremely high peak power pulse that is used to pulse charge through a series spark gap in the central electrode of the short pulse adapter stage of the pulser. This short pulse adapter then discharges an extremely short 3 ns high current pulse to the field emission electron tube. This pulse generates electron emission from the cathode and the electrons are then accelerated toward an exit window that functions as the anode.

As mentioned above, due to the lack of an inward deflection in the thin exit window of the field emission tube, it was decided that gaseous conditions existed inside the tube. Under normal conditions, the thin metal window would be noticeably drawn in by the high vacuum. Experiments using the technique of calorimetric dosimetry carried out

directly in front of the tube exit window showed negligible energy outputs. Therefore a modified electron beam tube exit system was fabricated.

#### 2.6.1 Refurbished Beam Tube

A modified electron beam tube flange and exit window system<sup>132</sup> was constructed to renew the output of the Febetron 706 system. This modification, Figure 17, was formed from a stainless steel chamber 4.75 inches in diameter and 1.25 inches thick, and fit with a Model 202-100 Perkin-Elmer 2 liter/second differential ion pump powered by a Model 222-0200 Perkin-Elmer IONPAK 200 power supply. The high vacuum current limiting power supply operated at a voltage between +4000 volts DC and +6000 volts DC and the system was capable of attaining pressures below  $1 \times 10^{-6}$  Torr.

The former anodic window of the field emission tube was cut away and a thin, approximately 0.001 inch stainless steel window and o-ring were set into the compartment. The compartment was attached by three threaded screws to the field emission tube window face plate flange of the Febetron 706 with a second o-ring seal. Initially, the thin window was placed 0.8 inches away from the original anode window location. Although an adequate vacuum was attained, further dosimetry experiments showed no improvement with this geometry so the window was set further into the compartment 0.4

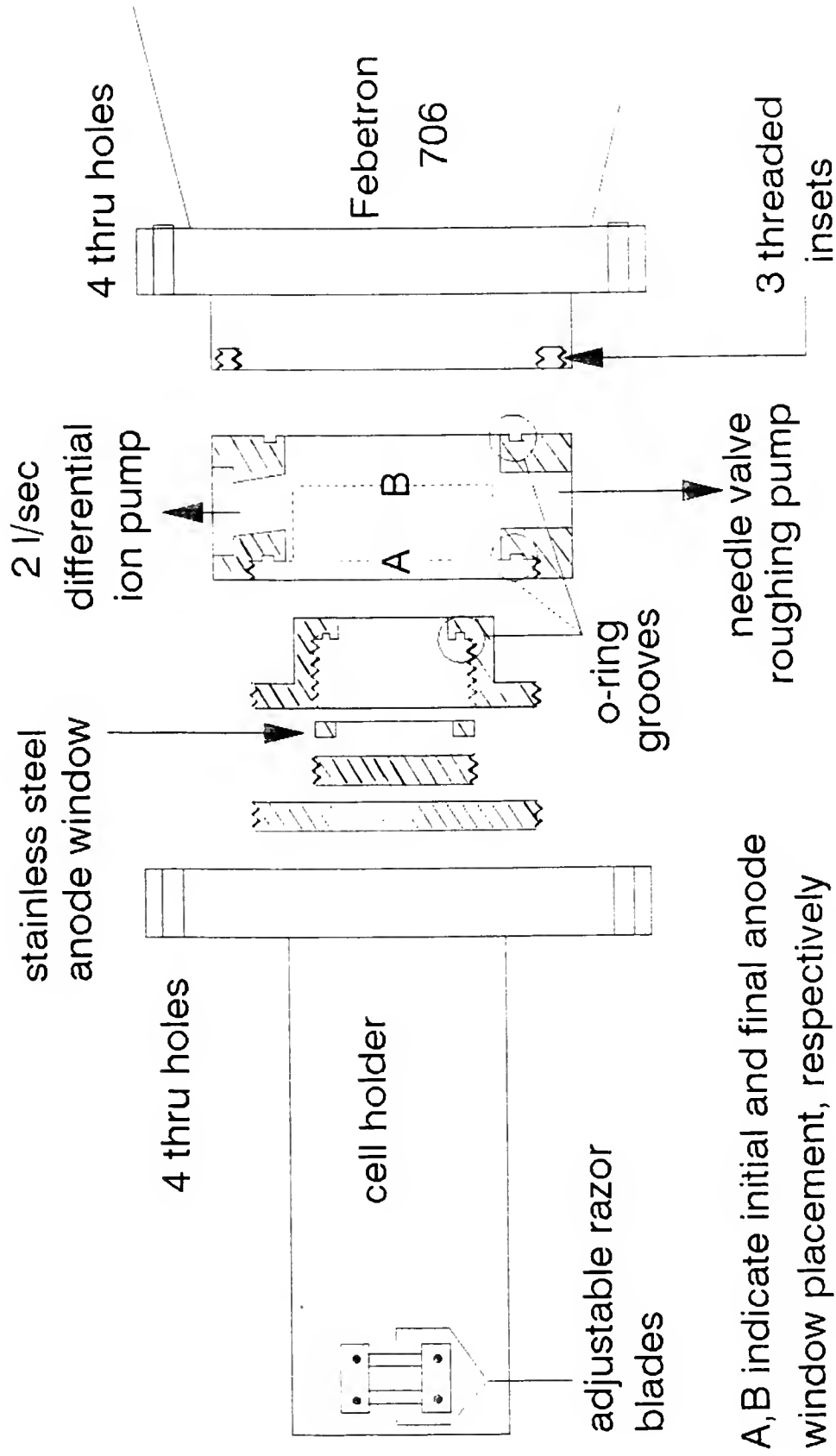


Fig. 17. Refurbished electron-beam tube with ion pump.

inches away from the original window location. After rough pumping the chamber down to a few microns of pressure and attaining the minimum +4000 volts DC required for proper operation of the ion pump, calorimetric dosimetry measurements were again performed.

### 2.6.2 Calorimetric Dosimetry

The total-beam calorimetric technique, as illustrated in Figure 18, involves the measurement of the heat deposition in an aluminum disk upon firing the Febetron 706 at maximum charge. The thickness and diameter of the disk, 0.033 inches and 1.385 inches respectively, were chosen to assure complete e-beam deposition. Aluminum is suitable due to its high thermal conductivity, specific heat, and low backscatter energy coefficient. The temperature of the calorimeter was conveniently measured by attaching a thermocouple and measuring the voltage output with a recording millivoltmeter. The thermocouple was attached to the aluminum disc in this particular calorimeter by drilling a small hole in the center, inserting the thermocouple wires, and swaging the aluminum around them with a punch. The calibration of the thermocouple/chart recorder was accomplished using room temperature of  $\approx 25^{\circ}\text{C}$  as the base line and normal body temperature of  $\approx 37^{\circ}\text{C}$  as the maximum scale value. For the maximum temperature reading, the disk was held firmly in the palm of the hand until a steady equilibrated signal was obtained.

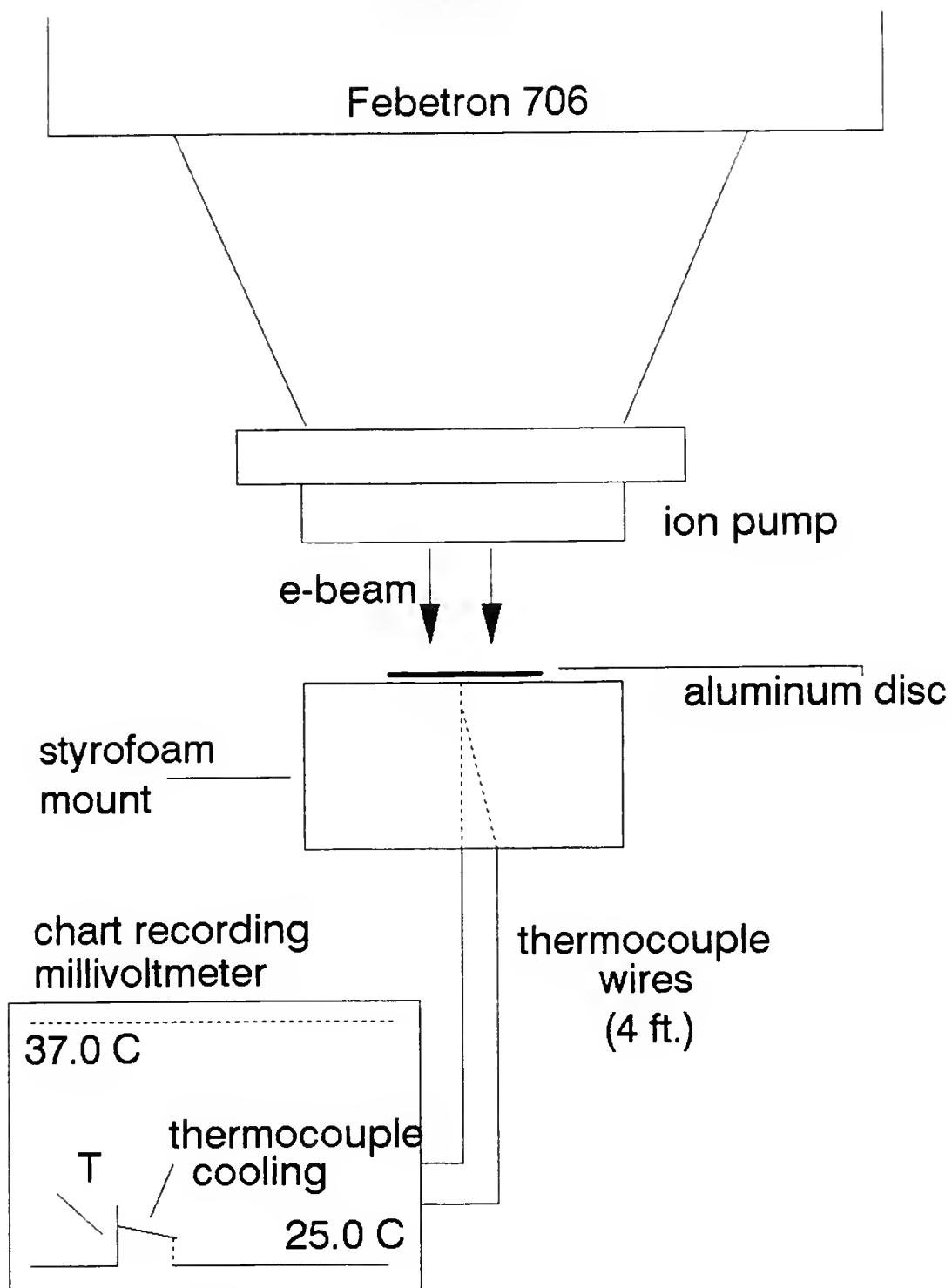


Fig. 18. Total beam calorimetric dosimetry arrangement.

Using the equation

$$Q = m C_p \Delta T \quad \text{II-5}$$

with  $Q$  = heat required to raise the specific heat of the calorimeter by  $\Delta J$ , Joules

$m = 2.3 \pm 0.05$  grams (mass of the aluminum disk)

$C_p = 0.22$  cal/ °C gram (specific heat of aluminum)

$\Delta T = 0.53$  °C (difference between pre- and post- pulse read from chart recorder)

a value of  $1.12 \pm 0.06$  Joules was determined as the beam energy absorbed per pulse. These positive results indicated that the placement of the new anode window was a critical factor with possible arcing complications arising when the new window was not located close enough in to the original window position.

## 2.7 Transient Recorder and Computer System

While early pulse radiolysis studies used the oscilloscope-Polaroid photograph technique for recording transient signals, development of sophisticated transient recorders followed that now have replaced this manual data analysis method.<sup>117</sup> Digital recorders now digitize the input signal in real time and can resolve the signal into separate channels thus providing a stored digitized record of the transient trace as a function of time. In addition, interfacing of the recorder with a computer allows for integrated control of the operational parameters such as time base, sensitivity, delays, signal processing, and data transfer.

The data acquisition and analysis system developed for this work is a second generation system having been preceded by a Biomation Model 610B transient recorder supported by an IMSAI 8080 S-100 bus microcomputer.<sup>128</sup> Current instruments include an Analogic Data Precision DATA 6000 waveform analyzer fitted with a Model 620 2-channel plug-in digitizer interfaced through a serial port at 9600 baud to a Tandy 1200 IBM-PC/compatible laboratory microcomputer.

The DATA 6000 has two signal-input ranges of  $\pm 1.2$  and  $\pm 3.6$  volts full scale, and a maximum sampling rate of 100 MHz. This sampling rate gives a period (time between sampled points) of 10 nanoseconds for collection of 512 points using an 8-bit recorder. Although the maximum period attainable is 300 seconds, a maximum period of 1 microsecond was used in this work giving a sampling rate of 1 MHz. The DATA 6000 is noted for its versatile capabilities of signal capture, processing and data transfer, although the lack of any fine control on the input voltage parameter was found to be a rather severe experimental limitation in this work. The DATA 6000 is controlled by a single internal 68000 microprocessor and a CRT display screen enables visual inspection of signals before data transfer.<sup>134</sup>

Data recording parameters were selected either manually through keypads on the front panel or remotely via computer control. Remote control of the DATA 6000 via an RS-232

serial interface port utilized three basic functions: control of data recording parameters, use of processing and display, and transfer of data to and from the digitizer. To use these functions, a computer program written in BASIC language provided either keystroke emulation by key code number or direct control using English commands. These operations were sent to the DATA 6000 as string commands and data transfers to the computer were sent in ASCII number format. Various timing loops set up in the BASIC program assured proper hand-shaking. During operation several parameters such as trigger source, timebase, screen display and marking were initially set manually and subsequently controlled remotely through the computer program. For short-lived transient signals, the multiple trace delayed mode with signal averaging was used which provides an enhancement to the S/N ratio in proportion to the square root of the number,  $n$ , of signals averaged.<sup>118</sup> Otherwise, the single trace delay mode was used with no signal averaging.

As shown in Figure 2, the triggering and delays were originated from a single initial manual trigger pendant delivering a 90 volt pulse derived from three 30 volt batteries in series with a standard RC trigger circuit. A typical timing sequence is presented in Figure 19. Delay of the Febetron firing was accomplished using an Evans Associates programmable time delay (PTD) module, Model 4145-2. Three such modules are present which could be used in series



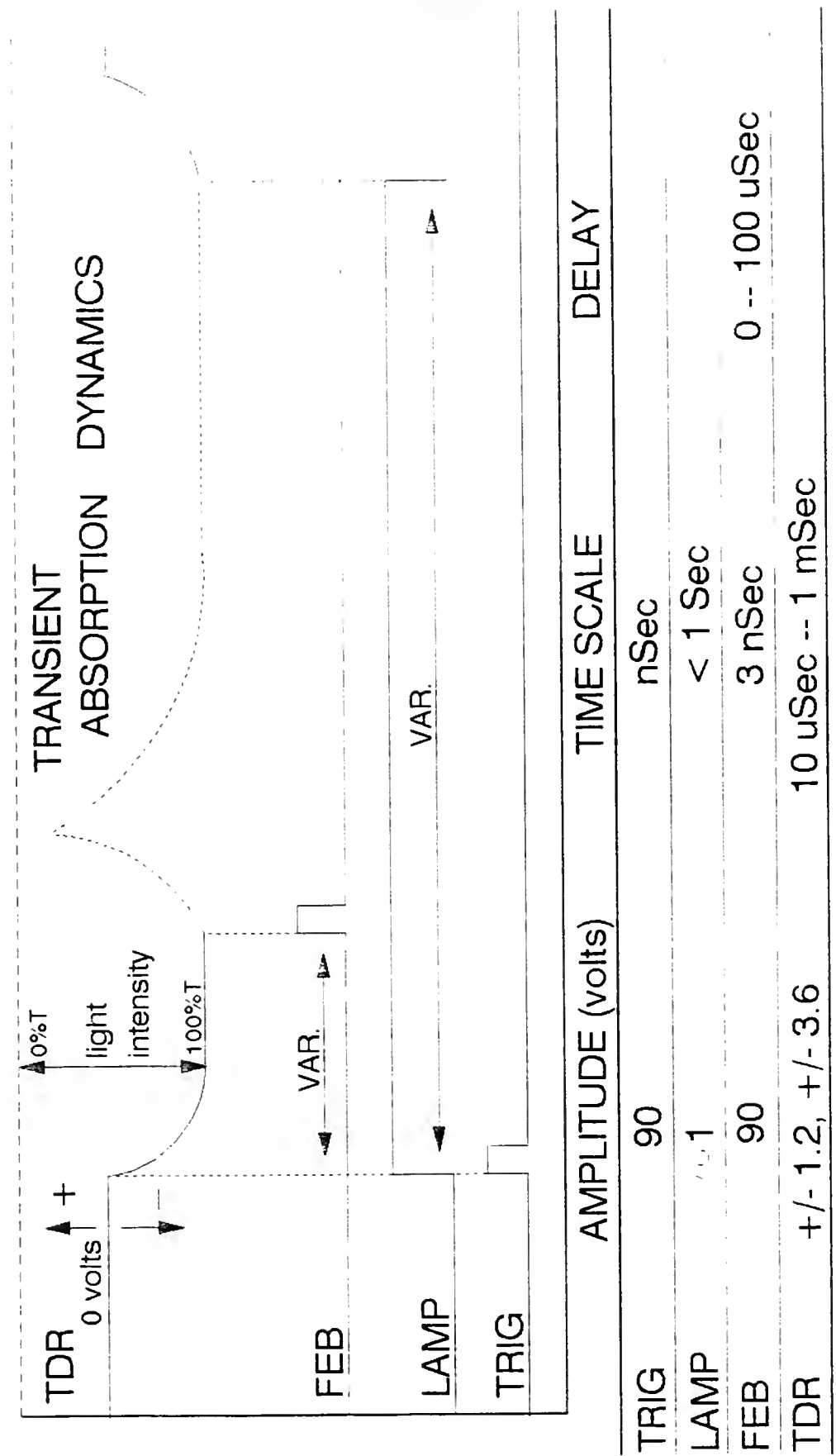


Fig. 19. Timing sequence for pulse radiolysis experiment.

for a maximum delay of 3 milliseconds. The voltage divider and amplifier in the circuit are required because the incoming trigger for the Febetron must be 90 volts in magnitude while the PTD uses a TTL type input and output. The lamp pulsing and shutter control was provided by a Vincent Associates shutter driver and timing unit, Model SD 10, which controlled a Model 225L Vincent Associates UNIBLITZ shutter. The shutter was not incorporated into the timing sequence but was manually switched on and off during a calibration procedure to set the zero and full light levels,  $V_0$  and  $V_m$  respectively. The lamp pulse duration was controlled by the shutter driver and timing unit which provides a positive going 5 volt square pulse with a variable 8 to 8,000 millisecond duration.

## 2.8 Computer Program

Full interaction between the operator and the computer/transient recorder was provided by a single BASIC program. This program, developed by J. Brogdon and R. J. Hanrahan with assistance from B. Yarborough and Brent Jones, was locally written in accordance with suggested BASIC routines provided by the DATA 6000 manufacturer.<sup>135</sup> A complete listing is provided in Appendix C. The BASIC source code was compiled from the RUN menu of Microsoft Quick BASIC version 4.0, and was executed directly from memory or from a separate executable program written to disk.

Initially, the opening menu would offer all options available, and upon full completion of any commands the main menu would again be presented. Prior to data collection the CALIBRATION command was used to set all data recording parameters and to provide a dark or no light trace, V0, and a full light trace, VM. The DATA command was entered during collection, storage, and averaging of actual traces by the DATA 6000. Upon completion of this loop three files were stored into computer memory: all digitized voltage values (QY(I)), a time dependent concentration file [QX(I), CON(I)], and a time dependent optical density file [QX(I), OD(I)]. After transfer of the data from the digitizer to the computer, the SAVE command could be executed to save a disk copy of the digitized voltage values. Using the PLOTTER command provided a graphical presentation of the digitized voltage optical trace on the computer CRT screen. Often hard copy of the graphical displays would be obtained to catalog the data.

The subroutine at line 1570 (LEFT & RIGHT BORDERS) allowed for selection of any portion of the trace followed by storage of either a concentration or optical density file corresponding to the section of the trace within the borders. The subroutine at line 3980 (LINEAR REGRESSIONS) provided linear least squares analysis of the concentration data to aid in determining the kinetics involved in the transient decays. Operation of the MANUAL command enables

adjustment for the true full light signal, VM. Even though the 100% light signal was set during the calibration steps, any fluctuation in the light during the actual data collection mode could be accounted for by taking an average of the light signal immediately preceding the pulse as an accurate measure of the true 100% light intensity. Selection of the molar absorption coefficient,  $E$ , which was dependent on the specific transient being observed was also done through the MANUAL command. The DIRECTORY command provided directory inspection to insure the storage of all files to disk and to access available memory.

## 2.9 Reagents and Sample Preparation

### 2.9.1 Sodium Tetrphenylborate and Sodium Azide

Kodak reagent-grade sodium tetrphenylborate and sodium azide were used as received.

### 2.9.2 $\text{IrCl}_6^{3-}$ (hydrate) and $\text{IrCl}_6^{2-}$

The sodium hexachloroiridate(III) hydrate and sodium hexachloridate(IV) complexes, which were obtained from Aldrich Chemical Company, were stored in a dessicator and used without purification.

### 2.9.3 Sodium Carbonate

Fisher Scientific Company-supplied  $\text{Na}_2\text{CO}_3$  was used in all the carbonate competition experiments.

#### 2.9.4 Sodium Hydroxide and Ethanol

Fisher Scientific Company-supplied NaOH and USP reagent quality 200 proof absolute  $\text{CH}_3\text{CH}_2\text{OH}$  from Florida Distillers Company were used in the hydrated electron dosimetry studies.

#### 2.9.5 Sulfuric Acid and Ferrous Ammonium Sulfate

Fisher Scientific Company  $\text{H}_2\text{SO}_4$  and  $\text{Fe}(\text{NH}_4)_2(\text{SO}_4)_2 \cdot 6\text{H}_2\text{O}$  were used as received for the Fricke dosimetry studies.

#### 2.9.6 Potassium Thiocyanate

Fisher Scientific Company KSCN was used as received for the thiocyanate dosimetry studies.

#### 2.9.7 Tert-Butyl Alcohol

Fisher Scientific Company reagent-grade  $(\text{CH}_3)_3\text{COH}$  was used as received for the hydrated electron rate-constant studies.

#### 2.9.8 Potassium Permanganate

Fisher Scientific Company reagent-grade  $\text{KMnO}_4$  and NaOH were used as received for the water distillation procedure.  $\text{KMnO}_4$  solid was dissolved in laboratory-distilled water that was made alkaline by addition of NaOH. Upon distillation, any organic impurities were removed by an oxidation reaction involving the  $\text{MnO}_4^-$  ion.

#### 2.9.9 Oxygen and Nitrogen

Liquid Air Corporation-supplied  $O_2$  and  $N_2$ , both of which were > 98% purity, were used as received for purging gases in the 'Super' Fricke studies and the hydrated electron studies, respectively.

#### 2.9.10 Nitrous Oxide

Matheson CP-grade  $N_2O$  with > 99.0% purity was used as received for generating oxidizing conditions for all studies involving the  $OH^\cdot$  radical reactions.

#### 2.9.11 Sample Preparation

Aqueous solutions were prepared by dissolving known amounts of solid reagents in doubly distilled water. A Model B5 Mettler analytical balance with 200 gram capacity and  $\pm 0.05$  milligram accuracy was used in all mass measurements. Reference spectra of the Iridium(III) chloride complex, Iridium(IV) chloride complex, and the Sodium Tetraphenylborate solution were measured using a Hewlett-Packard model 2400 UV/VIS spectrophotometer.

### 2.10 Sample Irradiation

Prior to radiolysis, solutions which were to be irradiated under oxidizing conditions were purged for approximately thirty minutes with nitrous oxide,  $N_2O$ . For work in-

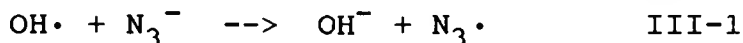
volving reducing conditions, nitrogen,  $N_2$ , was used as the purge gas. Purging of the solutions was done by introducing a disposable pipette directly into the 60 milliliter separatory funnel serving as the upper reservoir of the solution flow cell. Gas flow was maintained throughout the pulse experiments. Prior to calibrating the DATA 6000, the solution was introduced by gravity flow into the modified cuvette, which was then inserted into the aluminum cell holder. The cell holder was designed to accommodate the solution cell to give reproducible positioning and uniform irradiation in the region that was sampled by the analyzing light beam. After completing the calibration procedure, the data collection routine was executed and the Febetron was charged and triggered. Typically, due to product buildup or gas bubble evolution on the inner surface of the electron beam entrance window, a fresh aliquot was flushed into the cell and the system was recalibrated after each pulse.

CHAPTER III  
THE PULSE RADIOLYSIS OF  
SODIUM TETRAPHENYLBORATE IN AQUEOUS SOLUTION

3.1 Experimental Results

3.1.1 Oxidation Intermediates of Tetraphenylborate Ions

The pulse radiolysis of aqueous sodium tetraphenylborate (TBP) solutions under oxidizing conditions was studied with two different methods of generating the oxidizing species. As mentioned previously, using  $N_2O$ -saturated solutions the predominant oxidant produced is the  $OH\cdot$  radical generated from the direct radiolysis of water and the interconversion of  $e_{aq}^-$  to  $OH\cdot$  by  $N_2O$ . Alternatively, a secondary oxidant,  $N_3\cdot$ , is prepared under conditions of  $N_2O$ -saturation and the addition of excess sodium azide,  $NaN_3$ . The azidyl radical,  $N_3\cdot$ , is formed from the oxidation of the azide anion by the  $OH\cdot$  radical,



Both the  $N_3^-$  anion and  $N_3\cdot$  radical have absorption maxima at wavelengths  $< 280$  nm.<sup>136</sup> Experiments with  $N_3\cdot$  radical were carried out to utilize the selective electron transfer pathway of oxidation as compared to other possible reactions of the  $OH\cdot$  radical with aromatic systems, namely abstraction of an H atom and addition of the  $OH\cdot$  radical to the aromatic ring.



The pulse radiolysis of a nitrous oxide-saturated ( $\text{N}_2\text{O} \approx 2.4 \times 10^{-2} \text{ M}$ ) solution of 10 mM NaTPB was carried out at room temperature. Using the Xenon arc lamp in the pulsing mode, the transient absorption signals were recorded at various wavelengths from 300 to 800 nm. Figure 20 shows the absorption signal recorded at 330 nm for a single pulse experiment. The appearance of an incipient secondary absorption occurring approximately 20 to 30 microseconds after the initiating e-beam pulse was characteristic in all the time-concentration traces recorded in the 300-400 nm range.

A transient absorption spectrum, Figure 21, was generated by plotting the maximum absorption or "end of pulse" values as a function of the wavelength at which they were recorded. This spectrum shows an absorption maximum at 330 nm; the only other transient spectral feature is a small absorption (ca. 10% of the main peak) centered at about 750 nm. This spectrum is to be compared with that reported by Liu et al. for the radical derived by  $\text{OH}\cdot$  addition to the phenyl groups of  $\text{TPB}^-$  -- a spectrum with a large absorption at 300 nm that was reported to change only slightly over the first few microseconds.<sup>76</sup>

Assuming the absorption at 330 nm is caused by the radical derived by the addition of  $\text{OH}\cdot$  to the phenyl groups of  $\text{TPB}^-$ , its extinction coefficient at the absorption maximum of 330 nm can be calculated from the transient spectra shown in Figure 21 (a) by making use of the value for  $G(\text{OH})$  in  $\text{N}_2\text{O}$ -saturated solutions equal to 5.4 ( $= G(\text{OH}) + G(\text{e}_{\text{aq}}^-)$ ).

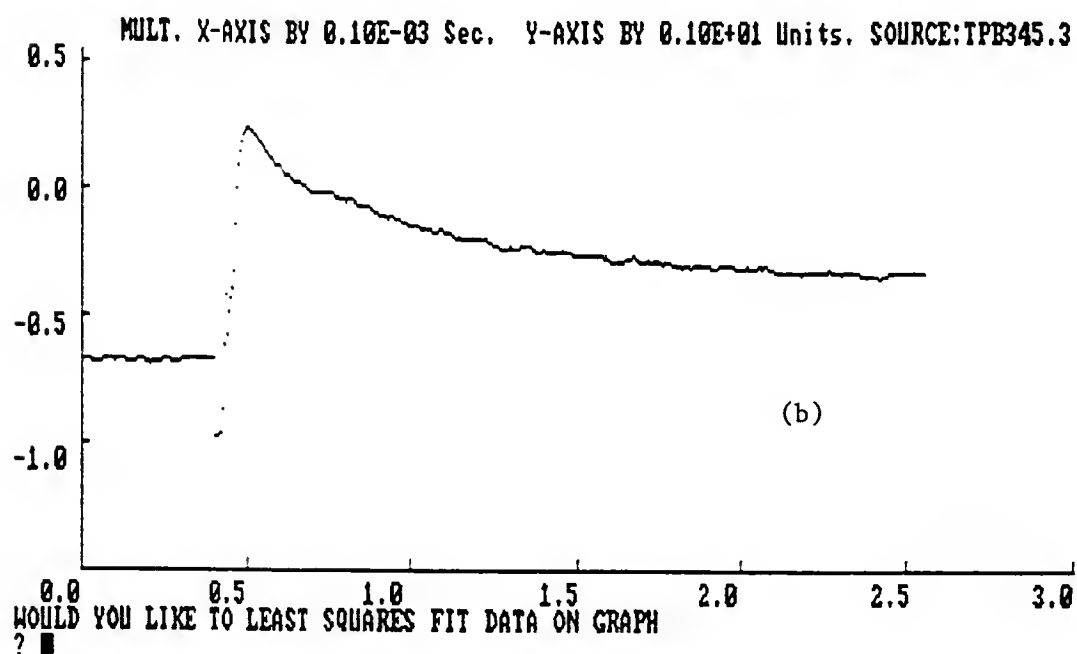
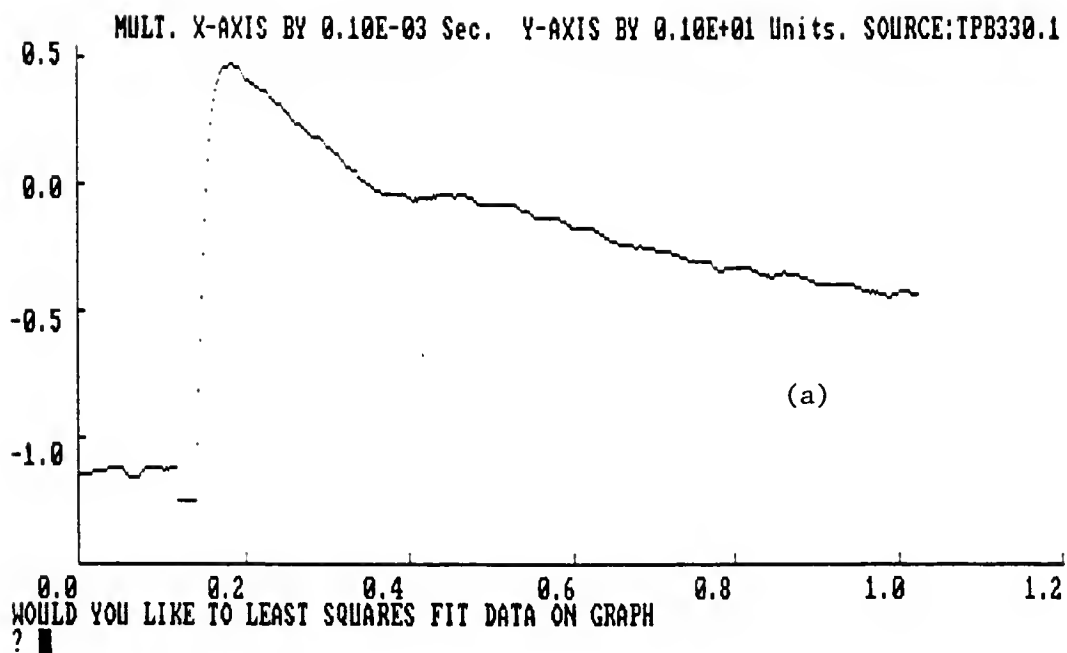


Fig. 20. Graphical displays of optical signal versus time following pulse radiolysis of  $\text{N}_2\text{O}$ -saturated 10 mM NaTPB solution. a) recorded at 330 nm, 200 nsec period, 100 usec full scale; b) recorded at 345 nm, 500 nsec period, 250 usec full scale.

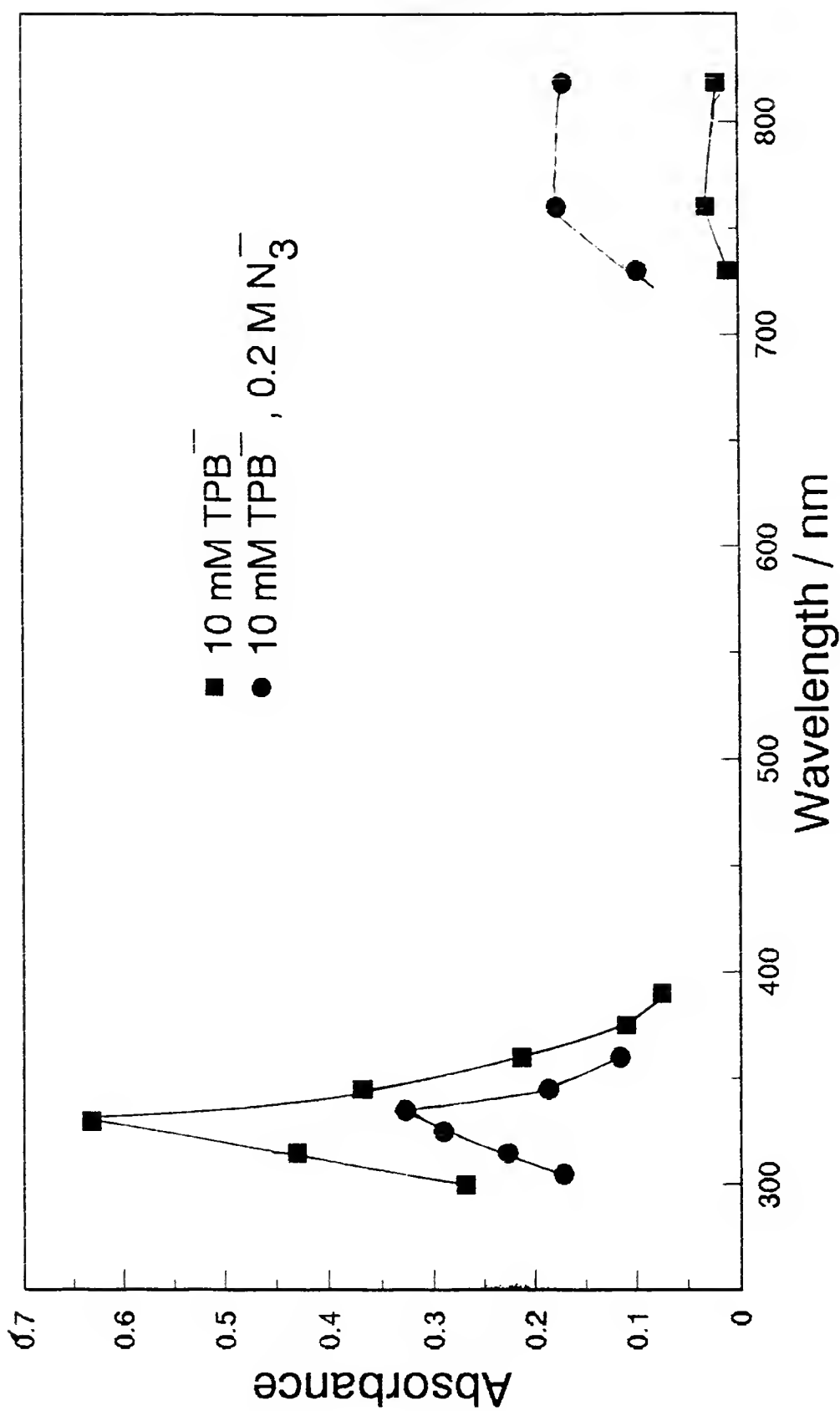


Fig. 21. Transient absorption spectra for:

a) N<sub>2</sub>O-saturated 10 mM NaTPB

b) N<sub>2</sub>O-saturated 10 mM NaTPB, 0.2 M NaN<sub>3</sub>

In  $N_2O$ -saturated  $TPB^-$  solutions, this total  $OH^\cdot$  yield of 5.4 will have been completely converted to the  $TPBOH^\cdot$  radical by the time optical measurements can be made. Thus the end of pulse optical density can be used to measure the extinction coefficient of the  $TPBOH^\cdot$  adduct. The value obtained from Figure 21 is approximately  $(10,000 \pm 10\%) M^{-1}cm^{-1}$  for the maximum peak at 330 nm.

The optical densities were calculated from the initial pre-pulse light intensity determined during calibration,  $V_f$ , and from the transmitted optical signal,  $V_t$ , using the equation

$$OD = -\log (V_t / V_f) = -\log[ (QY(I) - V_o) / V_f ] \quad III-2$$

$V_f$  is obtained from subtracting the dark signal,  $V_o$ , from the initial 100% light intensity,  $V_m$ , determined under the experimental conditions prior to irradiation and  $V_t$  is obtained from subtracting  $V_o$  from the digitized optical signal,  $QY(I)$ .

The pulse radiolysis of a  $N_2O$ -saturated solution of 10 mM NaTPB, with excess  $NaN_3 \approx 0.2 M$ , was carried out at various wavelengths yielding typical absorption traces, as shown in Figure 22. The accompanying transient absorption spectrum is plotted in Figure 21. The transient absorption traces resulting from the NaTPB with added  $NaN_3$  conditions also illustrate a secondary transient production. The

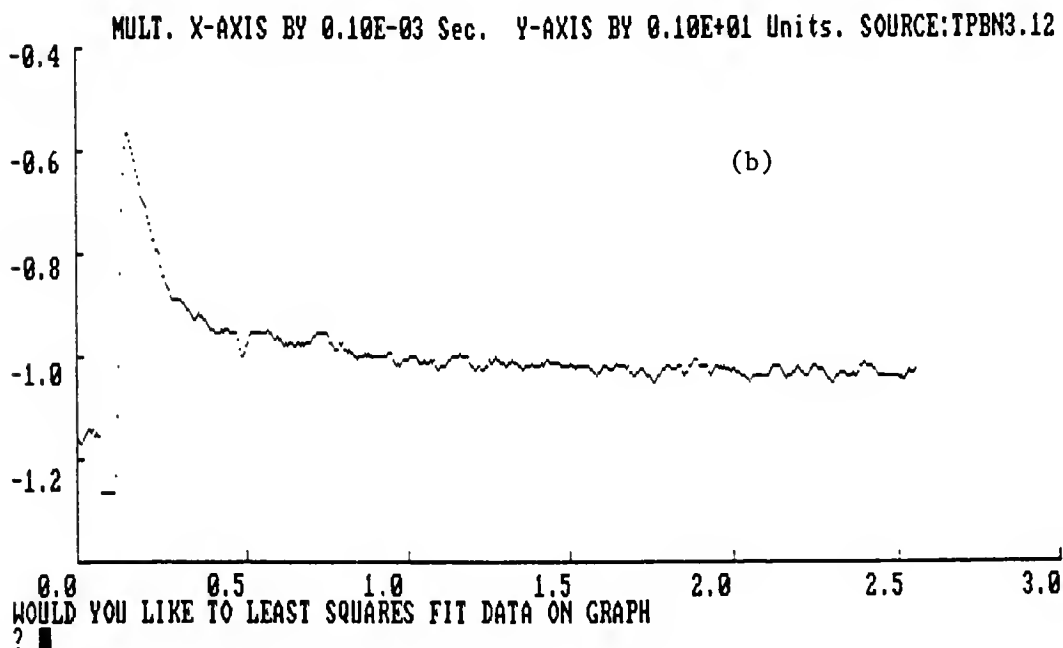
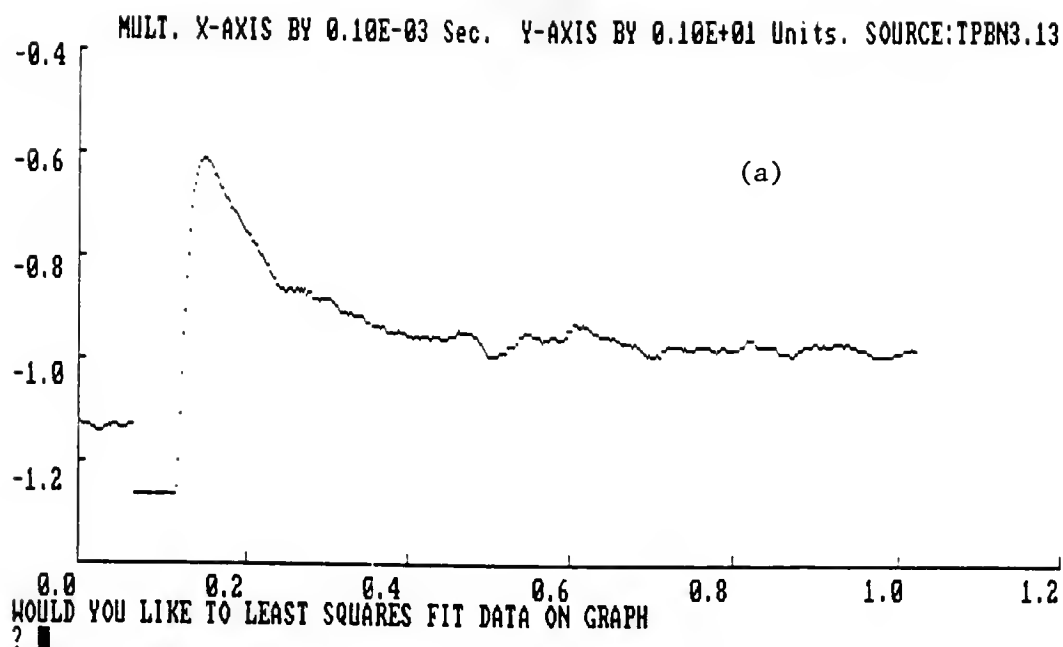


Fig. 22. Graphical display of optical signal versus time following pulse radiolysis of  $\text{N}_2\text{O}$ -saturated 10 mM NaTPB, 0.2 M  $\text{NaN}_3$  solution. a) recorded at 330 nm, 200 nsec period, 100 usec full scale; b) recorded at 330 nm, 500 nsec period, 250 usec full scale.

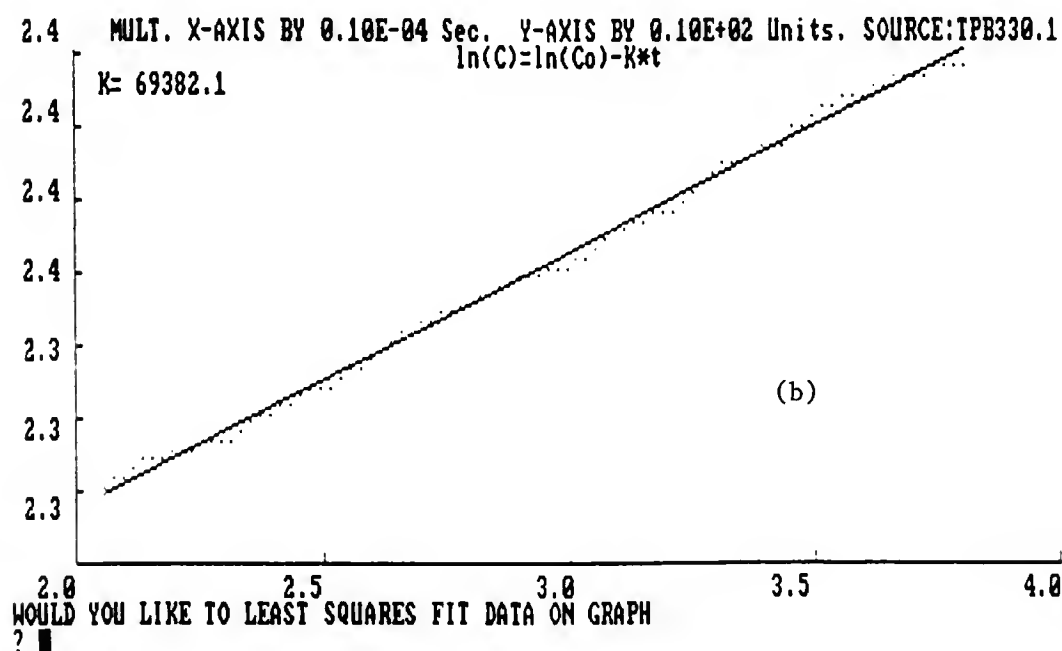
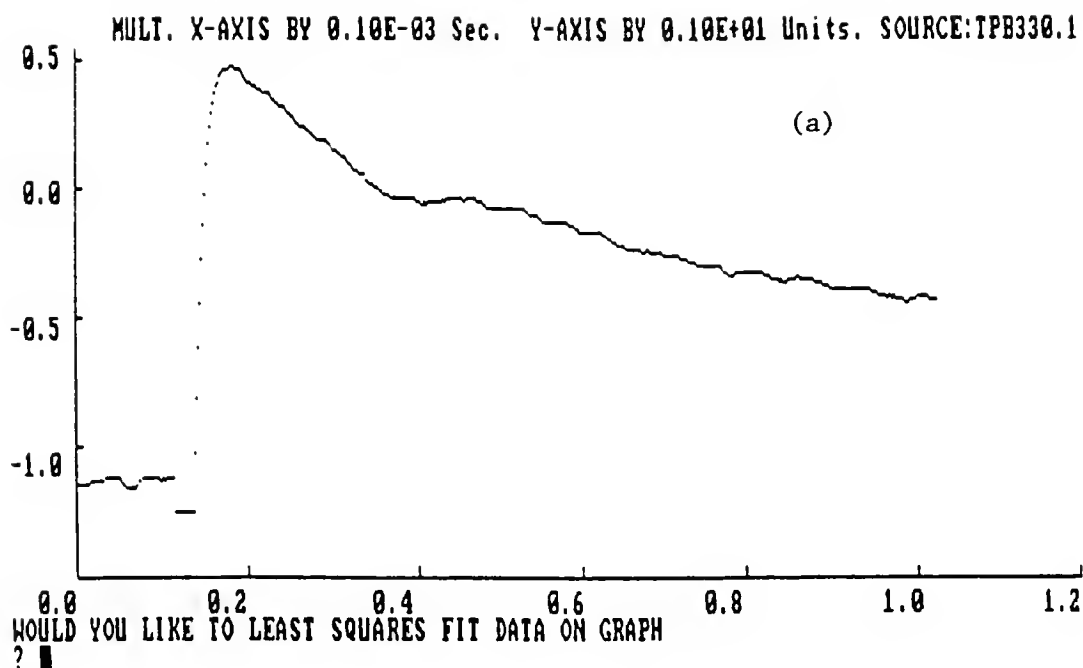
transient absorption spectrum contains two absorption bands, one at 330 nm and a broad band above 700 nm. This transient absorption spectrum as well as the associated kinetics of the 330 nm decay are in good agreement with published results obtained under similar solution conditions.<sup>75,76</sup>

### 3.1.2 Transient Kinetics

Kinetic analysis of the optical traces was carried out using a curve fitting routine from the BASIC program, and the best fit was judged from the correlation coefficient and visual inspection. Figures 23 and 24 show typical curve fits for both the initial and secondary transients produced under N<sub>2</sub>O-saturated millimolar NaTPB conditions. Analogous curve fitting was carried out on the experimental absorption traces obtained from N<sub>2</sub>O-saturated solutions of NaTPB containing excess NaN<sub>3</sub>. The resulting decay rate constants are presented in Table 2.

### 3.1.3 Carbonate Competition Method

The reaction of OH• radicals with the TPB<sup>-</sup> anion occurs too rapidly to be observed directly using the experimental conditions previously described. However, the formation rate of the OH• radical reaction with TPB<sup>-</sup> can be obtained by the carbonate competition method<sup>137</sup> using a secondary scavenger, CO<sub>3</sub><sup>2-</sup>, which competes with the TPB<sup>-</sup> anion for the OH• radical. The two competing reactions are



WOULD YOU LIKE TO LEAST SQUARES FIT DATA ON GRAPH  
 INICPT=  $2.16E+01$  (STD DEV=  $1.27E-02$ ) SLOPE=  $6.94E+04$  (STD DEV=  $4.26E+02$ )  
 R= .9983794 E= 10000 STD DEV PTS=  $2.020695E-02$

Fig. 23. Curve fit of data; a) transient trace presented from Figure 20 (a); b) First-order fitting routine applied to data between  $x = 20$  and  $x = 40$  micro-seconds.

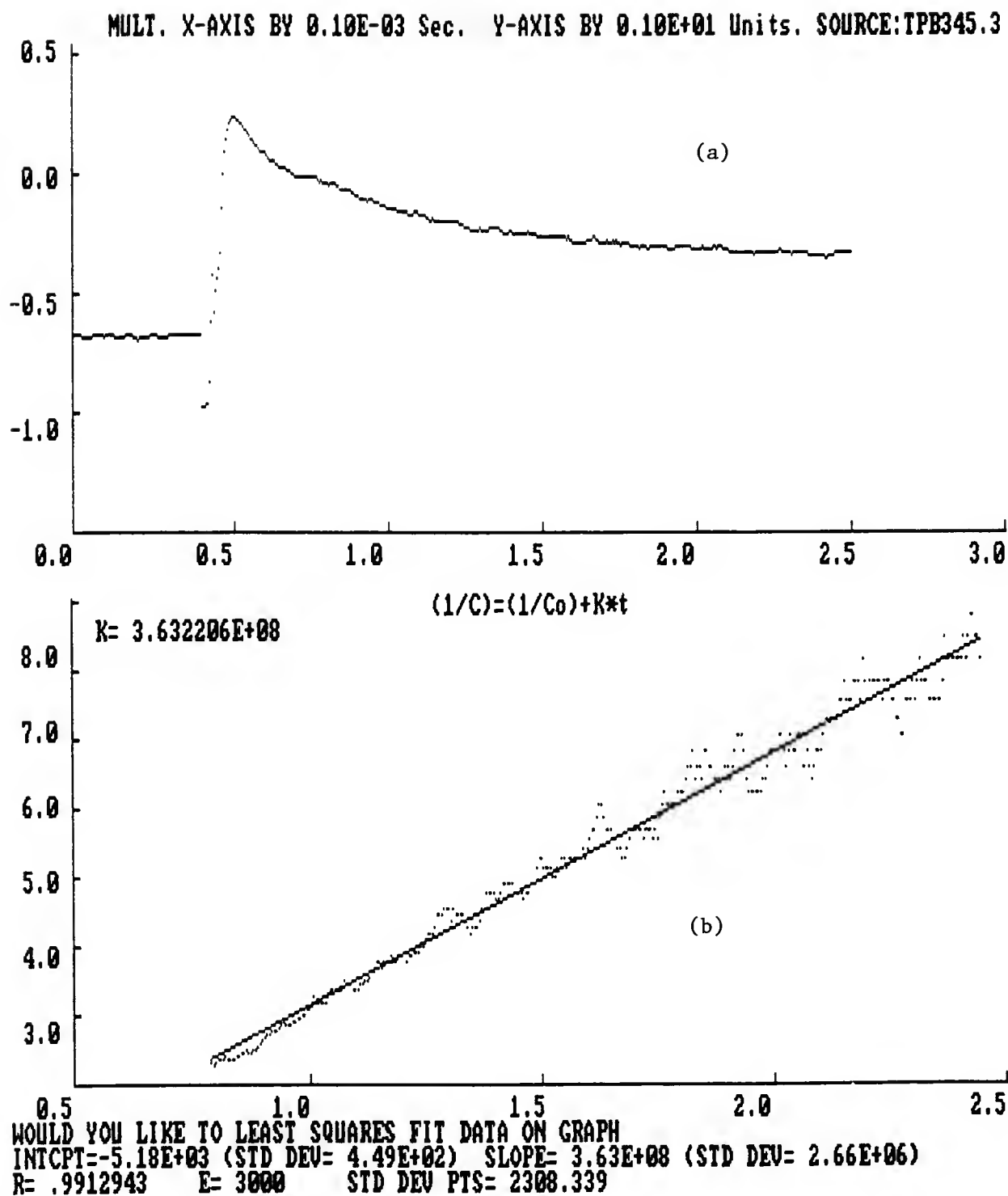


Fig. 24. Curve fit of data; a) transient trace presented from Figure 20 (b); b) Second-order fitting routine applied to data between  $x = 80$  and  $x = 250$  microseconds.

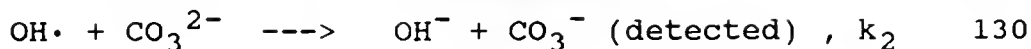
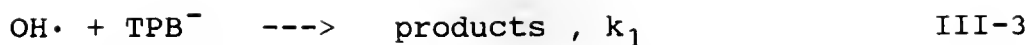


Table 2  
Transient Decay Rate Constants

N <sub>2</sub> O-saturated Solutions	Initial Transient Decay Rate Constant ( $\times 10^4 \text{ sec}^{-1}$ )	Secondary Transient Decay Rate Constant ( $\times 10^8 \text{ M}^{-1}\text{sec}^{-1}$ )
10 mM NaTPB	$5.88 \pm 0.98$	$3.76 \pm 0.42$
10 mM NaTPB 0.2 M NaN <sub>3</sub>	$8.25 \pm 0.59$	$3.10 \pm 0.91$
	a) 2	a) 4
	b) $3.9 \pm 0.2$	b) --

a) reported by Horii and Taniguchi

b) reported by Liu et al.



Using the He-Ne laser experimental setup, the  $\text{CO}_3^-$  radical anion was monitored as a function of added  $\text{TPB}^-$  anion. The  $\text{CO}_3^-$  radical anion has an extinction coefficient on the order of  $1000 \text{ M}^{-1} \text{ cm}^{-1}$ , a known formation rate constant of  $4.1 \times 10^8 \text{ M}^{-1} \text{ s}^{-1}$ , and a broad absorption band centered on 600-610 nm.<sup>138</sup> The equation representing the competition is

$$[\text{CO}_3^-]_{\text{inf.}} = \frac{k_2[\text{CO}_3^{2-}]}{k_2[\text{CO}_3^{2-}] + k_1[\text{TPB}^-]} \times [\text{OH}\cdot]_0 \quad \text{III-4}$$

with  $[\text{CO}_3^-]_{\text{inf.}}$  = end of pulse concentration of  $\text{CO}_3^-$  ion  
 $[\text{OH}\cdot]_0$  = initial concentration of  $\text{OH}\cdot$  (includes  
 primary  $\text{OH}\cdot$  from water radiolysis and  
 from interconversion of  $\text{e}_{\text{aq}}^-$  by  $\text{N}_2\text{O}$ )

Taking  $[\text{OH}\cdot]_0$  as equivalent to the  $[\text{CO}_3^-]_{\text{inf.}}$  generated with no  $\text{TPB}^-$  present, or  $[\text{CO}_3^-]_0$ , equation III-4 can be rearranged to

$$\frac{[\text{CO}_3^-]_0}{[\text{CO}_3^-]_{\text{inf.}}} = 1 + \frac{k_1[\text{TPB}^-]}{k_2[\text{CO}_3^{2-}]} \quad \text{III-5}$$

From a plot of  $[\text{CO}_3^-]_0 / [\text{CO}_3^-]_{\text{inf.}}$  versus  $[\text{TPB}^-] / [\text{CO}_3^{2-}]$ , as shown in Figure 25,  $k_1/k_2$  is found to be 15. Substitution of  $k_2$ , the  $\text{CO}_3^-$  reference formation rate constant gives a rate constant for the formation (reaction III-3 above) of the initial transient =  $(6.2 \pm 0.6) \times 10^9 \text{ M}^{-1}\text{sec}^{-1}$ .

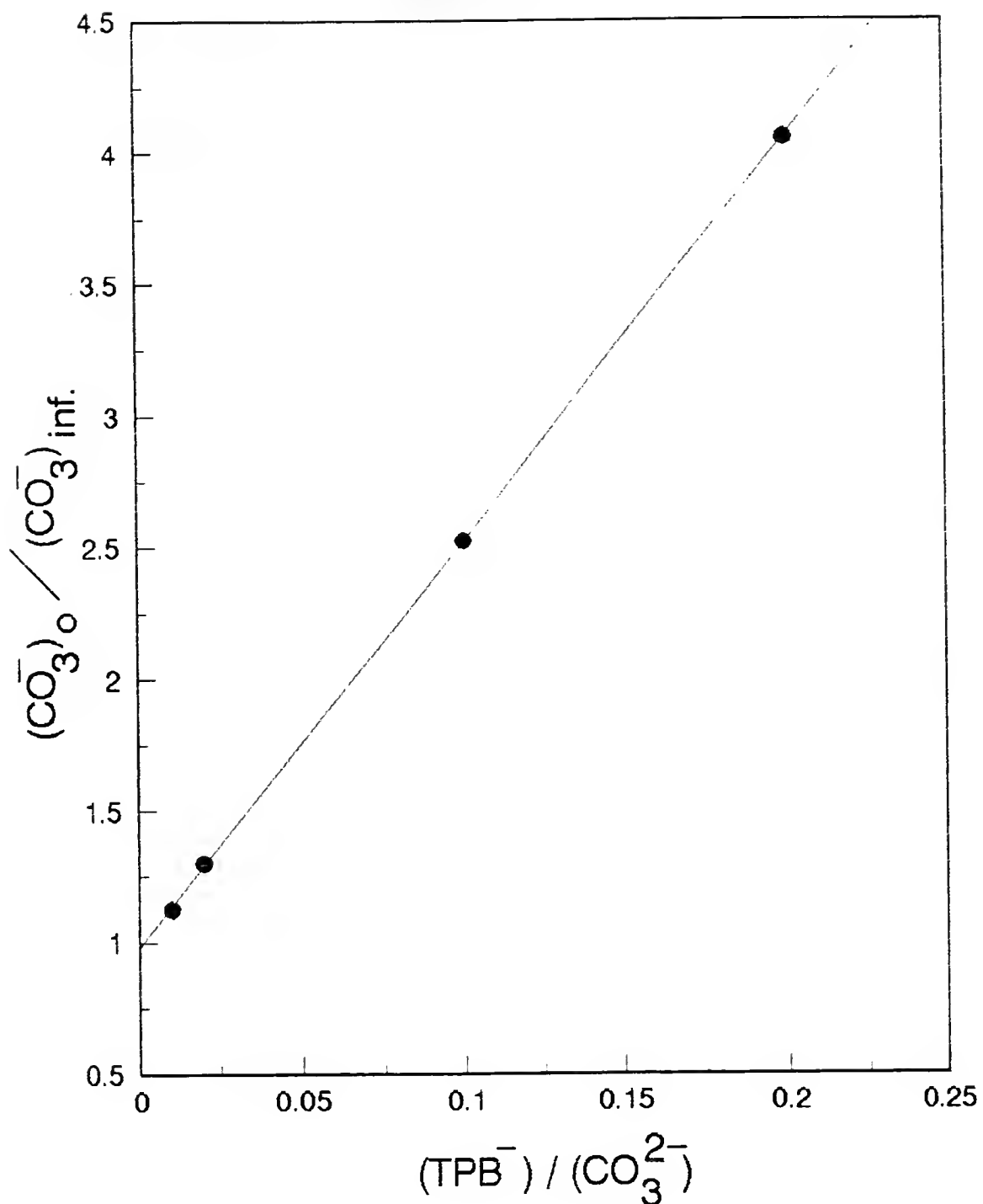


Fig. 25. Carbonate competition experiment for determining the  $\text{OH} + \text{TPB}^-$  rate constant.

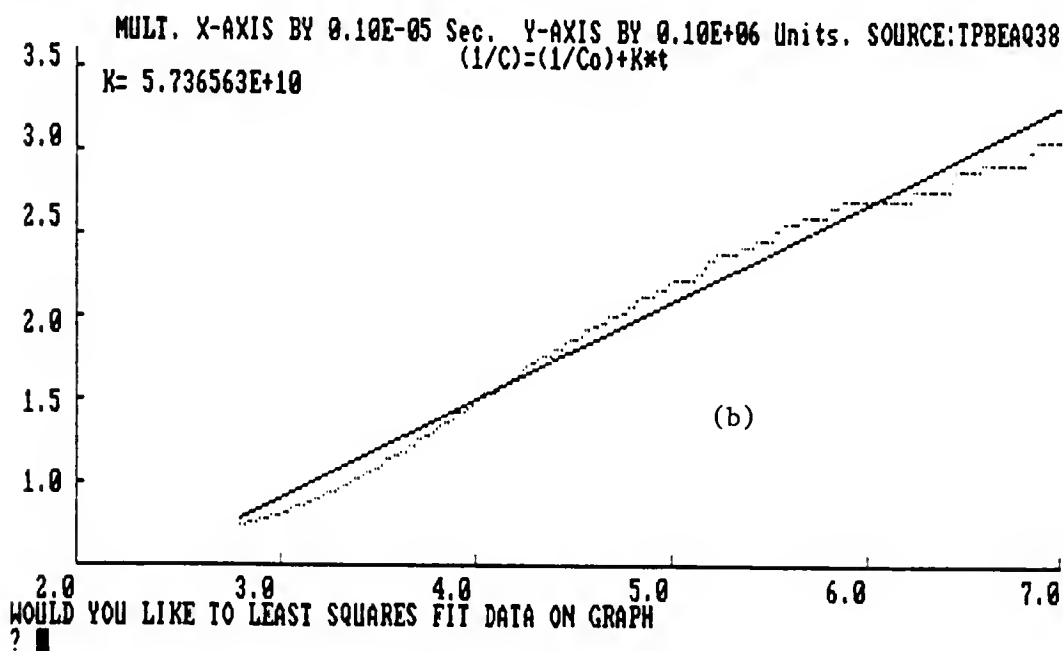
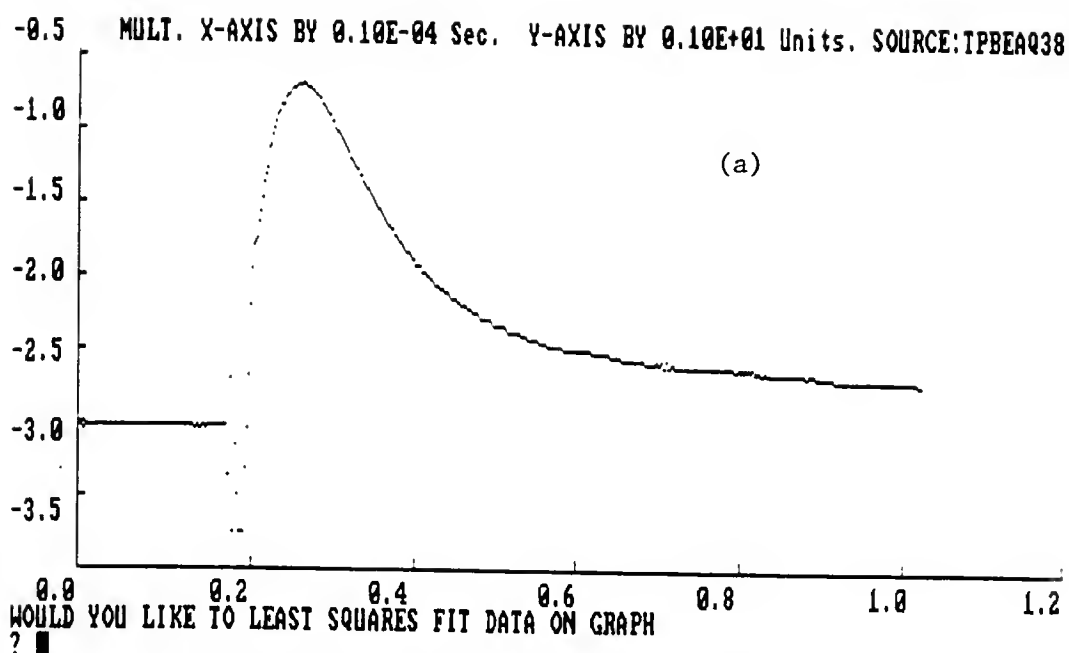
Radical formation rate constants for  $\text{TPB}^\cdot$  equal to  $1.4 \times 10^9 \text{ M}^{-1}\text{s}^{-1}$  and  $7.1 \times 10^8 \text{ M}^{-1} \text{ s}^{-1}$  have been reported for the electron transfer reaction involving  $\text{TPB}^-$  and  $\text{N}_3^\cdot$ .<sup>75,76</sup>

#### 3.1.4 Reduction Intermediates of Tetraphenylborate Ions

Pulse radiolysis experiments were performed using reducing conditions to examine the possibility of a rapid reaction between the  $\text{TPB}^-$  ion and  $e_{\text{aq}}^-$ . Because the  $\text{TPB}^-$  anion is a strong reducing agent and negatively charged, this reaction was presumed unlikely. However, by monitoring the  $e_{\text{aq}}^-$  transient signal as a function of added  $\text{TPB}^-$  any such reaction would be evinced by either a decrease in the magnitude of the end of pulse  $e_{\text{aq}}^-$  transient absorption or a change in the  $e_{\text{aq}}^-$  transient decay kinetics. A typical transient trace of the pulse experiments conducted on approximately 10 mM NaTPB solutions under reducing conditions is shown in Figure 26. The life-time of the  $e_{\text{aq}}^-$  transient was found to be approximately 8-10 microseconds with a best fit analysis giving a second order decay rate constant of  $5.7 \times 10^{10} \text{ M}^{-1}\text{s}^{-1}$ .

#### 3.1.5 Computer Simulation

Modeling calculations were utilized to help establish the detailed chemical mechanism of multi-step reactions found in aqueous pulse radiolysis systems. Differential rate equations for the suspected reaction sequence are



WOULD YOU LIKE TO LEAST SQUARES FIT DATA ON GRAPH  
 INTCPT= $-8.54\text{E}+04$  (STD DEV=  $2.85\text{E}+03$ ) SLOPE=  $5.74\text{E}+10$  (STD DEV=  $5.63\text{E}+08$ )  
 R= .9901459 E= 14860 STD DEV PTS= 9860.368

Fig. 26. a) Graphical display of optical signal versus time following pulse radiolysis of an  $\text{N}_2$ -saturated 10 mM NaTPB, 0.04 M t-butanol solution; 20 nsec period, 10 usec full scale; b) Curve fit of data between  $x = 3$  and  $x = 7$  microseconds.

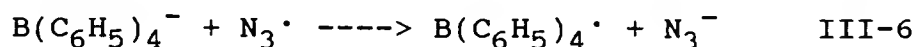
integrated to give computer-simulated time-dependent concentration profiles that are compared with those measured experimentally. These comparisons help to establish, or validate, proposed mechanisms. The computer modeling was done using a Gear integrator program.<sup>139</sup> This program, written by R. L. Brown<sup>140</sup> of NIST, was modified in this laboratory to run under Microsoft FORTRAN 77 on an MS-DOS-based microcomputer.

The input parameters to the program consist of a listing of all mechanistic steps and their rate constants (see Appendix B), the identification of all reactants with their initial concentrations, and the time-step which controls the 50 computation intervals.

### 3.2 Discussion

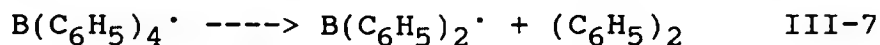
#### 3.2.1 Electron Transfer

The oxidation intermediates of TPB<sup>-</sup> ions in aqueous solutions have been examined by Horii and Taniguchi,<sup>75</sup> and Liu et al.<sup>76</sup> From their results with N<sub>2</sub>O-saturated solutions of NaTPB and NaN<sub>3</sub>, the proposed route to the formation of several major products is a rapid electron transfer from B(C<sub>6</sub>H<sub>5</sub>)<sub>4</sub><sup>-</sup> to N<sub>3</sub><sup>•</sup> yielding the B(C<sub>6</sub>H<sub>5</sub>)<sub>4</sub><sup>•</sup> radical and N<sub>3</sub><sup>-</sup>, or



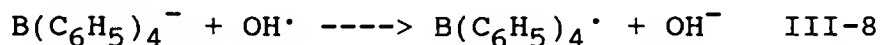
As shown earlier the azidyl radical, N<sub>3</sub><sup>•</sup>, is produced initially from primary OH radical reaction with N<sub>3</sub><sup>-</sup>, reaction

III-1. The transient absorbing at 330 nm and 800 nm (Figure 21) is attributed to the  $B(C_6H_5)_4^\cdot$  radical. Both peaks decay with the same first-order rate constant, indicating that they represent different absorbances of the same transient species.<sup>76</sup> Loss of the 330 nm peak is attributed to a rapid self-decomposition first-order decay, producing a second transient that undergoes a relatively slower decay. Horii and Taniguchi proposed the reaction,<sup>75</sup>



The secondarily-produced transient  $B(C_6H_5)_2^\cdot$  was suggested to disappear following second-order kinetics, although no product species were discussed.<sup>75</sup>

The pulse results from our oxidation experiments on TPB solutions containing no added  $N_3^-$  anion could be interpreted as above, i.e. a rapid electron transfer from  $B(C_6H_5)_4^-$  to  $OH^\cdot$ , instead of  $N_3^\cdot$ , or

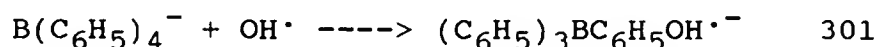


yielding the  $B(C_6H_5)_4^\cdot$  radical. As shown in Table 2, the decay kinetics of the transients produced with and without added  $N_3^-$  are similar, that is a rapid, first-order decay followed by a secondary transient decay. However, comparison of the transient spectra, Figure 21, suggests that two different transients are formed. With added azide, the transient spectral feature at 750 - 800 nm is about 70% of

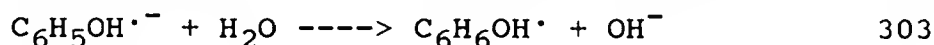
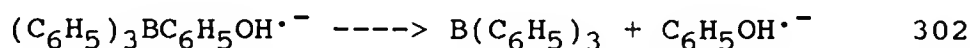
the magnitude of the main peak centered at 330 nm. With no added azide, the transient spectral feature at 750 - 800 nm is < 10% of the magnitude of the main peak centered at 330 nm.

### 3.2.2 OH Addition

An alternate mechanism to the electron transfer from  $\text{TPB}^-$  to  $\text{OH}^\bullet$ , as described above, is the addition of the  $\text{OH}^\bullet$  radical to the aromatic ring, which would lead to an  $\text{OH}^\bullet$  adduct transient species different from the  $\text{TPB}^\bullet$  radical, or



The following self-decomposition first-order decay scheme has been considered for the observed loss of this  $\text{OH}^\bullet$  addition adduct.

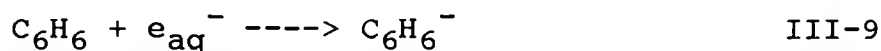


Triphenylborate and its hydrolysis products,  $(\text{C}_6\text{H}_5)\text{B}(\text{OH})_2$  and  $(\text{C}_6\text{H}_5)_2\text{BOH}$ , all have absorptions at wavelengths below 300 nm.<sup>74</sup> The secondarily-produced transient  $\text{C}_6\text{H}_5\text{OH}^{\bullet-}$ , is suggested to undergo a rapid hydrolysis, yielding the hydroxycyclohexadienyl radical  $\text{C}_6\text{H}_6\text{OH}^\bullet$ . The hydrolysis of  $\text{C}_6\text{H}_5\text{OH}^{\bullet-}$  has been reported in a previous aqueous phenol pulse radiolysis study.<sup>141</sup> In neutral solutions a slow reaction between the solvated electron,  $e_{\text{aq}}^-$ , and phenol



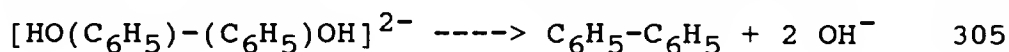
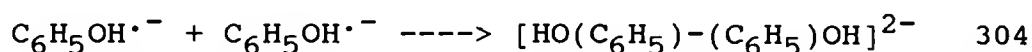
that forms  $\text{C}_6\text{H}_5\text{OH}^{\cdot-}$  was reported. The radical anion,  $\text{C}_6\text{H}_5\text{OH}^{\cdot-}$ , subsequently undergoes rapid protonation by  $\text{H}_2\text{O}$  to yield  $(\text{C}_6\text{H}_5)(\text{OH})\text{H}^{\cdot}$ . This species is a structural isomer of the hydroxycyclohexadienyl radical,  $\text{C}_6\text{H}_6\text{OH}^{\cdot}$ . A molar extinction coefficient of  $(3800 \pm 800) \text{ M}^{-1} \text{ cm}^{-1}$  at a wavelength maximum of 330 nm was assigned to the  $(\text{C}_6\text{H}_5)(\text{OH})\text{H}^{\cdot}$  radical.

Another possible competing reaction pathway for the  $\text{C}_6\text{H}_5\text{OH}^{\cdot-}$  radical anion would be a bimolecular radical anion reaction. The bimolecular disappearance of negatively charged radical species has been previously suggested in pulse radiolysis studies involving the reaction of the hydrated electron,  $e_{\text{aq}}^-$ , with benzene.<sup>58</sup> In this aqueous benzene study,  $\text{C}_6\text{H}_6^-$ , the addition product of  $e_{\text{aq}}^-$  and benzene, was reported to decay via a rapid bimolecular process before protonation in solutions of pH neutral to 13.



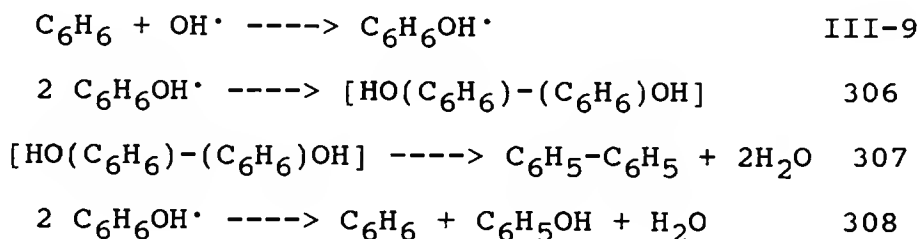
No specific products of the radical anion reaction, III-10, were discussed.

In the present study, concerning the combination reaction of  $\text{C}_6\text{H}_5\text{OH}^{\cdot-}$ , a possible reaction forming a charged dimer species, with subsequent formation of biphenyl and hydroxide ion, is proposed below



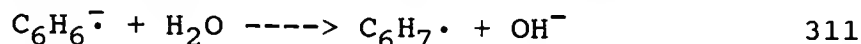
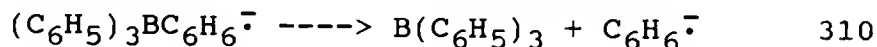
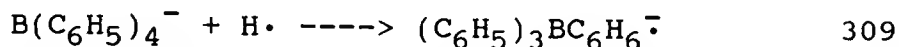
The scheme involving radical combination leading to an intermediate dimer is prominent in the mechanism involving the radiolysis of aqueous benzene, discussed below.

The hydroxycyclohexadienyl radical,  $C_6H_6OH^\cdot$ , mentioned above (reaction 303), is an important intermediate in the formation of major products in the radiolysis of aqueous benzene solutions; the results of which are in good agreement with the end products derived from Co-60 steady-state  $\gamma$ -radiolysis of NaTPB solutions carried out in this lab.<sup>86</sup> The proposed mechanism concerning the benzene oxidation<sup>55,64,65</sup> is described as

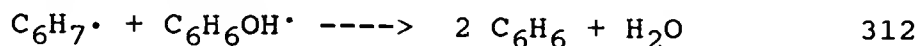


The hydroxycyclohexadienyl radical,  $C_6H_6OH^\cdot$ , has a reported absorption maxima at 313 nm.<sup>58</sup> The combined bimolecular rate constant for its disappearance via reactions 306 and 308 has been determined to be  $(7.05 \pm 0.35) \times 10^8 \text{ M}^{-1}\text{s}^{-1}$ .<sup>58</sup> The disproportionation to combination ratio for the disappearance of  $C_6H_6OH^\cdot$  was found to be  $< 0.4$ , indicating that the combination reaction 306 is predominant.<sup>63</sup> The major products produced are biphenyl, benzene and phenol. In the Co-60  $\gamma$ -radiolysis of aerated 0.05 M sodium tetraphenylborate solutions the products and their G-values were found to be biphenyl, 1.9; benzene, 1.3; and phenol, 0.41.<sup>68</sup>

It is also reasonable to expect the  $H\cdot$  atom to add to  $TPB^-$  ion, giving a transient species that decomposes via a two-step process giving the cyclohexadienyl radical



The  $(C_6H_5)_3BC_6H_6^-$  transient has been proposed by Liu et al. as the weakly absorbing species at higher wavelengths (Figure 21) in the pulse radiolysis of  $TPB^-$  solutions without added azide.<sup>76</sup> The cyclohexadienyl radical could also react with the hydroxycyclohexadienyl radical in a bimolecular process producing benzene<sup>56</sup>



Concerning the reduction of  $TPB^-$ , a rapid reaction between  $e_{aq}^-$  and  $TPB^-$  appears to be negligible from the results of the NaTPB pulse radiolysis under reducing conditions. Comparison of Figure 26 with  $e_{aq}^-$  traces found in the hydrated electron dosimetry experiments, Appendix A, shows little difference in either the magnitude or kinetic behavior of the  $e_{aq}^-$  transient signal. The  $e_{aq}^-$  transient signal decayed with a second order rate constant of  $5.7 \times 10^{10} M^{-1}s^{-1}$  with added  $TPB^-$ ; for the  $e_{aq}^-$  dosimetry experiments, the  $e_{aq}^-$  signal exhibited a second-order decay =  $4.4 \times 10^{10} M^{-1}s^{-1}$ .

### 3.2.3 Computer Simulations

Computer simulations were carried out with a Gear integrator utilizing the data set consisting of the elementary reaction steps describing the transients of irradiated pure water (Appendix B). The mechanistic scheme also includes reactions of  $e_{aq}^-$  with  $N_2O$ , and  $OH^\cdot$  with  $TPB^-$ .

Figure 27 illustrates typical results of the simulated calculations for conditions involving  $N_2O$ -saturated solutions containing 10 mM  $TPB^-$ . Time-concentration profiles for all species in the system are predicted over the ca. 200 microsecond data collection time period. Experimental data points indicate the observed decay of the transient trace produced in a typical experimental run, recorded at 330 nm (Figure 20 (b)). These experimental data points represent the combined absorbance of all the components in the system contributing to the absorption trace at 330 nm. Dotted lines show predicted yields of the various individual transients formed. The solid line represents the combined concentrations of the following intermediates; the initial  $OH^\cdot$  adduct  $(C_6H_5)_3BC_6H_5OH^\cdot$  with a molar extinction coefficient of  $10,000\text{ M}^{-1}\text{ cm}^{-1}$ , the radical anion  $C_6H_5OH^\cdot$  and the hydroxycyclohexadienyl radical  $C_6H_6OH^\cdot$  with molar extinction coefficients of  $3800\text{ M}^{-1}\text{ cm}^{-1}$ , and the intermediate dimers,  $[HO(C_6H_6)-(C_6H_6)OH]$  and  $[HO(C_6H_5)-(C_6H_5)OH]^{2-}$  with molar extinction coefficients of  $7,500\text{ M}^{-1}\text{ cm}^{-1}$ .

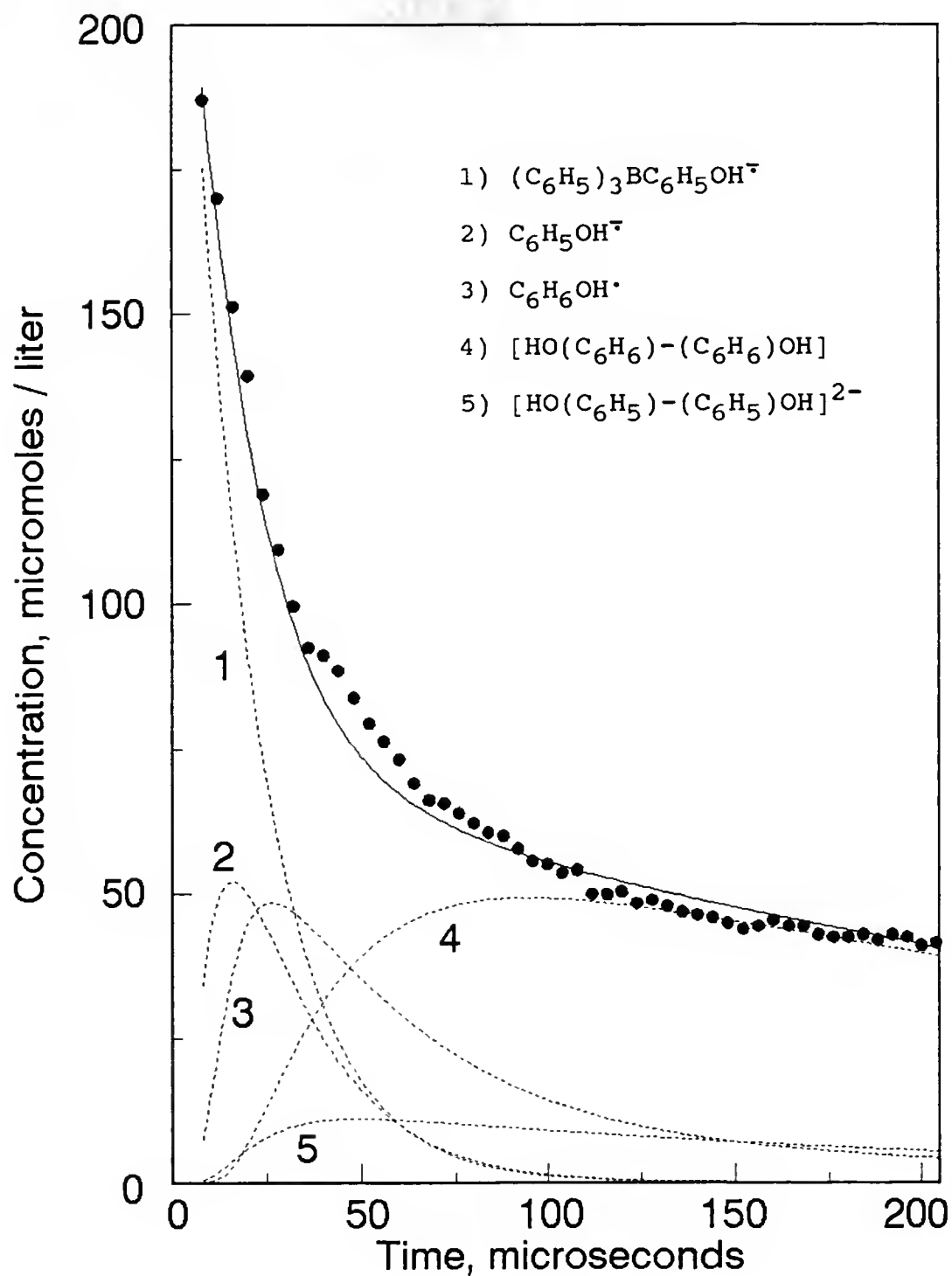


Fig. 27. Comparison of experimental and computer-simulated transient concentrations versus time plots during the pulse radiolysis of a 10 mM NaTPB solution;  
 (—) summation of individual transients;  
 (·) typical experimental results;  
 (---) computed individual transient traces.

### 3.3 Conclusions

Results obtained in this work lead to the conclusion that the identity of the transient species, absorbing upon pulse radiolysis of  $N_2O$ -saturated NaTPB solutions, is very much dependent on the nature of the oxidizing species produced in the system. The aqueous azide NaTPB solution experiments presented here, taken together with the results of others,<sup>75,76</sup> indicate that the one electron oxidation product of  $TPB^-$ , the  $TPB^\bullet$  radical, is the species that absorbs at 330 and 775 nm.

However, experiments in aqueous NaTPB solutions without added azide indicate formation of a different transient species, proposed to be the  $OH^\bullet$  adduct of  $TPB^-$ , or  $(C_6H_5)_3B(C_6H_5)OH^\bullet$ . This  $OH^\bullet$  addition product exhibits a strong absorption at 330 nm. A weak absorption at 750 nm constitutes approximately 10% of the magnitude of the main 330 nm peak. As mentioned earlier, this weak absorbance could be due to the  $H^\bullet$  addition product of  $TPB^-$ , since the addition of  $H^\bullet$  to aromatic systems with resonating  $\pi$ -bond systems has been observed. Alternatively, the weak 750 nm absorption could be indicative of the  $TPB^\bullet$  radical product formation, which would indicate that the one electron transfer mechanism occurs to a small extent in the  $N_2O$ -saturated TPB solutions without added azide.

The present study provides information regarding the fate of the  $TPBOH^\bullet$  adduct immediately following its forma-

tion, whereas the previous account mentioned only alluded to the TPBOH<sup>-</sup> adduct transient absorption spectrum.<sup>76</sup> Kinetic analysis of this transient species indicates that it undergoes a rapid first-order disappearance within the first 20 microseconds that is suggested to be a self-decomposition. It is presumed that this initial transient loss leads to the observed secondary absorption, which was found to decay on a longer timescale by second order decay kinetics.

A primary interest in this work was to establish a plausible reaction mechanism involving the radiolysis of TPB solutions. Evidence obtained from the pulse radiolysis experiments has lead to the formulation of a scheme that can explain the production of various organic products such as biphenyl, benzene, and phenol, reported from previous steady-state radiolysis studies on aqueous aerated TPB solutions sealed from the atmosphere.<sup>68</sup> For further validation of the mechanism presented in this study for the pulse radiolysis conditions, one could perform numerical integration of the scheme for both the pulse and steady-state radiolysis systems under equivalent solution conditions. Initial attempts to carry out this work have been encouraging.

CHAPTER IV  
THE PULSE RADIOLYSIS OF IRIDIUM HEXACHLOROIRIDATE  
IN AQUEOUS SOLUTION

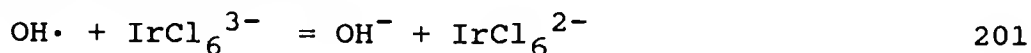
4.1 Results

4.1.1 Absorption Spectra

Initial experiments performed with the  $\text{IrCl}_6^{3-}$  and  $\text{IrCl}_6^{2-}$  ions involved measurement of the aqueous solution absorption spectra of these complexes. These absorption spectra, Figure 28, of millimolar aqueous solutions of the  $\text{IrCl}_6^{3-}$  and  $\text{IrCl}_6^{2-}$  complex ions were in agreement with the results of other authors.<sup>111,142</sup> Between 400 and 500 nm,  $\text{IrCl}_6^{2-}$  has a characteristic spectrum with an absorption maximum at 488 nm (extinction coefficient ca. 4000). In contrast, the  $\text{IrCl}_6^{3-}$  complex has no appreciable absorption in this wavelength range. Thus all pulse absorption data were recorded at 488 nm.

4.1.2  $\text{N}_2\text{O}$ -Saturated Iridium(III) Solutions

The reaction of  $\text{OH}\cdot$  radicals with  $\text{IrCl}_6^{3-}$  occurs too rapidly to be observed directly under our experimental conditions. A method involving competition kinetics, the carbonate competition method described earlier, was used to determine the rate constant for the reaction





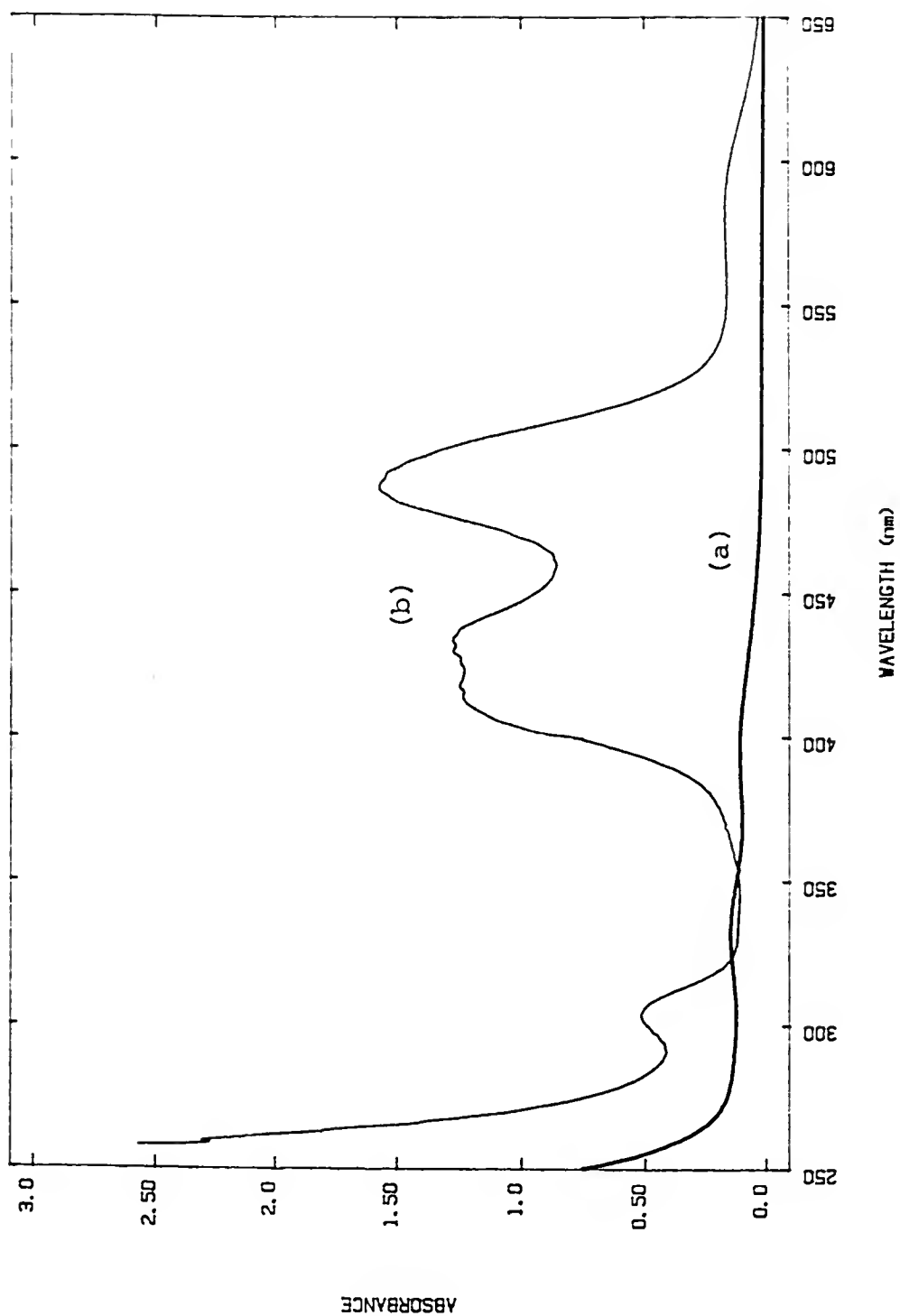
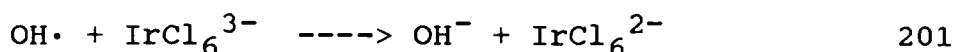
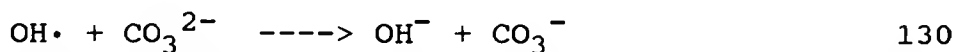


Fig. 28. UV-VIS spectra of:  
a) 1 mM  $\text{IrCl}_6^{3-}$ ; b) 0.5 mM  $\text{IrCl}_6^{2-}$

A series of experiments was performed using N<sub>2</sub>O-saturated solutions containing, typically,  $1 \times 10^{-3}$  M IrCl<sub>6</sub><sup>3-</sup> and various amounts of CO<sub>3</sub><sup>2-</sup> from 2 to  $14 \times 10^{-3}$  M. Under these conditions the hydrated electron, e<sub>aq</sub><sup>-</sup>, is converted to OH•. The equations representing the competition are



The end-of-pulse Ir(IV) absorption, Ir(IV)<sub>0</sub>, was first monitored for a millimolar solution of Ir(III) to obtain the maximum Ir(IV) produced, i.e. without any added CO<sub>3</sub><sup>2-</sup>. The end-of-pulse Ir(IV) absorption, Ir(IV)<sub>inf.</sub>, was then obtained for a series of solutions with added CO<sub>3</sub><sup>2-</sup>. A plot, Figure 29, of [Ir(IV)<sub>0</sub>]/[Ir(IV)<sub>inf.</sub>] versus the added CO<sub>3</sub><sup>2-</sup> concentration yields a slope,  $k_{130}/(k_{201}[\text{Ir(III)}])$ , equal to 85 M<sup>-1</sup>. Substitution of the Ir(III) concentration of 1 mM and  $k_{130} = 4.1 \times 10^8$  into the slope expression above gives a rate constant for reaction 130 above, equal to  $(4.9 \pm 0.6) \times 10^9 \text{ M}^{-1}\text{s}^{-1}$ . Broszkiewicz measured a somewhat higher value of  $8.9 \times 10^9 \text{ M}^{-1}\text{s}^{-1}$  for this reaction.<sup>111</sup> However, the lower value gives satisfactory results in the computer simulation studies.

In all the experiments on the pulse radiolysis of CO<sub>3</sub><sup>2-</sup>/IrCl<sub>6</sub><sup>3-</sup> solutions, using concentrations of IrCl<sub>6</sub><sup>3-</sup> of  $1 \times 10^{-3}$  M and concentrations of CO<sub>3</sub><sup>2-</sup> from 2 to  $14 \times 10^{-3}$  M,

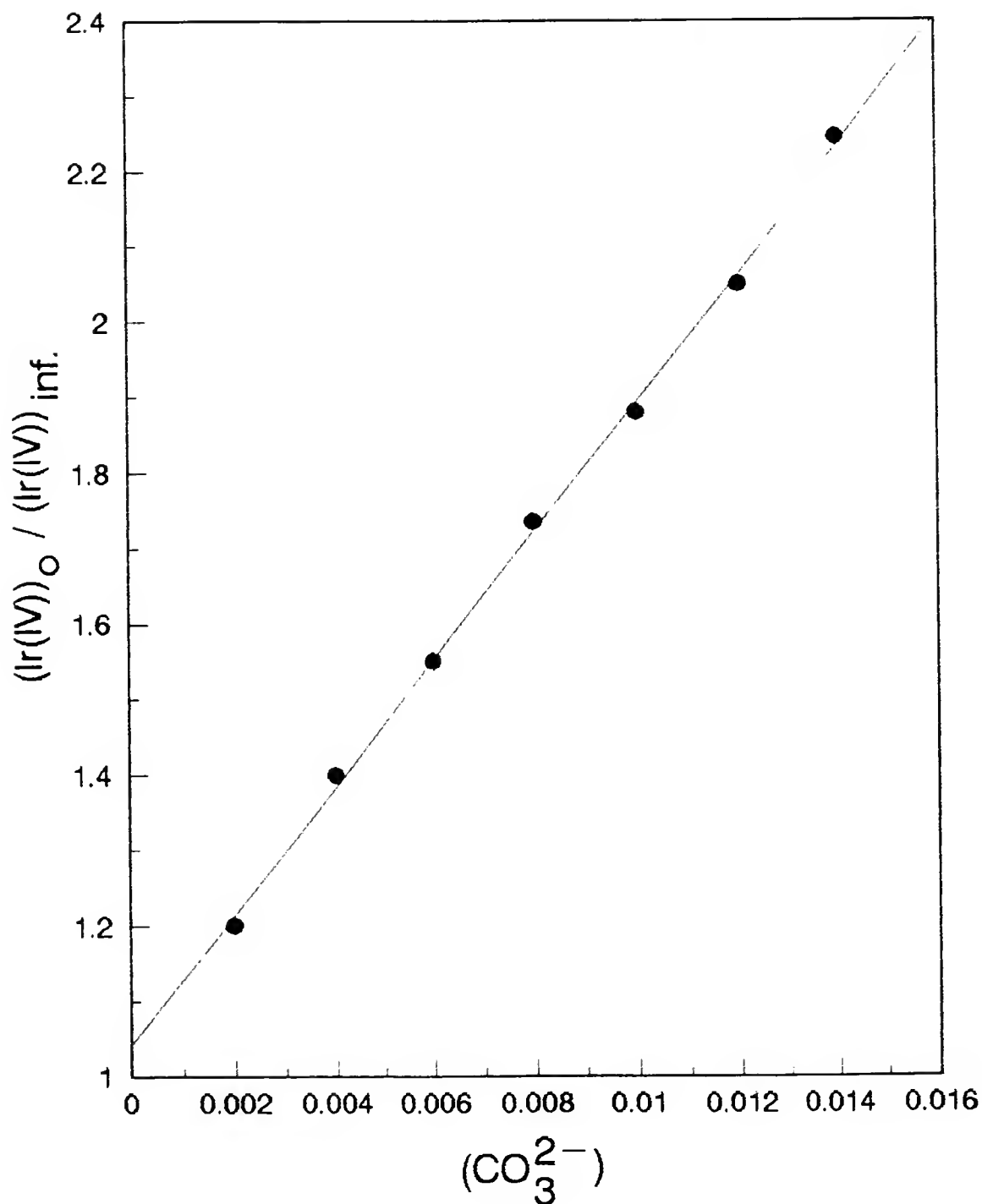
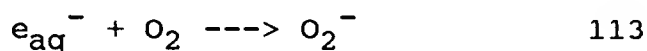


Fig. 29. Carbonate competition experiment for the determination of the  $\text{OH} + \text{Ir(IV)}$  rate constant.

the product,  $\text{IrCl}_6^{2-}$ , disappears rather rapidly as shown in Figure 30 (a). If the decay is fitted as a simple second-order process in  $\text{IrCl}_6^{2-}$ , an apparent rate constant of  $4 \times 10^7 \text{ M}^{-1}\text{s}^{-1}$  is obtained. However, loss of the Ir(IV) via a bimolecular disproportionation reaction is not reasonable mechanistically. An interpretation of the cause of the decay of the  $\text{IrCl}_6^{2-}$  optical signal in these experiments is discussed below. Interestingly, as seen in Figure 30 (b), the product iridium (IV) complex is almost inert, or stable over approximately 400 microseconds, when the experiment is performed with added  $\text{N}_2\text{O}$  using a neutral medium, i.e. with no added NaOH or  $\text{Na}_2\text{CO}_3$ .

#### 4.1.3 Nitrogen and Air-saturated Ir(III) Solutions

Experiments were performed on the pulse radiolysis of both nitrogen and air-saturated Ir(III) aqueous solutions to further investigate the reactivity of the Ir(IV) species. Using  $\text{N}_2$ -saturated solutions, roughly equal amounts of the reducing and oxidizing species,  $e_{\text{aq}}^-$  and  $\text{OH}\cdot$  respectively, are produced. The  $\text{N}_2$ -saturation purges all dissolved atmospheric oxygen, an efficient electron scavenger, from the solution, thus eliminating the reaction



In the pulse radiolysis of air-saturated solutions, which contain  $\text{O}_2$  at 0.25 mM, the superoxide anion,  $\text{O}_2^-$ , plays an important role<sup>40</sup> due to its formation from the reaction

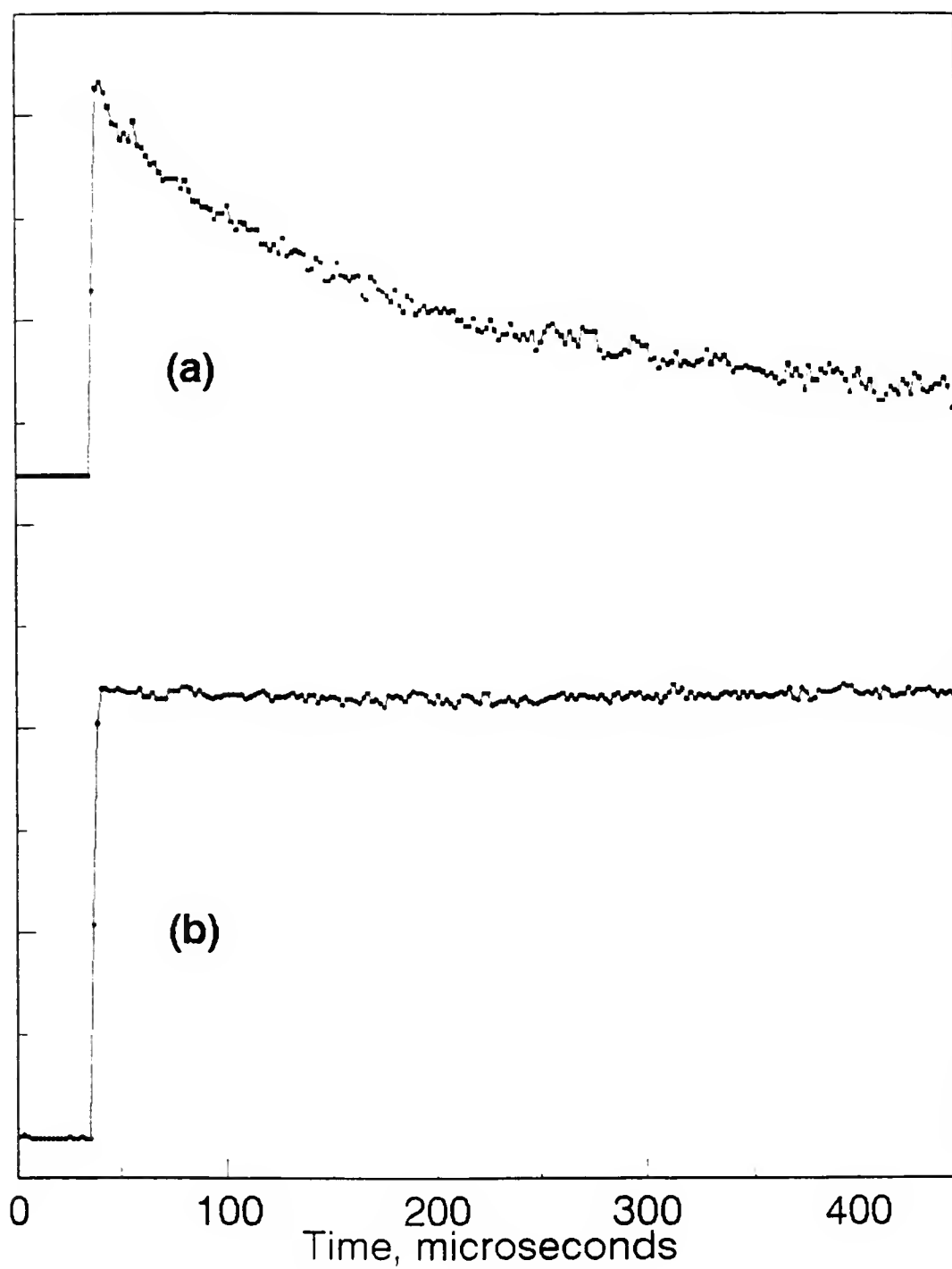


Fig. 30. Graphical display of  $\text{IrCl}_6^{2-}$  optical signal versus time following pulse radiolysis of  $\text{N}_2\text{O}$ -saturated solutions of (a) 1 mM  $\text{IrCl}_6^{3-}$  and 5 mM  $\text{CO}_3^{2-}$ ; (b) 1 mM  $\text{IrCl}_6^{3-}$ .

above, and the reaction

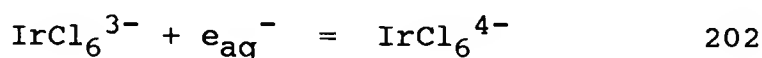


With a pK of 4.88 for  $\text{HO}_2$ ,  $\text{O}_2^-$  is the predominant species above pH = 5. The perhydroxyl radical,  $\text{HO}_2^\cdot$ , or  $\text{O}_2^-$  in basic media, can act as an oxidizing or reducing agent depending on the solute present.

The transient Ir(IV) oxidation product was found to be unstable in both  $\text{N}_2$ - and air-saturated solutions, as shown in Figure 31. The spectra of Ir(IV) disappeared rapidly in the  $\text{N}_2$ -saturated solutions with a second-order rate constant of  $5 \times 10^8 \text{ M}^{-1}\text{s}^{-1}$  and moderately rapid with a second-order rate constant of  $1 \times 10^7$  in the case of air-saturated solutions. These rate constants establish the time-scale of the phenomena. Additionally, since concentrations of the oxidizing and reducing reactants (originating from OH and  $e_{\text{aq}}^-$  respectively) are expected to be nearly equivalent, the rate constants should correctly describe the actual reactions.

#### 4.1.4 Reduction of Ir(III)

The rate constant for the reduction of the  $\text{IrCl}_6^{3-}$  complex



was obtained by applying pseudo-first-order kinetics.

Formation of the hydrated electron in water was observed

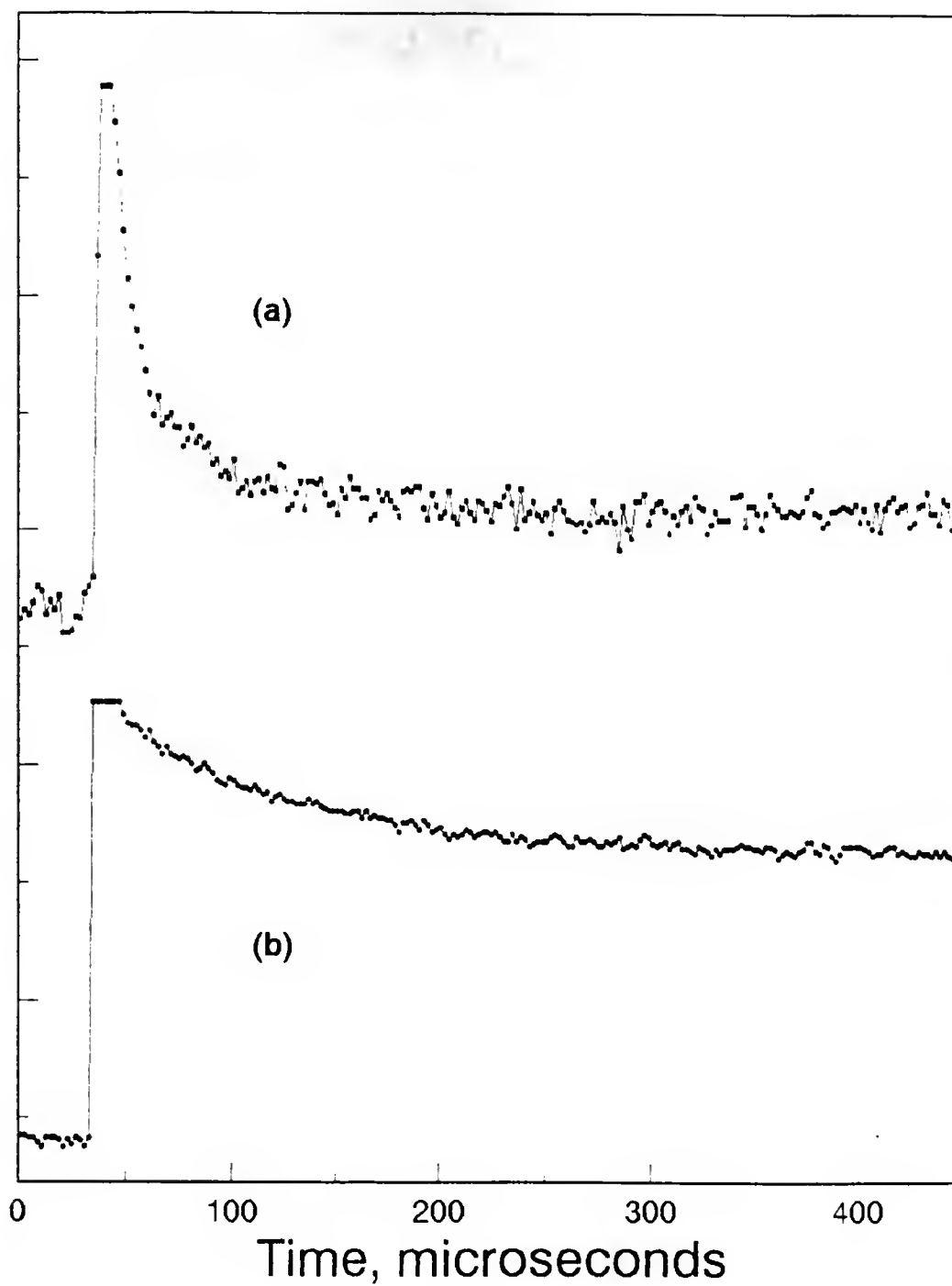


Fig. 31. Graphical display of  $\text{IrCl}_6^{2-}$  optical signal versus time following pulse radiolysis of neutral 1 mM  $\text{IrCl}_6^{3-}$  solutions saturated with (a)  $\text{N}_2$ ; (b) air.

using a 50 MHz sampling rate with our transient digitizer and its decay was followed at 632.8 nm. The rate expression for reaction 202 above is

$$-d[e_{aq}^-]/dt = k_{202} [Ir(III)] [e_{aq}^-] \quad IV-1$$

By making the concentration of Ir(III) high compared to the expected concentration of  $e_{aq}^-$ ,  $k_{202} [Ir(III)]$  is treated as a constant and the rate expression reduces to

$$-d[e_{aq}^-]/dt = k' [e_{aq}^-] \quad IV-2$$

where  $k' = k_{202} [Ir(III)]$ . Expression IV-2 is a first-order rate expression. The first-order decay rate constant for  $e_{aq}^-$ ,  $k'$ , was determined using the appropriate fit routine in the BASIC data analysis program found in Appendix C. These first-order rate constants for the  $e_{aq}^-$  decay were determined and plotted versus the concentration of added Ir(III) complex, Figure 32. The nitrogen-saturated solutions were made 0.1 M in t-Butanol to remove  $OH\cdot$  radicals. The value for the rate constant corresponding to reaction 202 above was found to be  $(6.1 \pm 0.3) \times 10^9 \text{ M}^{-1}\text{s}^{-1}$ .

#### 4.2 Discussion

The results presented above agree in general respects with those of Broszkiewicz;  $OH\cdot$  radicals react rapidly with  $IrCl_6^{3-}$  to produce the (IV) oxidation state of iridium via reaction 201 (Table 5). Our measured rate constant is



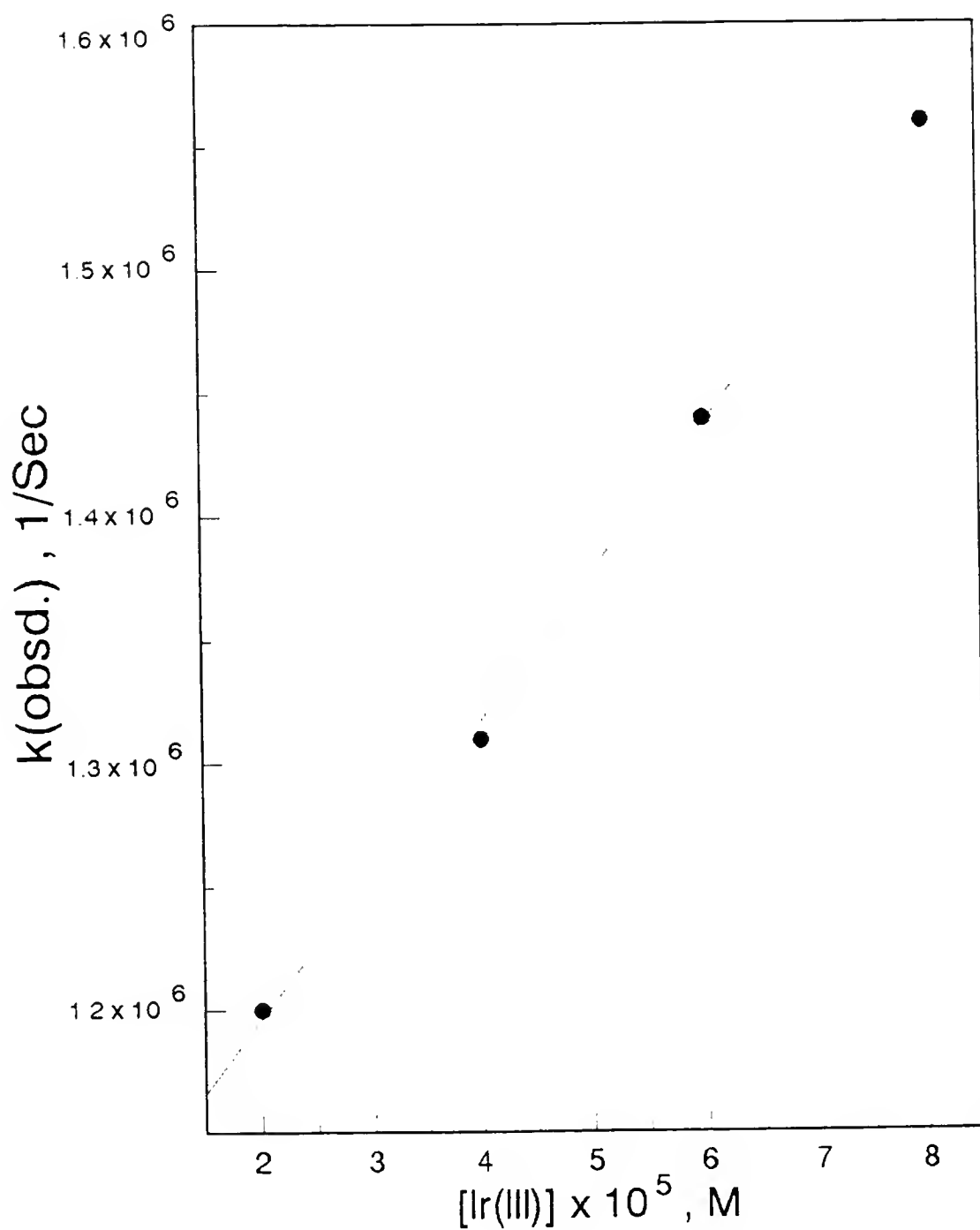


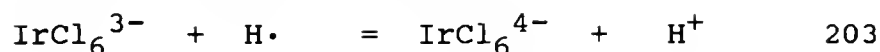
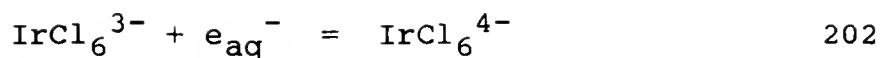
Fig. 32. Change in first-order decay of the hydrated electron with  $\text{IrCl}_6^{3-}$  concentration.

slower than that seen by Broszkiewicz, as mentioned earlier. Broszkiewicz also noted that  $\text{IrCl}_6^{2-}$  is "stable within the period of ca. 0.5 ms, though its relative instability, when compared with solutions of  $\text{IrCl}_6^{2-}$  as prepared from solid salt indicates that radiation produces either an active form of  $\text{IrCl}_6^{2-}$  of higher reactivity towards water, or a system in which this compound is more readily reduced."<sup>111</sup> In addition, Broszkiewicz reported that  $\text{IrCl}_6^{2-}$  is not capable of being further oxidized by any primary radiolysis product, but that it is capable of being reduced within a few microseconds.

In agreement with the earlier work mentioned,<sup>111</sup> it was found that the  $\text{IrCl}_6^{2-}$  species is stable when formed in neutral solutions saturated with  $\text{N}_2\text{O}$ , which converts  $e_{\text{aq}}^-$  to  $\text{OH}\cdot$  radical. In contrast, however, the  $\text{Ir(IV)}$  complex is rather short-lived under our circumstances in either of three conditions: 1) when formed in a neutral  $\text{N}_2$ -saturated solution, 2) when formed in an air-saturated solution in the absence of  $\text{N}_2\text{O}$  (i.e., with both  $e_{\text{aq}}^-$  and  $\text{OH}\cdot$  transients present, and 3) when formed in an alkaline,  $\text{N}_2\text{O}$ -saturated solution.

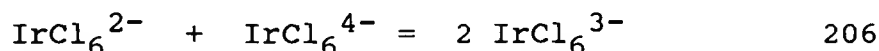
#### 4.2.1 Loss of Iridium (IV) in Nitrogen-Saturated Solutions

As noted in the earlier work,<sup>111</sup> iridium (III) is readily reduced to iridium (II) by either hydrated electrons via reaction 202 or by hydrogen atoms via reaction 203



Our measured rate constant for the reduction of  $\text{IrCl}_6^{3-}$  by reaction 202 is in good agreement with earlier reported values.<sup>110,111</sup>

Broszkiewicz suggested that the oxidation state (II) compound disappears rapidly via disproportionation to Ir(III) and Ir(I). While no evidence was found contrary to this possibility, an alternate suggestion is discussed below.  $\text{N}_2$ -saturated solutions pulse-irradiated in the absence of  $\text{N}_2\text{O}$  contained Ir(II) formed by reactions 202 and 203. In addition, Ir(IV) formed from reaction 201 was produced under these conditions. Thus it is suggested that under these circumstances, the most likely route of disappearance of Ir(II) is an electron transfer involving Ir(IV)



Interestingly, this reaction was proposed by Dainton<sup>108</sup> in connection with steady-state radiolysis of iridium (III) systems at natural pH, as studied by endproduct analysis.

#### 4.2.2 Loss of Iridium (IV) in Aerated Solutions

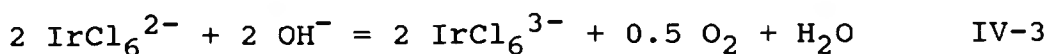
Air-saturated solutions showed a similar decay of the  $\text{IrCl}_6^{4-}$  absorption, although to a lesser extent than the  $\text{N}_2$ -saturated solutions. However, in the aerated solutions

millimolar concentrations of dissolved  $O_2$  (an effective  $e_{aq}^-$  scavenger) were in competition with Ir(III) for  $e_{aq}^-$  and  $H\cdot$  atoms. Thus only a portion of the  $H\cdot$  atom and  $e_{aq}^-$  yields reacted via processes 202 and 203. The superoxide anion,  $O_2^-$ , formed from reactions 113 and 117, can act as either an oxidant or reductant depending on the solute present. The  $IrCl_6^{2-}$  complex has a standard reduction potential,  $E^0$ , = +1.02 V.<sup>143</sup> Thus the  $O_2^-$  anion, with a standard reduction potential of -0.33,<sup>143</sup> is identified as the reductant of  $IrCl_6^{2-}$  in the aerated system.

#### 4.2.3 Loss of Iridium (IV) in Basic, $N_2O$ -Saturated Solutions

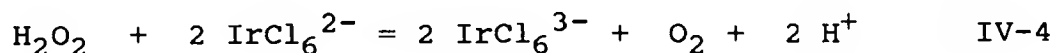
As indicated previously, our experimental conditions differ somewhat from those used by Broszkiewicz in that there exists a much higher instantaneous concentration of  $OH\cdot$  radicals leading to net formation of  $H_2O_2$ . As suggested by Broszkiewicz, there is no obvious method to oxidize the iridium (IV) compound, but its disappearance by reduction is a clear possibility. For this disappearance to occur, it is necessary that some other component in the solution be oxidizable. After elimination of all other obvious possibilities, it was concluded that the only plausible reductant is hydrogen peroxide, or actually the  $HO_2^-$  anion in basic solution.

As noted by several workers,<sup>144-146</sup> iridium (IV) chloride will ultimately decompose in alkaline aqueous solution, with formation of hydrated species. However, this process requires hundreds of hours and is far too slow to be relevant to our pulse radiolysis conditions. Fine<sup>147</sup> reports a rapid and quantitative reduction of iridium (IV) chloride in aqueous solutions at pH > 11 as a necessary preliminary step to any subsequent hydroxylation reactions. In concentrated alkaline solution and in the absence of other reducing agents, a reaction with hydroxide ion was suggested by Fine<sup>147</sup>



However, in view of the rate constants reported by Fine, this reaction is too slow to explain our results obtained at the pH values of our solutions (pH ca. 10). It was confirmed by simple benchtop experiments that the decay of the characteristic  $\text{IrCl}_6^{2-}$  spectrum in millimolar alkaline solution is very slow.

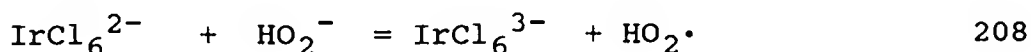
Dainton<sup>108</sup> proposed that iridium (IV) is capable of oxidizing hydrogen peroxide according to the net reaction



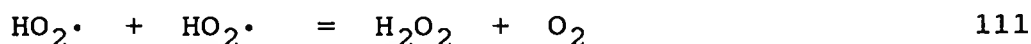
This reaction has also been mentioned by Waltz and Adamson.<sup>101</sup> However, it was found in the present study that the reaction of  $\text{H}_2\text{O}_2$  with  $\text{IrCl}_6^{2-}$  in neutral solution is

only moderately rapid, requiring typically ten to fifteen minutes to produce a substantial color change in neutral, millimolar solutions of each reagent.

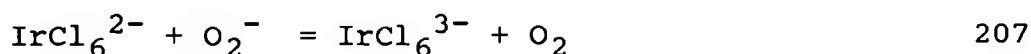
In contrast with the above observations, it was found that if millimolar solutions of  $\text{H}_2\text{O}_2$  and  $\text{IrCl}_6^{2-}$  were suddenly also made ca. 1 millimolar in  $\text{OH}^-$  by adding three drops of 0.1 molar NaOH to 20 ml. of solution, the color change indicating transformation of Ir (IV) to Ir (III) was essentially instantaneous; that is, the color changed as rapidly as the solution could be mixed by swirling. These results suggest that the redox process that causes a destruction of the  $\text{IrCl}_6^{2-}$  optical signal in the experiments mentioned above, involves the peroxide anion



The peroxide anion,  $\text{HO}_2^-$ , can act as either an oxidant or reductant depending on the solute present. As mentioned earlier, the  $\text{IrCl}_6^{2-}$  complex has a standard reduction potential,  $E^0$ , = +1.02 V.<sup>142</sup> Thus the  $\text{HO}_2^-$  anion, with a standard reduction potential of -0.15 V,<sup>143</sup> is attributed as the reductant of  $\text{IrCl}_6^{2-}$  for the conditions described above. The hydroperoxy free radical is consumed by several subsequent processes, in particular



Also, in solutions of  $\text{pH} > 5$ ,  $\text{HO}_2\cdot$  is converted into the reducing species  $\text{O}_2^-$  which could also contribute to the loss of the  $\text{IrCl}_6^{2-}$  optical signal



Reaction 208 was confirmed directly by stopped-flow experiments using a Durrum Model 110 instrument with a Nicolet digital oscilloscope. A rate constant of approximately  $1 \times 10^6 \text{ M}^{-1}\text{s}^{-1}$  was found for this process. Since the time response of the stopped-flow apparatus is limited by a finite mixing time, this value may represent a lower limit on the rate constant. Computer simulations of our pulse radiolysis data indicate a rate constant of  $4.7 \times 10^8 \text{ M}^{-1}\text{s}^{-1}$  for this reaction.

#### 4.2.4 Computer Simulations

The consistency of the above postulates has been examined by carrying out computer simulations with a Gear integrator utilizing the data set consisting of the elementary reaction steps describing transients of irradiated pure water (Appendix B). The mechanistic scheme also includes reactions of  $\text{e}_{\text{aq}}^-$  with  $\text{N}_2\text{O}$  and with  $\text{IrCl}_6^{3-}$ , and of  $\text{OH}\cdot$  radical with  $\text{IrCl}_6^{3-}$ , or with  $\text{CO}_3^{2-}$  (if present).

Figure 33 shows a typical result of the simulation calculations for conditions involving  $5 \times 10^{-3} \text{ M}$  carbonate,  $2.5 \times 10^{-2} \text{ M}$   $\text{N}_2\text{O}$ , and  $1 \times 10^{-3} \text{ M}$   $\text{IrCl}_6^{3-}$ . Experimental data

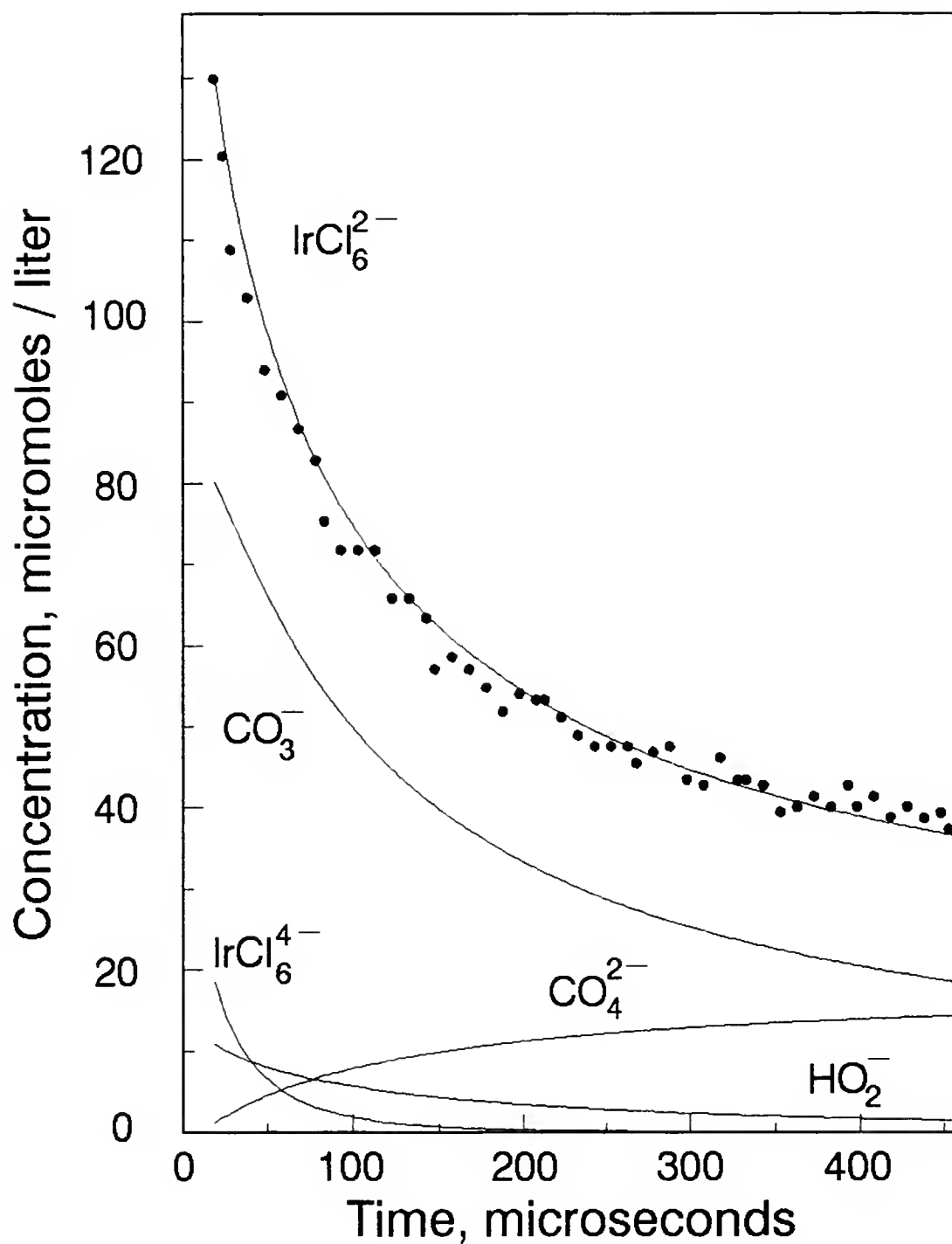


Fig. 33. Comparison of experimental and computer-simulated  $\text{IrCl}_6^{2-}$  concentration versus time plots during the pulse radiolysis of a  $\text{N}_2\text{O}$ -saturated solution containing 1 mM  $\text{IrCl}_6^{3-}$  and 5 mM  $\text{Na}_2\text{CO}_3$ . (—) computed; (•) typical experimental results.



points showing formation and decay of the  $\text{IrCl}_6^{2-}$  transient in a typical run are indicated. The Gear integrator predicts time-concentration behavior of all species in the system; the figure also illustrates predicted yields of  $\text{CO}_3^-$ ,  $\text{CO}_4^{2-}$ ,  $\text{IrCl}_6^{2-}$ ,  $\text{IrCl}_6^{4-}$  and  $\text{HO}_2^-$ .

Further simulation calculations for conditions involving  $1 \times 10^{-3}$  M  $\text{IrCl}_6^{3-}$  solutions saturated with air, and nitrogen are presented in Figures 34 and 35 respectively. It will be seen that the agreement between measured and predicted behavior for  $\text{IrCl}_6^{2-}$  is reasonable but not perfect for the various solution conditions.

The results of simulated calculations performed for all solution conditions mentioned previously are presented in Figure 36. These concentration-versus-time profiles are to be compared with the experimental digitized optical traces of the  $\text{IrCl}_6^{2-}$  species shown in Figures 30 and 31.

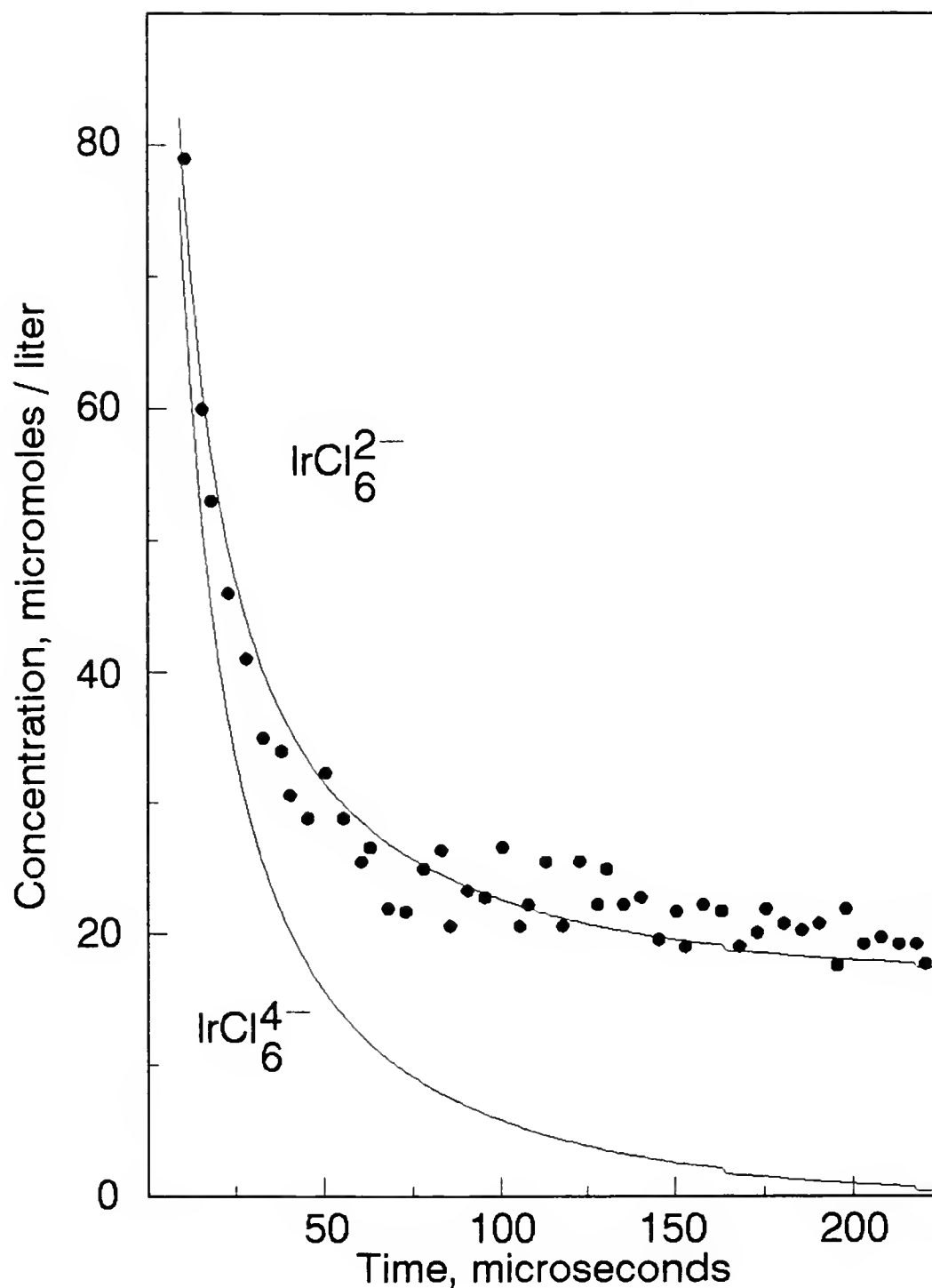


Fig. 34. Comparison of experimental and computer-simulated  $\text{IrCl}_6^{2-}$  concentration versus time plots during the pulse radiolysis of a nitrogen-saturated solution containing 1 mM  $\text{IrCl}_6^{3-}$ . (—) computed; (•) typical experimental results.

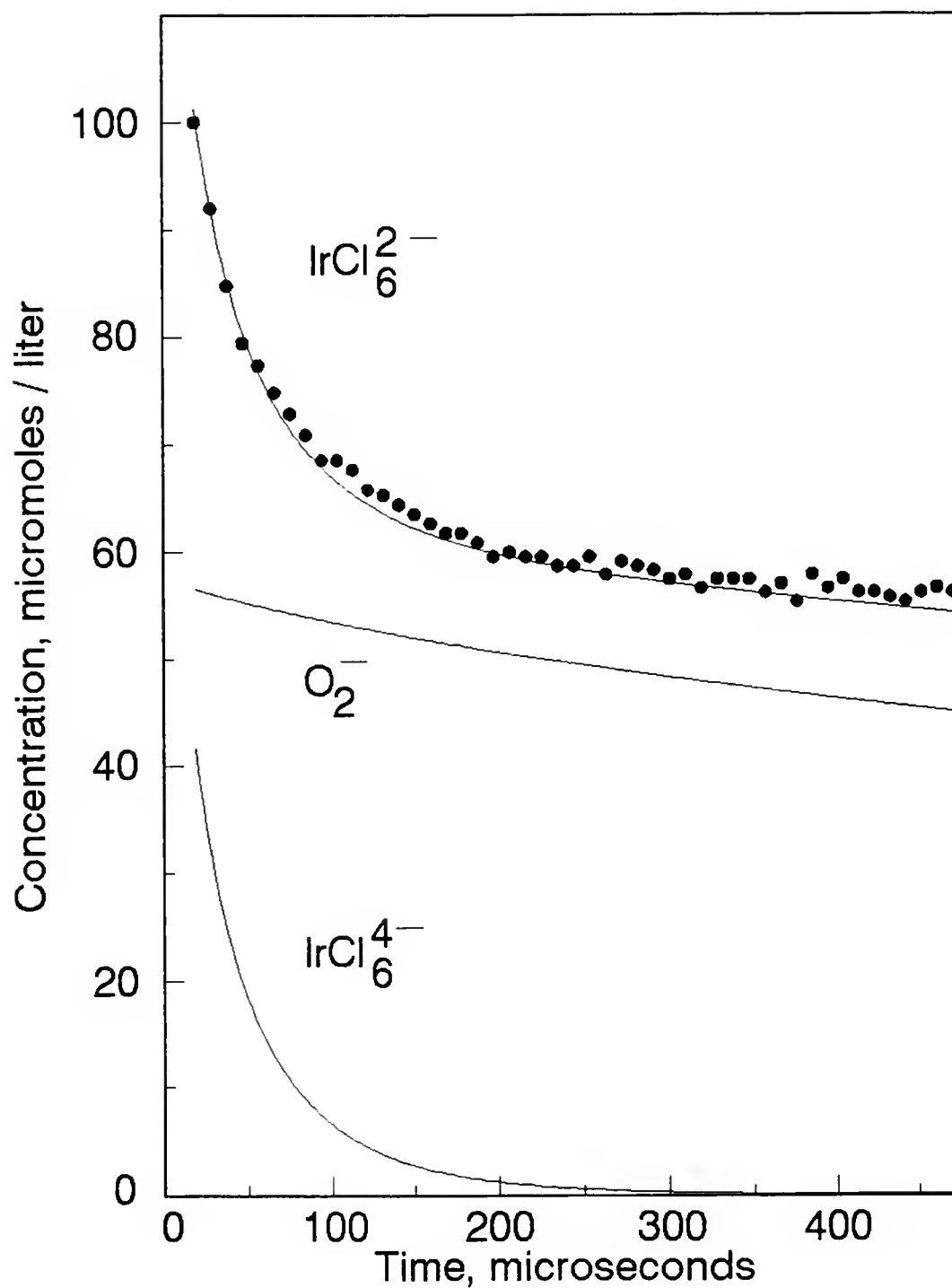


Fig. 35. Comparison of experimental and computer-simulated  $\text{IrCl}_6^{2-}$  concentration versus time plots during the pulse radiolysis of an air-saturated solution containing 1 mM  $\text{IrCl}_6^{3-}$ . (—) computed; (•) typical experimental results.

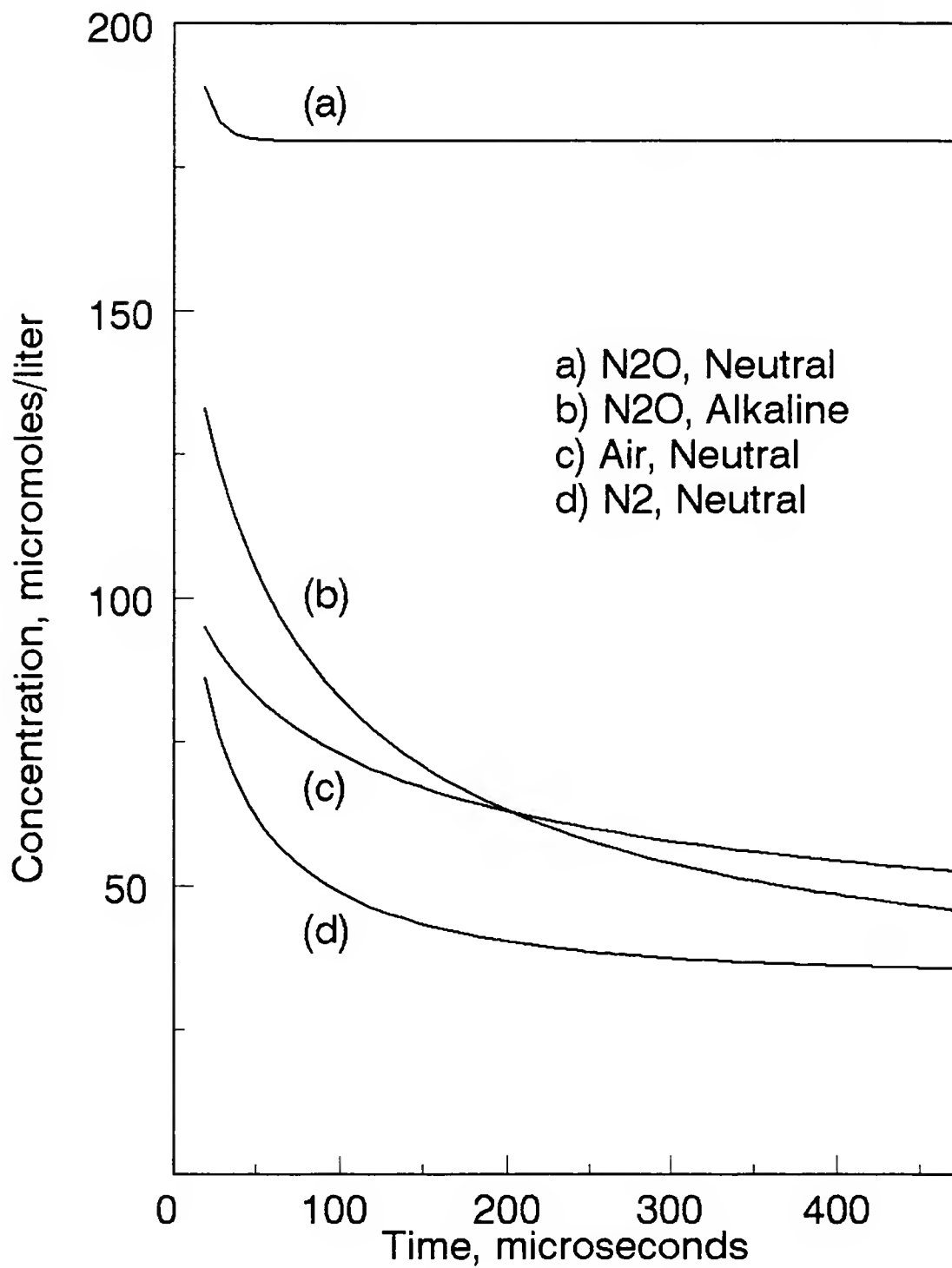


Fig. 36. Computer simulations of the transient  $\text{IrCl}_6^{2-}$  trace under various solution conditions.

### 4.3 Conclusions

Aqueous solutions of  $\text{IrCl}_6^{3-}$ , and the one-electron oxidation or reduction products,  $\text{IrCl}_6^{2-}$  and  $\text{IrCl}_6^{4-}$  respectively, form a relatively complex reaction system. However, the method of pulse radiolysis allows for the collection of some experimental evidence on the early stages of the redox reactions involved. It is entirely possible there are further nuances in the chemistry of the iridium complexes that have not been included at this time. For instance, several authors have suggested the participation of partially hydrolyzed iridium chloride complexes, such as  $\text{IrCl}_5(\text{OH}_2)^-$ .<sup>148-150</sup>

Results from this work lead to the following conclusions. The reported relative stability, i.e. no evidence of decay for the ca. 500-microsecond period of observation, of the  $\text{IrCl}_6^{2-}$  under neutral  $\text{N}_2\text{O}$ -saturated conditions was confirmed. The transient  $\text{IrCl}_6^{2-}$  complex formed during the pulse radiolysis of aqueous millimolar  $\text{IrCl}_6^{3-}$  solutions was found to be unstable under conditions of neutral air saturation, neutral nitrogen saturation, and alkaline nitrous-oxide saturation. For each of the solution conditions, an appropriate species has been identified and discussed as the most likely reductant for the one-electron reduction of the  $\text{IrCl}_6^{2-}$  complex. In the case of alkaline  $\text{N}_2\text{O}$ -saturated  $\text{IrCl}_6^{3-}$  solutions, pertinent benchtop experiments, as well

as stopped-flow techniques, were utilized to identify the peroxide anion,  $\text{HO}_2^-$ , as the reducing species.

Further work might confirm the proposed reaction between the Ir(IV) and Ir(II) species produced from the pulse radiolysis of nitrogen-saturated Ir(III) solutions, reaction 206. The Ir(II) complex could be exclusively formed by pulse irradiating, under totally reducing conditions, Ir(III) solutions containing trace amounts of Ir(IV) added as a minor solute. Subsequent analysis and comparison of the resulting Ir(IV) decay to the Ir(IV) decay presented earlier in this study could substantiate an electron transfer involving Ir(II) and Ir(IV).

Lastly, as mentioned previously the reaction rate constant of  $4.9 \times 10^9 \text{ M}^{-1}\text{s}^{-1}$  for the oxidation of Ir(III) by  $\text{OH}^\bullet$  was attained by the carbonate competition method. This value is somewhat less than the reported value of  $8.9 \times 10^9 \text{ M}^{-1}\text{s}^{-1}$ .<sup>111</sup> This referenced value was attained by applying the kinetic competition method using t-butyl alcohol as the competing species, rather than the carbonate anion. It is suspected that the lower value reported under the experimental conditions in this study could be due to complications arising from the data analysis of the end-of-pulse Ir(IV) concentrations. In the presence of added carbonate under alkaline conditions, the Ir(IV) complex undergoes a rapid decay immediately upon its formation from  $\text{OH}^\bullet$  reaction with

Ir(III). However, these end-of-pulse Ir(IV) concentrations must be referenced to the end-of-pulse Ir(IV) concentrations derived from stable Ir(IV) traces that are obtained when no competing species, i.e. carbonate, is present. The discrepancy in the rate constants could be explored by attempting the t-butyl alcohol competition method for the reaction of  $\text{OH}^\cdot$  with Ir(IV) under the experimental conditions described in this work.

## APPENDICES



APPENDIX A  
CHEMICAL DOSIMETRY FOR A PULSED RADIATION SOURCE

Chemical dosimetry involves the determination of the average absorbed dose in a material from a radiation-induced chemical change produced in a suitable substrate. The fraction of the total dose or flux from the radiation source that is absorbed will induce the chemical change in the system, and the most common unit of absorbed dose is the rad, which is defined as

$$1 \text{ rad} = 100 \text{ erg/g} = 6.24 \times 10^{13} \text{ ev/g} = 0.01 \text{ J/kg} \quad \text{A-1}$$

These systems consist of a bulk component, which absorbs the deposited radiation, and a minor component, which reacts with any radiation-induced species of the bulk to produce the observed chemical change that is quantitatively measured. Calculation of the absorbed dose requires the knowledge of an accurate G-value or radiation chemical yield which is defined as

$$G(x) = n(x)/E = \# \text{ molecules} / 100 \text{ eV} \quad \text{A-2}$$

with  $n(x)$  = the amount of  $x$  produced, destroyed, or changed by an absorbed energy,  $E$ . The dosimetry system should have the same atomic composition and density as the sample to be irradiated; thus all systems presented in this work are aqueous solutions that contain various solutes dissolved in the bulk water solvent. Optimal response characteris-

tics of the chemical dosimeter are as follows: the dosimeter should be 1) proportional to the radiation dose over a large range that covers from 10 rads up to 100 Mrads for radiation chemistry experiments, 2) independent of both the dose rate and the radiation's energy and LET, 3) independent of temperature and 4) highly precise, i.e. to  $< 5\%$ .<sup>40</sup>

Chemical dosimetry procedures for use with pulsed radiation sources are different from standard systems used with steady-state radiolysis. Larger dose rates occur with pulsed sources ( $10^8$  to  $10^{12}$  rad sec<sup>-1</sup>) compared to continuous dose rates ( $10$  to  $10^3$  rad sec<sup>-1</sup>) from Co-60  $\gamma$ -ray sources. The possibility of primary radical-radical interactions, as opposed to primary radical-solute interactions, lead to a net loss of measured product. This effect causes the G-value determined at lower dose rates to be inaccurate for pulse experiments. Also, with the pulse radiolysis experimental setup, one can measure transient species on the microsecond-to-millisecond time scales as opposed to chemical analysis carried out after the completion of a series of radiation-induced reactions.<sup>40</sup>

Multiple chemical dosimetry systems were utilized in this work, and Table 3 shows the various properties involved in the chemical analysis for each respective system. The first system applied, using the 1.4 ml non-flow

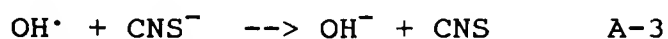
reaction cell, was a modified version of the standard Ferrous sulfate or Fricke system.<sup>151</sup> This system (1mM  $\text{Fe}(\text{NH}_4)_2(\text{SO}_4)_3 \cdot 6\text{H}_2\text{O}$ , 0.4 M  $\text{H}_2\text{SO}_4$ , air-saturated) involves the radiation-induced oxidation of ferrous ions to the ferric state ( $\text{Fe}^{2+} \rightarrow \text{Fe}^{3+}$ ) in the presence of oxygen at low pH. In the modified version (10mM  $\text{Fe}(\text{NH}_4)_2(\text{SO}_4)_3 \cdot 6\text{H}_2\text{O}$ , 0.4 M  $\text{H}_2\text{SO}_4$ ,  $\text{O}_2$ -saturated) recommended for pulse experiments, the solution is oxygen-saturated and a relatively higher initial  $[\text{Fe}^{2+}]$  is used. Detection of the product species,  $\text{Fe}^{3+}$ , was carried out after the completion of all relevant reactions, approximately thirty minutes, as is the practice with the standard Fricke system.

Table 3  
Physical Constants of the Dosimetry Systems\*

	Super Fricke	Thiocyanate	Hydrated Electron
Species detected	$\text{Fe}^{3+}$	$(\text{CNS})_2^-$	$e_{\text{aq}}^-$
G(product) <u>#molecules</u> 100 eV	16.1	5.8	2.63
$\lambda$ , monitored (nm)	304 (Beckman)	472 (xenon-arc)	632.8 (laser)
$\epsilon$ , ( $\text{M}^{-1}\text{cm}^{-1}$ )	2205	7580	14860
$\rho$ , (g/ml)	1.024	1.001	1.012

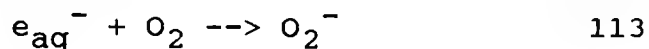
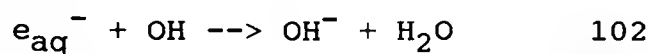
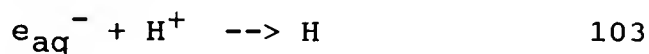
\* See references 40 and 151

The other systems used -- thiocyanate and hydrated electron -- involved transient species detection methods using the pulse radiolysis detection instrumentation. The thiocyanate system (10 mM KCNS, N<sub>2</sub>O-saturated) involves a potassium thiocyanate aqueous solution that, when irradiated under oxidizing conditions, produces a transient species, (CNS)<sub>2</sub><sup>-</sup>, formed in a two-step sequence from the OH<sup>•</sup> radical

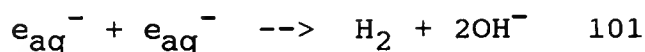


The purpose of the N<sub>2</sub>O saturation is to convert the hydrated electron, e<sub>aq</sub><sup>-</sup>, to OH that eliminates any optical interferences from e<sub>aq</sub><sup>-</sup> and produces a larger yield of the product species, (CNS)<sub>2</sub><sup>-</sup>, which decays via a second-order process with a rate constant of 3 x 10<sup>9</sup> M<sup>-1</sup>sec<sup>-1</sup>.<sup>151</sup>

In the hydrated electron system (0.1 M NaOH, 0.1 M ethanol, N<sub>2</sub>-saturated) the hydrated electron, e<sub>aq</sub><sup>-</sup>, a primary radical species produced by the direct interaction of the radiolysis of water, is monitored. Alkaline conditions, alcohol addition, and nitrogen-purging help to minimize the following reactions of the primary e<sub>aq</sub><sup>-</sup>.



The hydrated electron decays via a bimolecular reaction



with a rate constant of  $2k = 1.2 \times 10^{10} \text{ M}^{-1} \text{ sec}^{-1}$ .<sup>151</sup>

Figure 35 shows the results of the accumulated absorbance detected in a 1.4 ml volume of a modified Fricke solution contained in the non-flow cell described earlier. The absorbance is plotted as a function of the number of pulses delivered with the resulting slope of 0.1 equal to the change in optical density per pulse.

Figures 36 and 37 show the transient traces of the  $(CNS)_2^-$  and hydrated electron,  $e_{aq}^-$ , respectively. The life-time of the  $(CNS)_2^-$  transient is shown to be approximately 30-40 microseconds and a best fit analysis gives a second order decay with  $k = 3.3 \times 10^9 \text{ M}^{-1}\text{sec}^{-1}$  while the life-time of the  $e_{aq}^-$  transient is approximately 8-10 microseconds with a best fit curve giving a second order decay with  $k = 4.3 \times 10^{10} \text{ M}^{-1}\text{sec}^{-1}$ .

Using the experimental  $\Delta A$  values determined along with the various constants collected in Table 3, the absorbed dose ( $D_D$ ), presented in Table 4, can be calculated as<sup>40</sup>

$$\begin{aligned}
D_D &= \text{moles product formed per kg} \frac{(\text{mol})}{(\text{kg})} \\
&\quad \times 6.022 \times 10^{23} \frac{(\text{molecules})}{(\text{mol})} \times \frac{100}{G(\text{product})} \frac{(\text{eV})}{(\text{molecule})} \\
&\quad \times 1.602 \times 10^{-19} \frac{(\text{J})}{(\text{eV})} \times 100 \frac{(\text{kg rad})}{(\text{J})} \quad \text{A-5}
\end{aligned}$$

$$= 9.647 \times 10^8 \times \frac{\text{moles product formed per kg}}{G(\text{product})} \text{ rads}$$

or,

$$D_D = 9.647 \times 10^8 \times \frac{\text{moles product formed per liter}}{\rho G(\text{product})} \text{ rads}$$

with,

$$\text{moles product formed per liter} = \frac{\Delta A}{\Delta \epsilon l}$$

then,

$$D_D = 9.647 \times 10^8 \times \frac{\Delta A}{\Delta \epsilon l \rho G(\text{product})} \text{ rads}$$

with,

$\Delta A$  = difference in absorbance between irradiated and non-irradiated solution

$\Delta \epsilon$  = difference in molar extinction coefficient of reactant and product at monitored wavelength

$l$  = optical pathlength, cm

$\rho$  = density of solution, g/ml

$G(\text{product})$  = number of moles of product formed per 100 eV of energy absorbed

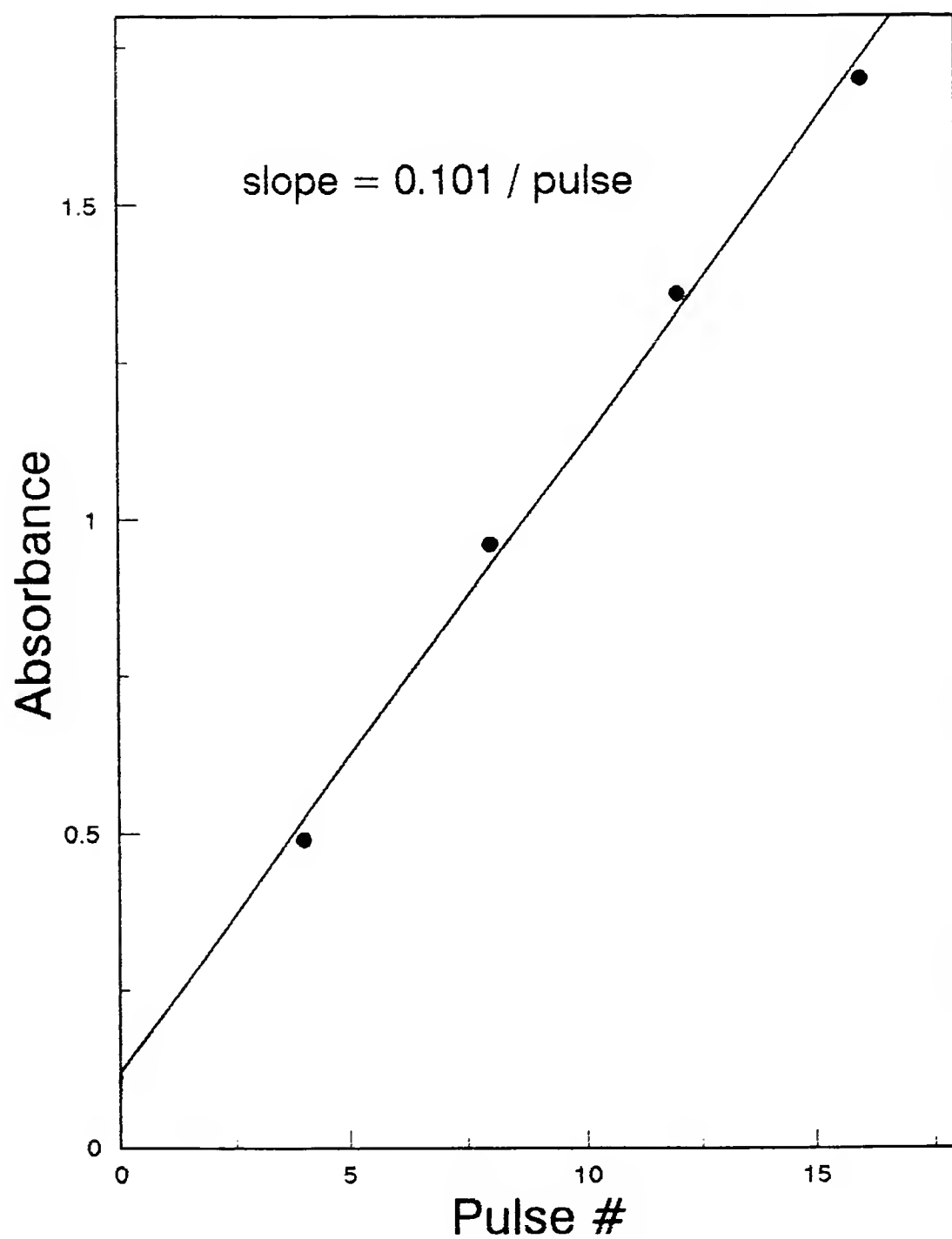


Fig. 37. Change in absorbance with accumulated radiation pulses for the modified Fricke dosimetry system.

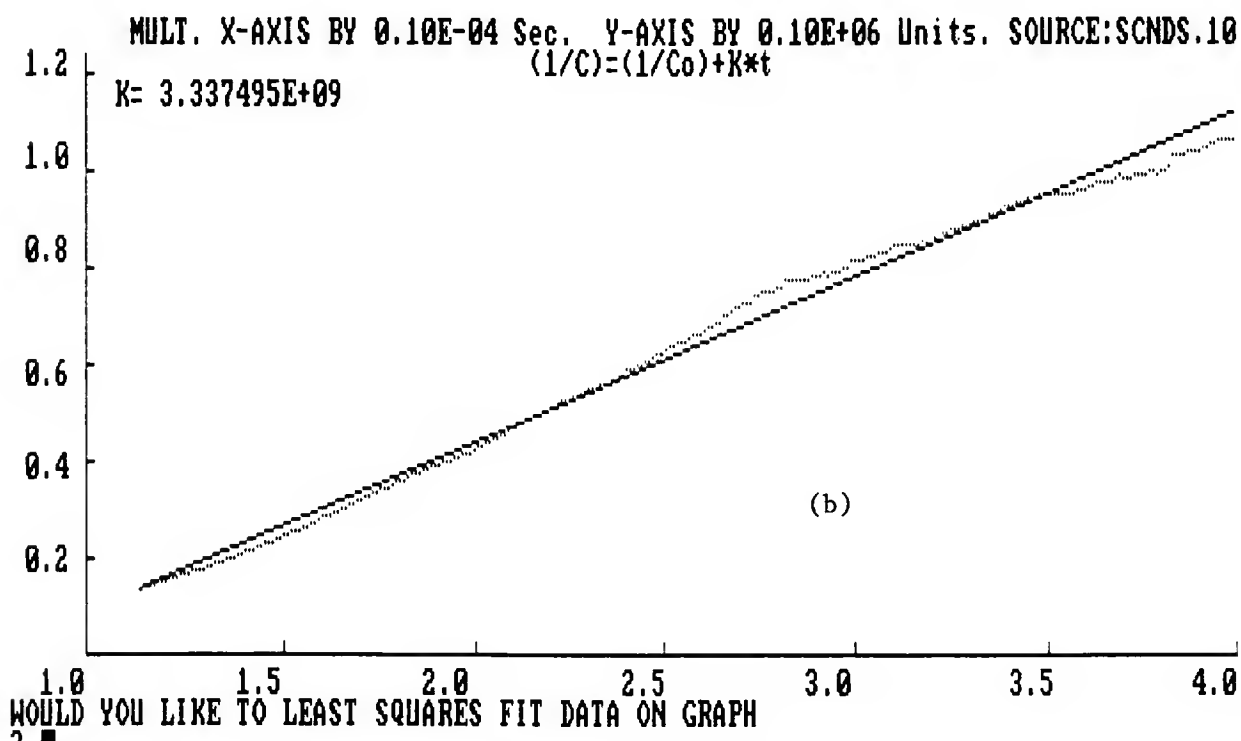
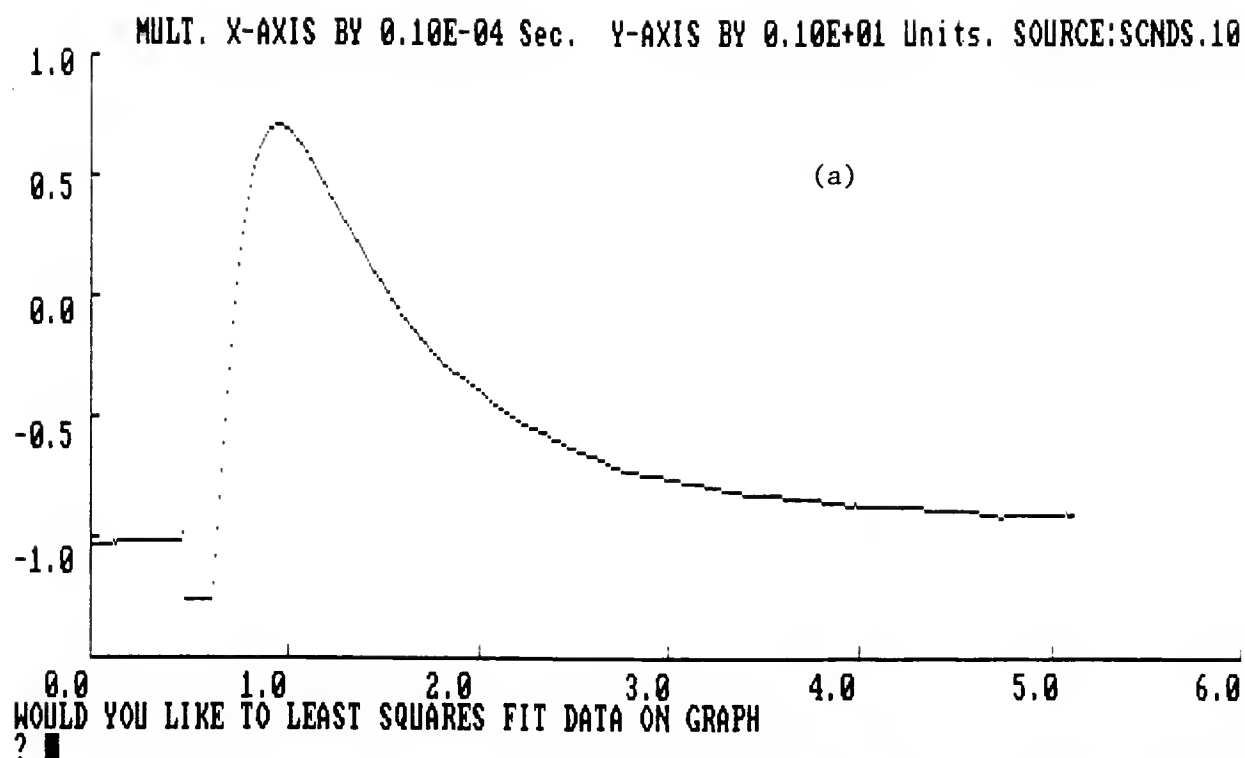


Fig. 38. Thiocyanate dosimetry system (a) graphical display of the optical signal following pulse radiolysis of  $N_2O$ -saturated solution containing 10 mM KCNS; data recorded at 472 nm, 100 nsec period, 50 usec full scale; (b) curve fit of data between  $x = 10$  to  $x = 40$  usec.



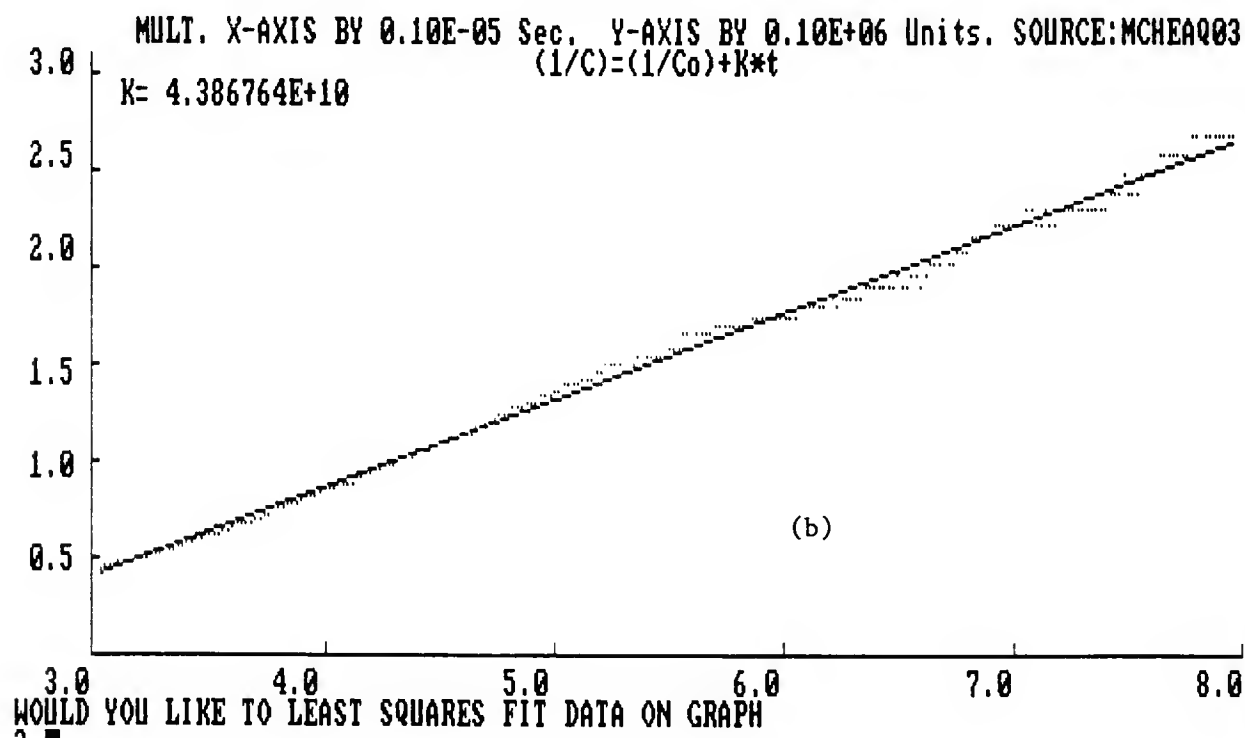
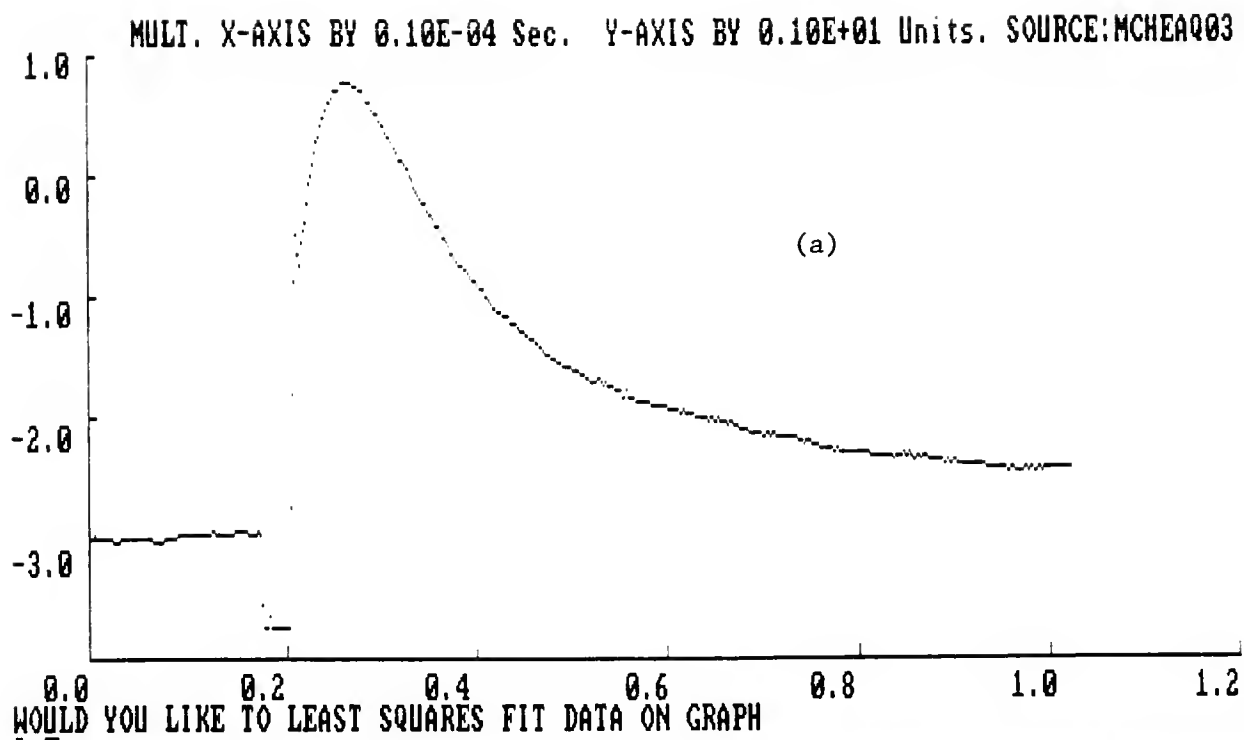


Fig. 39. Hydrated electron dosimetry system (a) graphical display of optical signal following pulse radiolysis of  $N_2$ -saturated solution containing 0.1 M NaOH and 0.1 M ethanol; data recorded at 632 nm, 20 nsec period, 10 usec full scale; (b) curve fit of data between  $x = 3$  and  $x = 8$  usec.

Table 4  
Absorbance Change and Absorbed Dose for  
Chemical Dosimetry Systems

System	$\Delta A$ / pulse	$D_D$ , rads
Super Fricke	$0.101 \pm 0.005$	$(2.5027 \pm .2741) \times 10^4$
Thiocyanate	a) $0.418 \pm 0.076$	$(8.709 \pm 1.739) \times 10^3$
	b) $1.129 \pm 0.332$	$(2.3542 \pm .5056) \times 10^4$
Hydrated Electron	a) $0.378 \pm 0.137$	$(9.220 \pm 2.001) \times 10^3$
	b) $1.103 \pm 0.267$	$(2.6894 \pm .6521) \times 10^4$

a) Maximum end of pulse absorption from transient trace

b) Results from extrapolation of best fit

## APPENDIX B RELEVANT REACTION SYSTEMS

The reactions used for the calculations of product concentrations in the aqueous tetraphenylborate and hexachloroiridate systems are listed in Table 5. The 100 series involves the well-known reactions describing transients of irradiated pure water<sup>152,153</sup> as well as the reactions relevant to  $N_2O$ - and air-saturated solutions. Reactions 101 - 107 and 118 describe the recombination of the primary radical species. Reactions 108-117 describe the reactions between the radicals and the molecular products.

Reactions 118-123 give the dissociation equilibria of  $H_2O$ ,  $HO_2$ , and  $H_2O_2$ . Reactions 124-128 should be important at pH 10 and above. Reactions 130-134 describe the carbonate anion and the carbonate radical anion,  $CO_3^{\cdot-}$ , produced in the pulse radiolysis of carbonate solutions containing  $N_2O$ .

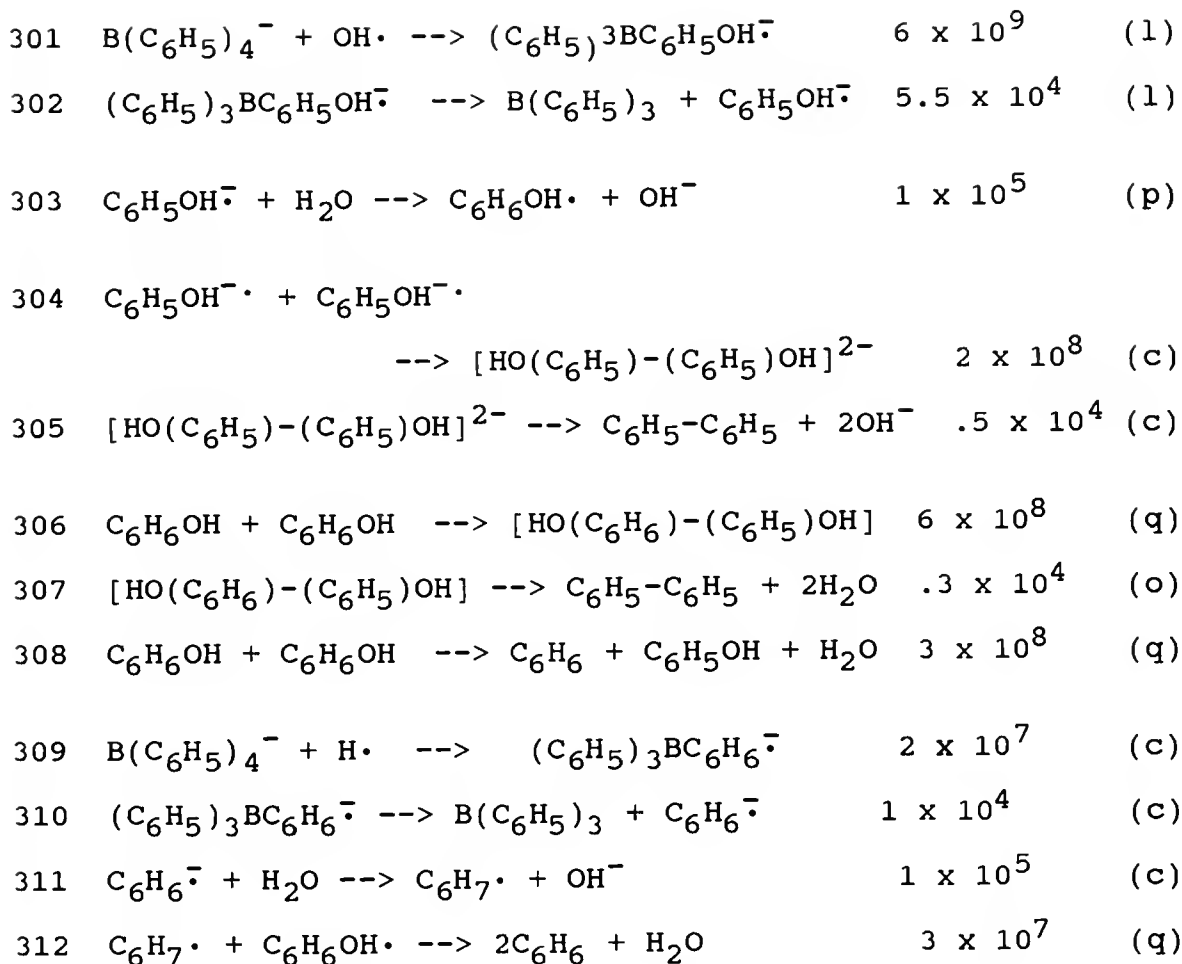
The 200 series involves all the reactions in the mechanistic scheme describing the  $IrCl_6^{3-}$  complex under the various conditions presented in the text. The 300 series involves all the reactions in the mechanistic scheme for the pulse radiolysis of  $N_2O$ -saturated solutions containing the  $TBP^-$  anion.

Table 5

## Chemical Reaction Systems for Computer Simulation Studies

No.	Reaction	Rate Constant ( $\text{M}^{-1}\text{s}^{-1}$ )	Ref.
101	$\text{e}_{\text{aq}}^- + \text{e}_{\text{aq}}^- \rightarrow \text{H}_2 + 2\text{OH}^-$	$5.4 \times 10^9$	(a)
102	$\text{e}_{\text{aq}}^- + \text{OH} \rightarrow \text{OH}^- + \text{H}_2\text{O}$	$3.0 \times 10^{10}$	(a)
103	$\text{e}_{\text{aq}}^- + \text{H}^+ \rightarrow \text{H}$	$2.4 \times 10^{10}$	(a)
104	$\text{e}_{\text{aq}}^- + \text{H} \rightarrow \text{H}_2 + \text{OH}^-$	$2.5 \times 10^{10}$	(a)
105	$\text{H} + \text{H} \rightarrow \text{H}_2$	$7.8 \times 10^9$	(a)
106	$\text{OH} + \text{OH} \rightarrow \text{H}_2\text{O}_2$	$5.3 \times 10^9$	(a)
107	$\text{H} + \text{OH} \rightarrow \text{H}_2\text{O}$	$7 \times 10^9$	(a)
108	$\text{e}_{\text{aq}}^- + \text{H}_2\text{O}_2 \rightarrow \text{OH} + \text{OH}^-$	$1.2 \times 10^{10}$	(a)
109	$\text{OH} + \text{H}_2 \rightarrow \text{H} + \text{H}_2\text{O}$	$4.9 \times 10^7$	(a)
110	$\text{OH} + \text{H}_2\text{O}_2 \rightarrow \text{HO}_2 + \text{H}_2\text{O}$	$2.7 \times 10^7$	(a)
111	$\text{HO}_2 + \text{HO}_2 \rightarrow \text{H}_2\text{O}_2 + \text{O}_2$	$2.7 \times 10^6$	(a)
112	$\text{O}_2^- + \text{HO}_2 \rightarrow \text{HO}_2^- + \text{O}_2$	$4.4 \times 10^7$	(a)
113	$\text{e}_{\text{aq}}^- + \text{O}_2 \rightarrow \text{O}_2^-$	$1.9 \times 10^{10}$	(a)
114	$\text{H} + \text{H}_2\text{O}_2 \rightarrow \text{OH} + \text{H}_2\text{O}$	$1 \times 10^{10}$	(a)
115	$\text{HO}_2 + \text{H} \rightarrow \text{H}_2\text{O}_2$	$1 \times 10^{10}$	(a)
116	$\text{HO}_2 + \text{OH} \rightarrow \text{H}_2\text{O} + \text{O}_2$	$6.6 \times 10^9$	(a)
117	$\text{H} + \text{O}_2 \rightarrow \text{HO}_2$	$1.9 \times 10^{10}$	(a)
118	$\text{H}^+ + \text{OH}^- \rightarrow \text{H}_2\text{O}$	$1.4 \times 10^{11}$	(b)
119	$\text{H}_2\text{O} \rightarrow \text{H}^+ + \text{OH}^-$	$2.6 \times 10^{-5}$	(b)
120	$\text{O}_2^- + \text{H}^+ \rightarrow \text{HO}_2$	$4.5 \times 10^{10}$	(c)
121	$\text{HO}_2 \rightarrow \text{H}^+ + \text{O}_2^-$	$8 \times 10^5$	(d)

122	$\text{H}^+ + \text{HO}_2^-$	$\rightarrow \text{H}_2\text{O}_2$	3	$\times 10^{10}$	(c)
123	$\text{H}_2\text{O}_2$	$\rightarrow \text{H}^+ + \text{HO}_2^-$	3	$\times 10^{-2}$	(e)
124	$\text{H}_2\text{O}_2 + \text{OH}^-$	$\rightarrow \text{HO}_2^- + \text{H}_2\text{O}$	1	$\times 10^{10}$	(c)
125	$\text{HO}_2^- + \text{H}_2\text{O}$	$\rightarrow \text{H}_2\text{O}_2 + \text{OH}^-$	5	$\times 10^7$	(f)
126	$\text{OH} + \text{OH}^-$	$\rightarrow \text{H}_2\text{O} + \text{O}^-$	1.2	$\times 10^{10}$	(g)
127	$\text{O}^- + \text{H}_2\text{O}$	$\rightarrow \text{OH} + \text{OH}^-$	9.3	$\times 10^7$	(g)
128	$\text{O}_2^- + \text{OH}$	$\rightarrow \text{OH}^- + \text{O}_2$	1.0	$\times 10^{10}$	(h)
129	$\text{N}_2\text{O} + \text{e}_{\text{aq}}^-$	$\rightarrow \text{OH}^- + \text{OH}$	8.7	$\times 10^9$	(a)
130	$\text{OH} + \text{CO}_3^{2-}$	$\rightarrow \text{OH}^- + \text{CO}_3^-$	4.1	$\times 10^8$	(i)
131	$\text{CO}_3^- + \text{CO}_3^-$	$\rightarrow \text{CO}_2 + \text{CO}_4^{2-}$	2	$\times 10^7$	(i)
132	$\text{CO}_3^- + \text{O}_2^-$	$\rightarrow \text{CO}_3^{2-} + \text{O}_2$	4	$\times 10^8$	(j)
133	$\text{CO}_3^{2-} + \text{H}_2\text{O}$	$\rightarrow \text{HCO}_3^- + \text{OH}^-$	1.78	$\times 10^4$	(k)
134	$\text{HCO}_3^- + \text{OH}^-$	$\rightarrow \text{CO}_3^{2-} + \text{H}_2\text{O}$	1	$\times 10^8$	(c)
201	$\text{IrCl}_6^{3-} + \text{OH}$	$\rightarrow \text{IrCl}_6^{2-} + \text{OH}^-$	4	$\times 10^9$	(l)
202	$\text{IrCl}_6^{3-} + \text{e}_{\text{aq}}^-$	$\rightarrow \text{IrCl}_6^{4-}$	6.8	$\times 10^9$	(l)
203	$\text{IrCl}_6^{3-} + \text{H}$	$\rightarrow \text{IrCl}_6^{4-} + \text{H}^+$	6	$\times 10^9$	(m)
204	$\text{IrCl}_6^{2-} + \text{e}_{\text{aq}}^-$	$\rightarrow \text{IrCl}_6^{3-}$	9.9	$\times 10^9$	(n)
205	$\text{IrCl}_6^{2-} + \text{H}$	$\rightarrow \text{IrCl}_6^{3-} + \text{H}^+$	9.2	$\times 10^9$	(n)
206	$\text{IrCl}_6^{4-} + \text{IrCl}_6^{2-}$	$\rightarrow 2\text{IrCl}_6^{3-}$	6	$\times 10^8$	(l)
207	$\text{IrCl}_6^{2-} + \text{O}_2^-$	$\rightarrow \text{IrCl}_6^{3-} + \text{O}_2$	1	$\times 10^7$	(l)
208	$\text{IrCl}_6^{2-} + \text{HO}_2^-$	$\rightarrow \text{IrCl}_6^{3-} + \text{HO}_2$	4.7	$\times 10^8$	(o)
209	$\text{IrCl}_6^{4-} + \text{IrCl}_6^{4-}$	$\rightarrow \text{IrCl}_6^{3-} + \text{IrCl}_6^{5-}$	5	$\times 10^8$	(n)




---

<sup>a</sup>ref. 153
<sup>n</sup>ref. 111.<sup>b</sup>ref. 37.<sup>o</sup>to give best fit.<sup>c</sup>assumed.<sup>p</sup>ref. 141<sup>d</sup>to give pK = 4.8 with  $k_{120}$ .<sup>q</sup>refs. 58, 60.<sup>e</sup>to give pK = 11.8 with  $k_{122}$ .<sup>f</sup>to give pK = 2.3 with  $k_{124}$ .<sup>g</sup>ref. 43.<sup>h</sup>ref. 154.<sup>i</sup>ref. 138.<sup>j</sup>ref. 155.<sup>k</sup>to give pK = 3.74 with  $k_{134}$ .<sup>l</sup>this work.<sup>m</sup>analogous to reaction 205.

# APPENDIX C INPUT DATA FILES

The data files used in the various computer integration simulations for the aqueous TPB and Iridium Chloride systems are presented below. Each input file consist of 1) title line, 2) reaction steps and appropriate rate constants, 3) initial reactant molar concentrations, 4) integration step size and time period parameters, 5) 1-50 time increments.

Simulation Tetraphenylborate System; N2O saturated

```

1110
1,EAQ+EAQ=H2+H2O2--,5.4E9
2,EAQ+OH=OH-+H2O,3.0E10
3,EAQ+HPLUS=H,2.4E10
4,EAQ+H=H2+OH-,2.5E10
5,H+H=H2,1.0E10
6,OH+OH=H2O2,5.3E9
7,H+OH=H2O,2.4E10
8,HPLUS+OH-=H2O,3E10
9,H2O=HPLUS+OH-,5.5E-6
10,EAQ+H2O2=OH+OH-,1.2E10
11,OH+H2=H+H2O,4.9E7
12,OH+H2O2=HO2.+H2O,2.7E7
13,HO2.+HO2.=H2O2+O2,2.7E6
14,O2-+HO2.=HO2-+O2,4.4E7
15,EAQ+O2=O2-,1.9E10
16,H+H2O2=OH+H2O,1E10
17,HO2.+H=H2O2,1E10
18,HO2.+OH=H2O+O2,1E10
19,H+O2=HO2.,1E10
20,O2-+HPLUS=HO2.,3E10
21,HPLUS+HO2-=H2O2,3E10
22,HO2.=HPLUS+O2-,1E6
23,H2O2=HPLUS+HO2-,3E-2
24,H2O2+OH-=HO2-,1E10
25,HO2-=H2O2+OH-,3E7
26,N2O+EAQ=OH-+OH,8.7E9
27,OH+OH-=O-+H2O,1.2E10
28,O-+H2O=OH+OH-,9.3E7
29,BP4-+OH=BP4OH-,6E9
30,BP4OH-=BP3+POH-,5.5E4
31,POH-=PHOH+OH-,1E5
32,PHOH+PHOH=X,6E8
33,X=C6H5-C6H5,.3E4
34,PHOH+PHOH=POH+C6H6,3E8

```

```

35,POH-+POH-=Y,2E8
36,Y=C6H5-C6H5,.5E4
37,BP4-+H=BP4H-,1E5
38,BP4H-=BP3+PH-,1E4
39,PH-+H2O=PH+OH-,1.0E7
40,PHOH+PH=C6H6+C6H6,3.5E7
END
EAQ,1.12E-4
HPLUS,1.12E-4
OH,1.12E-4
H,2.91E-5
H2,.975E-5
H2O2,1.5E-5
H2O,55
OH-,1E-7
N2O,2.5E-2
BP4-,1E-2
END
1.0E-30,1.0E-33,4E-6,0.00345
1,2,3,4,5,6,7,8,9,10,
11,12,13,14,15,16,17,18,19,20,
21,22,23,24,25,26,27,28,29,30,
31,32,33,34,35,36,37,38,39,40,
41,42,43,44,45,46,47,48,49,50

```

Simulation Hexachloroiridate System; N2O saturated, alkaline  
1110

```

1,EAQ+EAQ=H2+H2O2--,5.4E9
2,EAQ+OH=OH-+H2O,3.0E10
3,EAQ+HPLUS=H,2.4E10
4,EAQ+H=H2+OH-,2.5E10
5,H+H=H2,7.8E9
6,OH+OH=H2O2,5.3E9
7,H+OH=H2O,7E9
8,HPLUS+OH-=H2O,1.43E11
9,H2O=HPLUS+OH-,2.6E-5
10,EAQ+H2O2=OH+OH-,1.2E10
11,OH+H2=H+H2O,4.9E7
12,OH+H2O2=HO2.+H2O,2.7E7
13,HO2.+HO2.=H2O2+O2,2.7E6
14,O2-+HO2.=HO2-+O2,4.4E7
15,EAQ+O2=O2-,1.9E10
16,H+H2O2=OH+H2O,1E10
17,HO2.+H=H2O2,1E10
18,HO2.+OH=H2O+O2,6.6E9
19,H+O2=HO2.,1.9E10
20,O2-+HPLUS=HO2.,4.5E10
21,HPLUS+HO2-=H2O2,3E10
22,HO2.=HPLUS+O2-,8E5
23,H2O2=HPLUS+HO2-,3E-2
24,H2O2+OH-=HO2-,1E10
25,HO2-=H2O2+OH-,5E7
26,OH+OH-=O-+H2O,1.2E10

```



```

27,O-+H2O=OH+OH-,9.3E7
28,N2O+EAQ=OH-+OH,8.7E9
29,OH+CO3--=OH-+CO3-,4.1E8
30,CO3-+CO3-=CO2+CO4--,2E7
31,CO3--=HCO3-+OH-,1.78E4
32,HCO3-+OH-=CO3--,1E8
33,CO3-+O2-=CO3--+O2,4E8
34,O2-+OH=OH-+O2,1.01E10
35,IR3+OH=IR4+OH-,4E9
36,IR3+EAQ=IR2,6.8E9
37,IR2+IR4=IR3+IR3,6E8
38,IR4+EAQ=IR3,9.9E9
39,IR4+H=IR3+HPLUS,9.2E9
40,IR3+H=IR2+HPLUS,6E9
41,IR4+HO2-=IR3+HO2.,4.7E8
42,IR4+O2-=IR3+O2,1E7
43,IR2+IR2=IR3+IR1,5E8
END
EAQ,1.5E-4
HPLUS,1.5E-4
OH,1.55E-4
H,3.14E-5
H2,2.57E-5
H2O2,3.88E-5
HO2,1.48E-6
HO2-, .53E-5
H2O,55
OH-,9E-4
IR3,1E-3
N2O,2.5E-2
CO3--,5E-3
HCO3-,9E-4
O2-,2E-7
END
1.0E-30,1.0E-33,9.25E-6,0.00345
1,2,3,4,5,6,7,8,9,10,
11,12,13,14,15,16,17,18,19,20,
21,22,23,24,25,26,27,28,29,30,
31,32,33,34,35,36,37,38,39,40,
41,42,43,44,45,46,47,48,49,50

```

Simulation Hexachloroiridate System; N2O saturated, neutral  
1110

```

1,EAQ+EAQ=H2+H2O2--,5.4E9
2,EAQ+OH=OH-+H2O,3.0E10
3,EAQ+HPLUS=H,2.4E10
4,EAQ+H=H2+OH-,2.5E10
5,H+H=H2,7.8E9
6,OH+OH=H2O2,5.3E9
7,H+OH=H2O,7E9
8,HPLUS+OH-=H2O,1.43E11
9,H2O=HPLUS+OH-,2.6E-5
10,EAQ+H2O2=OH+OH-,1.2E10

```

```

11,OH+H2=H+H2O,4.9E7
12,OH+H2O2=HO2.+H2O,2.7E7
13,HO2.+HO2.=H2O2+O2,2.7E6
14,O2-+HO2.=HO2-+O2,4.4E7
15,EAQ+O2=O2-,1.9E10
16,H+H2O2=OH+H2O,1E10
17,HO2.+H=H2O2,1E10
18,HO2.+OH=H2O+O2,6.6E9
19,H+O2=HO2.,1.9E10
20,O2-+HPLUS=HO2.,4.5E10
21,HPLUS+HO2-=H2O2,3E10
22,HO2.=HPLUS+O2-,8E5
23,H2O2=HPLUS+HO2-,3E-2
24,N2O+EAQ=OH-+OH,8.7E9
25,O2-+OH=OH-+O2,1.01E10
26,IR3+OH=IR4+OH-,4E9
27,IR3+EAQ=IR2,6.8E9
28,IR2+IR4=IR3+IR3,6E8
29,IR4+EAQ=IR3,9.9E9
30,IR4+H=IR3+HPLUS,9.2E9
31,IR3+H=IR2+HPLUS,6E9
32,IR4+HO2-=IR3+HO2.,4.7E8
33,IR4+O2-=IR3+O2,1E7
34,IR2+IR2=IR3+IR1,5E8
END
EAQ,1.5E-4
HPLUS,1.5E-4
OH,1.55E-4
H,3.14E-5
H2,2.57E-5
H2O2,3.88E-5
HO2,1.48E-6
H2O,55
OH-,1E-7
IR3,1E-3
N2O,2.5E-2
END
1.0E-30,1.0E-33,9.25E-6,0.00345
1,2,3,4,5,6,7,8,9,10,
11,12,13,14,15,16,17,18,19,20,
21,22,23,24,25,26,27,28,29,30,
31,32,33,34,35,36,37,38,39,40,
41,42,43,44,45,46,47,48,49,50

```

Simulation Hexachloroiridate System; Nitrogen saturated

1110

```

1,EAQ+EAQ=H2+H2O2--,5.4E9
2,EAQ+OH=OH-+H2O,3.0E10
3,EAQ+HPLUS=H,2.4E10
4,EAQ+H=H2+OH-,2.5E10
5,H+H=H2,7.8E9
6,OH+OH=H2O2,5.3E9
7,H+OH=H2O,7E9

```

```

8,HPLUS+OH-=H2O,1.43E11
9,H2O=HPLUS+OH-,2.6E-5
10,EAQ+H2O2=OH+OH-,1.2E10
11,OH+H2=H+H2O,4.9E7
12,OH+H2O2=HO2.+H2O,2.7E7
13,HO2.+HO2.=H2O2+O2,2.7E6
14,O2-+HO2.=HO2-+O2,4.4E7
15,EAQ+O2=O2-,1.9E10
16,H+H2O2=OH+H2O,1E10
17,HO2.+H=H2O2,1E10
18,HO2.+OH=H2O+O2,6.6E9
19,H+O2=HO2.,1.9E10
20,O2-+HPLUS=HO2.,4.5E10
21,HPLUS+HO2-=H2O2,3E10
22,HO2.=HPLUS+O2-,8E5
23,H2O2=HPLUS+HO2-,3E-2
24,O2-+OH=OH-+O2,1.01E10
25,IR3+OH=IR4+OH-,4E9
26,IR3+EAQ=IR2,6.8E9
27,IR2+IR4=IR3+IR3,6E8
28,IR4+EAQ=IR3,9.9E9
29,IR4+H=IR3+HPLUS,9.2E9
30,IR3+H=IR2+HPLUS,6E9
31,IR4+HO2-=IR3+HO2.,4.7E8
32,IR4+O2-=IR3+O2,1E7
33,IR2+IR2=IR3+IR1,5E8
END
EAQ,1.5E-4
HPLUS,1.5E-4
OH,1.55E-4
H,3.14E-5
H2,2.57E-5
H2O2,3.88E-5
HO2,1.48E-6
H2O,55
OH-,1E-7
IR3,1E-3
END
1.0E-30,1.0E-33,9.25E-6,0.00345
1,2,3,4,5,6,7,8,9,10,
11,12,13,14,15,16,17,18,19,20,
21,22,23,24,25,26,27,28,29,30,
31,32,33,34,35,36,37,38,39,40,
41,42,43,44,45,46,47,48,49,50

```

Simulation Hexachloroiridate System; Aerated

1110

```

1,EAQ+EAQ=H2+H2O2--,5.4E9
2,EAQ+OH=OH-+H2O,3.0E10
3,EAQ+HPLUS=H,2.4E10
4,EAQ+H=H2+OH-,2.5E10
5,H+H=H2,7.8E9
6,OH+OH=H2O2,5.3E9

```

```

7,H+OH=H2O,7E9
8,HPLUS+OH-=H2O,1.43E11
9,H2O=HPLUS+OH-,2.6E-5
10,EAQ+H2O2=OH+OH-,1.2E10
11,OH+H2=H+H2O,4.9E7
12,OH+H2O2=HO2.+H2O,2.7E7
13,HO2.+HO2.=H2O2+O2,2.7E6
14,O2-+HO2.=HO2-+O2,4.4E7
15,EAQ+O2=O2-,1.9E10
16,H+H2O2=OH+H2O,1E10
17,HO2.+H=H2O2,1E10
18,HO2.+OH=H2O+O2,6.6E9
19,H+O2=HO2.,1.9E10
20,O2-+HPLUS=HO2.,4.5E10
21,HPLUS+HO2-=H2O2,3E10
22,HO2.=HPLUS+O2-,8E5
23,H2O2=HPLUS+HO2-,3E-2
24,O2-+OH=OH-+O2,1.01E10
25,IR3+OH=IR4+OH-,4E9
26,IR3+EAQ=IR2,6.8E9
27,IR2+IR4=IR3+IR3,6E8
28,IR4+EAQ=IR3,9.9E9
29,IR4+H=IR3+HPLUS,9.2E9
30,IR3+H=IR2+HPLUS,6E9
31,IR4+HO2-=IR3+HO2.,4.7E8
32,IR4+O2-=IR3+O2,1E7
33,IR2+IR2=IR3+IR1,5E8
END
EAQ,1.5E-4
HPLUS,1.5E-4
OH,1.55E-4
H,3.14E-5
H2,2.57E-5
H2O2,3.88E-5
HO2,1.48E-6
H2O,55
OH-,1E-7
IR3,1E-3
O2,2.5E-4
END
1.0E-30,1.0E-33,9.4E-6,0.00345
1,2,3,4,5,6,7,8,9,10,
11,12,13,14,15,16,17,18,19,20,
21,22,23,24,25,26,27,28,29,30,
31,32,33,34,35,36,37,38,39,40,
41,42,43,44,45,46,47,48,49,50

```

APPENDIX D  
PULSE RADIOLYSIS COMPUTER PROGRAM

```
1  /
2  /
3  /      *****      DATA GRABBER      *****
4  /
5  /      ***** File DEBEST8.BAS, OCT. 12, 1989 *****
6  /
7  / PULSE RADIOLYSIS DATA ACQUISITION PROGRAM FOR DATA
   / PRECISION 6000
8  / TRANSIENT DIGITIZER INTERFACED THROUGH A SERIAL PORT AT
   / 9600 BAUD
9  / WITH AN IBM-PC COMPATIBLE MICROCOMPUTER.
10 /
11 / FOR USE WITH MICROSOFT QUICK BASIC COMPILER VERSION 4.0
   / WITH 8087
12 / COPYRIGHT 1988, 1989 BY JOHN BROGDON AND ROBERT
   / HANRAHAN
15 / RADIATION CHEMISTRY LAB, 406 NSC, U OF FLA GAINESVILLE
   / 32611
18 / TEL 904-392-1442 OR 376-7754
19 /
20 / WORK DONE UNDER DOE CONTRACT DE-AS05-76ERO-3106
21 /
23 / COMPILE FROM THE QBASIC DIRECTORY WITH THE WORKFILE ON
   / B:, AS FOLLOWS
24 / BC B: DEBEST8/O/X/E/C:6000; THE LAST SETS UP THE
25 / COMMUNICATION BUFFER; THEN LINK. IN TURBO BASIC THE
26 / METACOMMAND $COM1 6000 IS SUPPOSED TO WORK BUT WE GET
   / ERRORS
28 / ABOUT EVERY NINTH DATA POINT WHEN WE TAKE DATASET FROM
   / DP 6000.
33 / IN BASICA, THE BUFFER MAY BE CHANGED WITH THE COMMAND
   / "BASIC/C:6000"
35 / WHEN ENTERING INTO THE BASIC MODE, BUT INTERPRETER IS
   / VERY SLOW
40 / AND SEVERAL TIMING LOOPS MUST BE CHANGED. SOME TIMING
   / LOOPS
43 / PRESENTLY MAY BE LONGER THAN NECESSARY ON A STANDARD
   / SPEED 4.77 MHZ
45 / COMPUTER **** BUT MIGHT NEED TO BE LONGER ON A FASTER
   / MACHINE
48 /
50 /
52 / **** NOTE, THE UNDERLINE _ _ _ IS A LINE CONTINUATION
   / IN QBASIC ****
72 / WARNING -- NOT ALL FEATURES HAVE BEEN FULLY TESTED. IN
   / PARTICULAR,
73 / THE COMMAND TO COMPARE SPECTRA HAS NOT BEEN USED
   / EXTENSIVELY.
```

```

75  DIM AGI$(100), BGI$(100), DSPM$(10), TRGSRC$(10), OD(512)
80  DIM QY(520), QX(512), VERLN(147), QLY(512), BTARY(3400),
    CON(512)
90  OPEN "com1:9600,n,8,1,cs,ds,cd" FOR RANDOM AS #1
100 ON ERROR GOTO 5220
110 SCREEN 2: KEY ON: CLS : GET (1, 80)-(639, 99), BTARY
120 DLY$ = "-3.0uS": PER$ = "200nS": SWP$ = "3"
130 DSPM = 2: YSC$ = "1.0": TRGSRC = 5
140 PRINT "FIRST TURN ON THE DP6000, THEN PRESS CONT"
145 FOR KKQ = 1 TO 520: QY(KKQ) = 0: NEXT
150 L = 1: EE = 3000: FLORD = 0: FLCAL = 0: FLDATA = 0
170 KEY OFF: B$ = "PROG;KEYSRQ=1;KEY=1017;KEY=1033;REMOTE"
180 GOSUB 1090
190 INPUT "IS MODE ON RUN OR EDIT"; B$
200 B$ = LEFT$(B$, 1)
210 IF B$ <> "R" AND B$ <> "E" GOTO 190
220 IF B$ = "R" GOTO 250
230 B$ = "KEY=1017"
240 GOSUB 1090
250 INPUT "IS EXECUTE ON RUN/STOP (YES or NO)"; B$
260 B$ = LEFT$(B$, 1)
270 IF B$ <> "Y" AND B$ <> "N" GOTO 250
280 IF B$ = "Y" GOTO 320
290 B$ = "KEY=1033"
300 GOSUB 1090
310 GOTO 250
320 DEF FNQSC (QS, QXS, QNS, QXO, QNO) = INT(QXO - (QXO - QNO)
    / (QXS - QNS) * (QXS - QS) + .5)
330 PRINT : GOTO 350
340 '***** MENU *****
350 PRINT : PRINT "RETURNING TO MENU": PRINT
360 PRINT "CALIBRATION      CALIBRATE DP6000 FOR EXPERIMENT"
370 PRINT "DATA              ACQUIRE DATA FROM DP6000"
380 PRINT "PLOTTER           PLOT RAW DATA ON SCREEN"
390 PRINT "LEAST SQUARES     LINEAR REGRESION FOR CURRENT DATA"
400 PRINT "LOAD              LOAD DATA FROM DISK"
410 PRINT "SAVE              SAVE DATA ON DISK"
420 PRINT "ORDER            CHOOSE ORDER OF REACTION"
430 PRINT "COMPARE          COMPARE DATA SETS ON GRAPH"
432 PRINT "MAN              MANUAL CHANGE V0,VM,L,OR E"
433 PRINT "DIR              DISK DIRECTORY"
435 PRINT "END              END SESSION "
436 FOR I = 1 TO 25
437 SOUND RND * 1000 + 37, 2
438 NEXT I
440 PRINT : INPUT "COMMAND"; B$
450 B$ = LEFT$(B$, 3)
455 IF B$ = "END" THEN END
460 RESTORE
470 FOR I = 1 TO 11
480 IF I = 11 THEN PRINT "BAD COMMAND": PRINT : GOTO 440
490 READ A$
500 IF B$ = A$ THEN GOTO 520

```

```

510 NEXT I
520 ON I GOSUB 570, 1140, 1480, 3950, 4940, 4780, 5140, 5330,
      8000, 9800
530 PRINT : GOTO 350
550 DATA "CAL","DAT","PLO","LEA","LOA","SAV","ORD","COM",
      "MAN","DIR"
555 GOTO 9999
560 /***** CALIBRATION *****/
570 PRINT : PRINT TAB(25); : PRINT "CALIBRATION"
580 DSPM$(1) = "SINGLE": DSPM$(2) = "2 SEPR": DSPM$(3) =
      "2 OVLY"
585 TRGSRC$(1) = "NONE": TRGSRC$(2) = "CH 1": TRGSRC$(3) =
      "CH 2"
586 TRGSRC$(4) = "LINE": TRGSRC$(5) = "EXT TRIG"
590 PRINT
592 PRINT "1)TIME DELAY=" + DLY$, "2)PERIOD=" + PER$, "3)#
      SWEEPS=" + SWP$,
593 PRINT "4)DSPL MODE=" + DSPM$(DSPM), "5) Y SCALE=" + YSC$,
      "6)NO CHANGE"
595 PRINT "7)TRIGGER=" + TRGSRC$(TRGSRC)
600 FLCAL = 1
610 PRINT
620 PRINT "WHICH NUMBER": B$ = INPUT$(1)
630 B = VAL(B$)
640 IF B < 1 OR B > 7 GOTO 620
650 ON B GOTO 660, 670, 680, 690, 700, 710, 702
660 INPUT "1)TIME DELAY= ", DLY$: GOTO 590
670 INPUT "2)PERIOD=", PER$: GOTO 590
680 INPUT "3)# SWEEPS=", SWP$: GOTO 590
690 PRINT : PRINT "CHOICES:", "1) SINGLE", "2) 2 SEPR",
      "3) 2 OVLY"
695 PRINT : INPUT "4)DSPL MODE=", DSPM: GOTO 590
700 INPUT "5)Y SCALE=", YSC$: GOTO 590
702 PRINT : PRINT "CHOICES:", "1)NONE", "2)CH 1", "3)CH 2",
      "4)LINE",
705 PRINT "5)EXT TRIG": INPUT "7)TRIGGER=", TRGSR: GOTO 590
710 PRINT "INIALIZING DP6000"
715 TRG$ = STR$(TRGSR)
720 B$ = "DARM;PROMPT=1;TRIG;TRGM=1;TMB;PERIOD=" + PER$ +
      ";TRGSRC=" + TRG$
730 GOSUB 1090
732 B$ = "TMB;KEY=1008;PERIOD=" + PER$ + ";KEY=1004;
      PERIOD=" + PER$ + ""
734 GOSUB 1090
740 B$ = "DELAY=" + DLY$ + ";DISP;DSPM=" + STR$(DSPM)
750 GOSUB 1090
760 B$ = "TRACE=1;X;TRCSRC=BUF.A2;XFILL=2;Y;YSCL=" + YSC$ +
      ";TRACE=2"
770 GOSUB 1090
780 B$ = "TRCSRC=BUF.A2;YSCL=" + YSC$ + ";X;XFILL=2;GRID=2;ARM"
790 GOSUB 1090
792 B$ = "TMB"
794 GOSUB 1090

```

```

800 PRINT : PRINT "V0="; V0, "VM="; VM + V0: PRINT
810 INPUT "DO YOU WANT TO CHANGE THE PARAMETERS OF THE
      EXPERIMENT"; B$
820 B$ = LEFT$(B$, 1)
830 IF B$ <> "Y" AND B$ <> "N" GOTO 810
832 B$ = "KEY=4001"
834 GOSUB 1090
836 B$ = "KEY=1008"
838 GOSUB 1090
840 IF B$ = "N" AND VM <> 0 THEN B$ = "DARM": GOSUB 1090: GOTO
      990
850 IF VM = 0 AND B$ = "N" THEN PRINT "YOU HAVE NO CHOICE (VM-
      V0=0)"
860 PRINT : INPUT "HAVE YOU TRIGGERED FOR NO LIGHT"; B$
870 B$ = LEFT$(B$, 1): IF B$ <> "Y" THEN 860
880 B$ = "BUF.A2(2)": GOSUB 7000
882 NO = MYINFO: B$ = "BUF.A2(150)": GOSUB 7000
884 Y1 = MYINFO: B$ = "BUF.A2(250)": GOSUB 7000
886 Y2 = MYINFO: B$ = "BUF.A2(350)": GOSUB 7000
888 Y3 = MYINFO
910 V0 = (Y1 + Y2 + Y3) / 3
912 B$ = "KEY=4001"
914 GOSUB 1090
916 B$ = "KEY=1008"
918 GOSUB 1090
920 PRINT : INPUT "HAVE YOU TRIGGERED FOR FULL LIGHT"; B$
930 B$ = LEFT$(B$, 1): IF B$ <> "Y" THEN 920
932 B$ = "BUF.A2(2)": GOSUB 7000
934 NO = MYINFO: B$ = "BUF.A2(150)": GOSUB 7000
936 Y1 = MYINFO: B$ = "BUF.A2(250)": GOSUB 7000
938 Y2 = MYINFO: B$ = "BUF.A2(350)": GOSUB 7000
939 Y3 = MYINFO
940 REM B$="BUF.A2(2);BUF.A2(400);BUF.A2(300);BUF.A2(500);DARM"
950 REM GOSUB 1090
960 REM INPUT #1,NO,Y1,Y2,Y3
970 VM = (Y1 + Y2 + Y3) / 3
980 VFULL = VM - V0
990 REM L = L / EE
1000 PRINT : PRINT "VMAX = "; VM; " V0 = "; V0; "L="; L,
      "E="; EE: PRINT
1010 PRINT "L-CHANGE L", "E-CHANGE E", "N-NO CHANGE ": B$ =
      INPUT$(1)
1020 IF B$ <> "L" AND B$ <> "E" AND B$ <> "N" GOTO 1010
1030 IF B$ = "L" THEN INPUT "L=", L: GOTO 1000
1040 IF B$ = "E" THEN INPUT "E=", EE: GOTO 1000
1050 LEFF = L * EE * 2.303
1060 QY(516) = V0: QY(517) = VM: QY(518) = L: QY(519) = EE
1070 RETURN
1080 '***** OUTPUT B$ TO DP6000 *****
1090 PRINT #1, B$
1100 FOR I = 1 TO 8000
1105 QQWER = LOG(I)
1110 NEXT I

```



```

1120 RETURN
1130 '***** DATA *****
1140 PRINT TAB(40); "DATA"
1150 IF FLCAL = 0 THEN PRINT "CALIBRATION NEEDED FIRST": GOSUB
    570
1160 B$ = "DARM;X;TRACE=1;TRCSRC=BUF.A2"
1170 GOSUB 1090
1172 B$ = "X;TRACE=2;TRCSRC=AVEGA2"
1173 GOSUB 1090
1174 FOR BADDOG = 1 TO 500: AHUNK1 = LOG(BADDOG): NEXT
1175 REM B$ = "PROG;SAVG;AVGCLR;AVGCNT=0;NAVG=" + SWP$ +
    ";KEY=1067;DISP;"
1176 B$ = "PROG;SAVG;AVGCLR;AVGCNT=0;"
1177 GOSUB 1090
1178 B$ = "NAVG=" + SWP$ + ";KEY=1067;DISP;"
1179 GOSUB 1090
1182 B$ = "AVGCLR;AVGCNT=0;CLRSUM"
1184 GOSUB 1090
1192 B$ = "X;TRACE=1;TRCSRC=BUF.A2;ARM"
1194 GOSUB 1090
1200 SWP = VAL(SWP$)
1210 FOR K = 1 TO SWP
1212 B$ = "KEY=4001"
1214 GOSUB 1090
1216 B$ = "KEY=1008"
1218 GOSUB 1090
1220 PRINT "TYPE T FOR TRIGGERED OR S FOR STOP.  ";
1230 B$ = INPUT$(1): PRINT B$
1240 IF B$ <> "T" AND B$ <> "S" THEN GOTO 1220
1250 IF B$ = "S" GOTO 1300
1260 B$ = "KEY=2001"
1270 GOSUB 1090
1280 PRINT "# SWEEPS="; K
1290 NEXT K
1300 B$ = "DARM;X;TRACE=2;TRCSRC=AVEGA2"
1309 GOSUB 1090
1310 REM GOSUB 7000
1311 B$ = "PERIOD": GOSUB 7000
1312 NO = MYINFO
1313 B$ = "PERIOD": GOSUB 7000
1314 PER = MYINFO
1315 B$ = "MIN": GOSUB 7000
1316 QMINY = MYINFO
1317 B$ = "MAX": GOSUB 7000
1318 QMAXY = MYINFO
1319 B$ = "DELAY": GOSUB 7000
1320 N = MYINFO
1329 REM INPUT #1,NO,PER,QMINY,QMAXY,N
1330 IF QMAXY <> QMINY THEN GOTO 1370
1340 PRINT "BAD DATA": PRINT NO, PER, QMINY, QMAXY, N
1350 REM IF LOC(1)<3 GOTO 1300
1360 REM INPUT #1,PER:GOTO 1300
1365 GOTO 350

```

```

1370 PRINT "creating file from avega2"
1371 PRINT #1, "AVEGA2|"
1372 FOR AAA = 1 TO 200: SAM = SAM + 3: NEXT
1378 PRINT "finist sam stall"
1380 FOR I = 1 TO 512
1383 REM QWQWQE = 2+3
1390 INPUT #1, QY(I)
1400 NEXT I
1405 PRINT "FINISH W INPUT INTO #1"
1410 FOR I = 1 TO 512
1420 QX(I) = I * PER
1425 IF VM = 0 THEN VM = -3: IF L = 0 THEN L = 39: IF V0 = 0
    THEN V0 = -1
1430 CON(I) = -LOG(ABS((QY(I) - V0) / VFULL)) / LEFF
1431 OD(I) = -LOG(ABS((QY(I) - V0) / VFULL)) / 2.303
1440 NEXT I
1450 QY(513) = PER: QY(514) = QMAXY: QY(515) = QMINY
1460 FLDATA = 1
1465 PRINT "going to main menu"
1470 RETURN
1480 '***** PLOTTER *****
1490 N = 1: QMINX = QX(1): QMAXX = QX(512)
1491 RHGRFLAG = 0
1500 IF FLDATA > 0 THEN GOTO 1520
1510 PRINT "NO DATA SOURCE. RETURNING TO MENU": RETURN
1520 INPUT "WHAT RESOLUTION WOULD YOU LIKE TO GRAPH (1 TO 20)";
    QRES
1525 IF QRES < 1 OR QRES > 20 THEN QRES = 1
1530 QN = 512: QFLG = 0: GOSUB 2160
1540 GOSUB 1570
1550 RETURN
1560 '***** LEFT & RIGHT BORDERS *****
1561 RHGRFLAG = 0
1570 PUT (0, QLNB + 11), BTARY, PSET: LOCATE INT((QLNB / 200) *
    25 + 1) + 2, 1
1571 IF RHGRFLAG = 1 THEN FOR ASEC = 1 TO 12000: AMIN =
    LOG(ASEC): NEXT
1575 PRINT "WOULD YOU LIKE TO LEAST SQUARES FIT DATA ON GRAPH"
1590 INPUT B$: B$ = LEFT$(B$, 1)
1600 IF B$ = "N" THEN RETURN
1610 IF B$ <> "Y" THEN GOTO 1590
1620 GET (QLNL, QLNT)-(QLNL, QLNB), VERLN
1630 PUT (0, QLNB + 11), BTARY, PSET: LOCATE INT((QLNB / 200) *
    25 + 1) + 2, 1
1640 INPUT "DO YOU WISH TO MOVE THE LEFT BORDER"; B$
1650 B$ = LEFT$(B$, 1)
1660 LNPOS = QLNL
1670 IF B$ = "N" THEN GOTO 1830
1680 IF B$ <> "Y" THEN GOTO 1630
1690 LNPOS = QLNL + 25
1700 C$ = "R"
1710 PUT (LNPOS, QLNT), VERLN

```

```

1720 PUT (0, QLNB + 11), BTARY, PSET: LOCATE INT((QLNB / 200) *
      25 + 1) + 2, 1
1730 PRINT "L-LEFT,R-RIGHT,S-STOP OR NUMBER OF SPACES "; : B$
      = INPUT$(1)
1740 D = VAL(B$) ^ 2
1750 IF D = 0 AND (B$ = "L" OR B$ = "R" OR B$ = "S") THEN C$ = B$
1760 IF C$ = "S" THEN GOTO 1830
1770 PUT (LNPOS, QLNT), VERLN
1780 IF C$ = "R" THEN LNPOS = LNPOS + D
1790 IF C$ = "L" THEN LNPOS = LNPOS - D
1800 IF LNPOS < QLNL THEN LNPOS = QLNL: C$ = "R"
1810 IF LNPOS > QLNR THEN LNPOS = QLNR: C$ = "L"
1820 PUT (LNPOS, QLNT), VERLN: GOTO 1720
1830 N = ((QMAXPX - QMINPX) * QSCLX * (LNPOS - QLNL)) / (QLNR -
      QLNL)
1840 N = INT((N - QX(1)) / QY(513))
1850 PUT (0, QLNB + 11), BTARY, PSET: LOCATE INT((QLNB / 200) *
      25 + 1) + 2, 1
1860 INPUT "DO YOU WISH TO MOVE THE RIGHT BORDER"; B$
1870 B$ = LEFT$(B$, 1)
1880 LNPOS = QLNR
1890 IF B$ = "N" THEN GOTO 2060
1900 IF B$ <> "Y" THEN GOTO 1850
1910 LNPOS = QLNR - 100
1920 C$ = "L"
1930 PUT (LNPOS, QLNT), VERLN
1940 PUT (0, QLNB + 11), BTARY, PSET: LOCATE INT((QLNB / 200) *
      25 + 1) + 2, 1
1950 PRINT "L-LEFT,R-RIGHT,S-STOP OR NUMBER OF SPACES "; : B$
      = INPUT$(1)
1960 D = VAL(B$) ^ 2
1970 IF D = 0 AND (B$ = "L" OR B$ = "R" OR B$ = "S") THEN C$ = B$
1980 IF C$ = "S" THEN GOTO 2060
1990 PUT (LNPOS, QLNT), VERLN
2000 IF C$ = "L" THEN LNPOS = LNPOS - D
2010 IF C$ = "R" THEN LNPOS = LNPOS + D
2020 IF LNPOS < QLNL THEN LNPOS = QLNL: C$ = "R"
2030 IF LNPOS > QLNR THEN LNPOS = QLNR: C$ = "L"
2040 PUT (LNPOS, QLNT), VERLN: GOTO 1940
2060 J = ((QMAXPX - QMINPX) * QSCLX * (LNPOS - QLNL)) / (QLNR - QLNL)
2070 J = INT((J - QX(1)) / QY(513))
2075 IF J < N THEN CC = J: J = N: N = CC
2076 IF J > 512 THEN J = 512
2077 IF N < 1 THEN N = 1
2078 CLOSE #1
2079 INPUT "CREATE A NEW FILE FOR COMP SIMU ?"; RNBANS$
2080 C$ = (LEFT$(RNBANS$, 1))
2081 IF C$ = "N" OR C$ = "" THEN GOTO 2106
2082 INPUT "CREAT 'OD' FILE (YES) ELSE CON FILE CREATED?";
      CLCANS$
2083 C$ = (LEFT$(CLCANS$, 1))
2084 IF C$ = "Y" THEN GOTO 9892
2093 INPUT "WHICH DRIVE"; DRV$: IF DRV$ = " " THEN DRV$ = "C"

```

```

2094 DRV$ = LEFT$(DRV$, 1)
2095 IF DRV$ = "A" OR DRV$ = "B" GOTO 2098
2096 IF DRV$ = "C" OR DRV$ = "D" GOTO 2098
2097 GOTO 2093
2098 DRV$ = DRV$ + ":"
2099 INPUT "FILE NAME"; FILENAME$
2100 B$ = DRV$ + LEFT$(FILENAME$, 8)
2101 OPEN "O", #1, B$
2102 FOR I = N TO J STEP 5
2103 PRINT #1, QX(I), ",", CON(I), ",",
2104 NEXT I
2105 CLOSE #1
2106 PUT (0, QLNB + 11), BTARY, PSET: LOCATE INT((QLNB / 200) *
25 + 1) + 2, 1
2110 INPUT "ORDER OF REACTION (0,1,2 or 3)"; ORDER
2120 IF ORDER < 0 OR ORDER > 3 GOTO 2100
2130 PUT (0, QLNB + 11), BTARY, PSET: LOCATE INT((QLNB / 200) *
25 + 1) + 2, 1
2140 GOSUB 3980
2150 RETURN
2160 '***** HERE COMES PLOTTER*****
2170 QQYY = 95: QQXX = 317
2180 REM qflg=0 - grid and plot , = 1 - grid only, = 2 - plot
only
2190 IF QFLG > 1 THEN 2910
2200 Q$ = "##.#"
2210 REM approximate number of vertical and horizontal
intervals
2220 QNINX = 5: QNINY = 4.8
2230 REM left and right borders
2240 QLNL = 40: QLNR = 639
2250 REM bottom and top borders
2260 QLNB = 164: QLNT = 9: QLOCX1 = 1
2270 SCREEN 2: CLS : KEY OFF
2280 QLOCY1 = INT(QLNT / 8 + .5)
2290 QLOCY2 = QLOCY1 + 1
2300 QLOCY3 = INT(QLNB / 8 + .625)
2310 QLOCY4 = QLOCY3 + 1
2320 QLOCY5 = QLOCY4 + 1
2330 QLOCX2 = INT(QLNL / 8 - 4)
2340 QLOCX3 = QLOCX2 + 1
2350 QLOCX4 = QLOCX3 + INT((QLNR - QLNL) / 8 + .625) - 1
2360 REM find "nice" x-scale intervals
2370 QMIN = QMINX: QMAX = QMAXX: QNIN = QNINX
2380 GOSUB 3500
2390 QSCLX = QSCL: QMINPX = QMINP: QMAXPX = QMAXP
2400 QNINPX = QNINP: QWDTX = QWDT
2410 REM find "nice" y-scale intervals
2420 QMIN = QMINY: QMAX = QMAXY: QNIN = QNINY
2430 GOSUB 3500
2440 QSCLY = QSCL: QMINPY = QMINP: QMAXPY = QMAXP
2450 QNINPY = QNINP: QWDTY = QWDT
2460 REM draw title

```

```

2470 LOCATE 1, 9
2480 IF FLDATA = 1 THEN DSRC$ = "DP6000"
2490 IF FLDATA = 2 THEN DSRC$ = FILENAME$
2492 RH33 = QSCLX: RH33 = RH33 * (1.0001)
2500 REM PRINT "MULTIPLY Y-AXIS BY";QSCLY;"Units
2501 PRINT "MULT. X-AXIS BY ";
2502 PRINT USING "#.##^"; RH33; : PRINT " Sec. Y-AXIS BY ";
2503 PRINT USING "#.##^"; QSCLY; : PRINT " Units. SOURCE:";
    DSRC$
2510 IF FLORD = 0 GOTO 2620
2520 LOCATE 2, 35
2530 IF ORDER = 1 THEN B$ = "ln(C)=ln(Co)-K*t"
2540 IF ORDER = 2 THEN B$ = "(1/C)=(1/Co)+K*t"
2550 IF ORDER = 3 THEN B$ = "(1/C)^2=(1/Co)^2+2*K*t"
2560 IF ORDER = 4 THEN B$ = "C=Co-K*t"
2570 PRINT B$
2580 IF B > 0 THEN LOCATE 3, 8
2590 IF B < 0 THEN LOCATE 3, INT(QLNR * 80 / 640 - .5) - 15
2600 PRINT "K="; K
2610 FLORD = 0
2620 QLOCWY = (QLOCY3 - QLOCY2 + 1) / QNINPY
2630 QLNWY = (QLNB - QLNT) / QNINPY
2640 REM draw vertical grid and labels
2650 FOR QI = 0 TO QNINPY
2660 IF QI = 0 THEN 2690
2670 LOCATE INT(QLOCY3 - QI * QLOCWY + 1), QLOCX2
2680 PRINT USING Q$; QMINPY + QI * QWDTY;
2690 QNLX1 = QNLB - QI * QLNWY
2700 NEXT QI
2710 GOSUB 3840
2720 LINE (QLNL, QNLB)-(QLNR, QNLB)
2730 QLOCWX = (QLOCX4 - QLOCX3 + 1) / QNINPX
2740 QLNWX = (QLNR - QLNL) / QNINPX
2750 REM draw horizontal grid and labels
2760 FOR QI = 0 TO QNINPX
2770 QLOC = QLOCY4
2780 LOCATE QLOC, INT(QLOCX3 + QI * QLOCWX + .5)
2790 PRINT USING Q$; QMINPX + QI * QWDTX;
2800 QNLX1 = QLNL + QI * QLNWX
2810 NEXT QI
2820 LINE (QLNL, QNLB)-(QLNL, QLNT)
2830 GOSUB 3730
2840 IF QFLG = 1 THEN RETURN
2850 REM draw qx-qy array
2860 FOR QI = N TO QN STEP QRES
2870 GOSUB 3440
2880 LINE (QX2, QY2)-(QX2, QY2), , B
2890 NEXT QI
2900 RETURN
2910 IF QSCL > 0 THEN 2930
2920 PRINT "NO GRID DRAWN, CHECK QFLG PARAMETER": RETURN
2930 FOR QI = N TO QN STEP QRES
2940 GOSUB 3440

```

```

2950 REM chek for points outside the grid
2970 IF QX2 < QLNL OR QX2 > QLNR OR QY2 > QLNB OR QY2 < QLNT
    THEN QFL2 = 1 ELSE QFL2 = 0
2980 IF QFL2 = 0 THEN LINE (QX2, QY2)-(QX2, QY2), , B
3110 NEXT QI
3430 RETURN
3440 REM routine for linear transformation from subject to
    object space
3460 QX2 = FNQSC(QX(QI) / QSCLX, QMAXPX, QMINPX, QLNR, QLNL)
3480 QY2 = FNQSC(QY(QI) / QSCLY, QMAXPY, QMINPY, QLNT, QLNB)
3490 RETURN
3500 REM routine to find "nice" scale intervals
3510 IF QMIN >= QMAX THEN BEEP: PRINT "Array can not be
    plotted": STOP
3520 QEPS = .025: QA = ABS(QMIN)
3530 IF ABS(QMIN) < ABS(QMAX) THEN QA = ABS(QMAX)
3540 QSCL = 10 ^ INT(LOG(ABS(QA)) / LOG(10))
3550 QMINA = QMIN / QSCL: QMAXA = QMAX / QSCL
3560 IF QMIN = 0 THEN QMIN = -1
3570 QD = (QMAXA - QMINA) / QNIN: QJ = QD * QEPS
3580 QE = INT(LOG(ABS(QD)) / LOG(10))
3590 QF = QD / 10 ^ QE: QV = 10
3600 IF QF < SQR(50) THEN QV = 5
3610 IF QF < SQR(10) THEN QV = 2
3620 IF QF < SQR(2) THEN QV = 1
3630 QWDT = QV * 10 ^ QE
3640 QG = INT(QMINA / QWDT)
3650 IF ABS(QG + 1 - QMINA / QWDT) < QJ THEN QG = QG + 1
3660 QMINP = QWDT * QG
3670 QH = INT(QMAXA / QWDT) + 1
3680 IF ABS(QMAXA / QWDT + 1 - QH) < QJ THEN QH = QH - 1
3690 QMAXP = QWDT * QH
3700 QNINP = QH - QG
3710 IF ABS(QMAXP) >= 10 OR ABS(QMINP) >= 10 THEN QSCL = QSCL *
    10: GOTO 3550
3720 RETURN
3730 REM routine to draw x tic marks
3740 QLNXB1 = QLNR
3750 QDTPX = INT((QLNR - QLNL) / QNINPX)
3760 QLNXB1 = QLNXB1 + QDTPX
3770 FOR QQ = 1 TO QNINPX
3780 QLNXB1 = QLNXB1 - QDTPX
3790 IF QLNXB1 < QLNL THEN RETURN
3800 QLNB3 = QLNB - 3
3810 LINE (QLNXB1, QLNB)-(QLNXB1, QLNB3)
3820 NEXT QQ
3830 RETURN
3840 REM routine to draw y tic marks
3850 QYLB1 = QLNB
3860 QDTYP = INT((QLNB - QLNT) / QNINPY)
3870 FOR QQ = 1 TO QNINPY
3880 QYLB1 = QYLB1 - QDTYP
3890 QLNL4 = QLNL + 4

```

```

3900 LINE (QLNL, QYLNBI)-(QLNL4, QYLNBI)
3920 IF QQ = QNINPY AND QDTYP = 1 THEN QQ = QQ - 34
3925 NEXT QQ
3930 RETURN
3940 '***** LINEAR REGRESSION*****
3950 INPUT "LEFT MOST BORDER (1-512)"; N
3960 INPUT "RIGHT MOST BORDER (1-512)"; J
3970 QLNB = 164
3980 DEFDBL P, S
3990 M = J - N + 1
4000 SX = 0: SY = 0: PX = 0: PY = 0: PC = 0
4010 IF ORDER < 1 OR ORDER > 4 THEN ORDER = 4
4020 FOR I = N TO J
4030 IF ORDER = 4 THEN QLY(I) = CON(I)
4040 IF ORDER = 1 THEN QLY(I) = LOG(ABS(CON(I)))
4050 IF ORDER = 2 THEN QLY(I) = 1 / CON(I)
4060 IF ORDER = 3 THEN QLY(I) = (1 / CON(I)) ^ 2
4061 RHGRFLAG = 1
4070 SX = SX + QX(I): SY = SY + QLY(I)
4080 PX = PX + QX(I) * QX(I): PY = PY + QLY(I) * QLY(I)
4090 PC = PC + QX(I) * QLY(I)
4100 NEXT I
4110 D# = M * PX - SX * SX
4120 A = (SY * PX - PC * SX) / D#
4130 B = (M * PC - SX * SY) / D#
4140 VX# = (PX - SX * SX / M) / (M - 1)
4150 VY# = (PY - SY * SY / M) / (M - 1)
4160 RR# = B * B * VX# / VY#
4170 R = SQR(RR#)
4180 E = SQR((1 - RR#) / (M - 2)) / R
4190 RE = (M - 1) * VY# * (1 - RR#)
4200 GB = ABS(E * B)
4210 GA = GB * SQR(PX / M)
4220 GP = SQR(RE / (M - 1))
4230 K = ABS(B): IF ORDER = 3 THEN K = K / 2
4240 PRINT "INTCPT="; : PRINT USING "###.##^"; A;
4250 PRINT " (STD DEV="; : PRINT USING "###.##^"; GA;
4260 PRINT ") SLOPE="; : PRINT USING "###.##^"; B;
4270 PRINT "(STD DEV="; : PRINT USING "###.##^"; GB;:PRINT ")"
4280 PRINT "R="; R; " E="; EE; " STD DEV PTS="; GP;
4290 IF R > .8 GOTO 4320
4300 PUT (0, QLNB - 64), BTARY, PSET
4305 LOCATE INT(((QLNB - 64) / 200) * 25 + 1) + 1, 1
4310 PRINT TAB(30); : PRINT "THIS IS NOT A WELL FIT CURVE"
4315 REM FOR LLKK = 1 TO 2000:MYBADD0G=LOG(LLKK):NEXT
4320 IF INKEY$ = "" THEN 4320
4330 PUT (0, QLNB + 11), BTARY, PSET: LOCATE INT((QLNB / 200) *
25 + 1) + 2, 1
4340 INPUT "WOULD YOU LIKE A PLOT OF THE RESULTS"; B$
4350 B$ = LEFT$(B$, 1)
4360 IF B$ = "N" THEN RETURN
4370 PUT (0, QLNB + 11), BTARY, PSET: LOCATE INT((QLNB / 200) *
25 + 1) + 2, 1

```

```

4380 IF B$ <> "Y" THEN GOTO 4330
4390 FLORD = 1
4400 INPUT "WHAT RESOLUTION WOULD YOU LIKE TO GRAPH (1 TO 10)";
      QRES
4405 IF QRES < 1 OR QRES > 20 THEN QRES = 1
4410 FOR I = N TO J
4420 CC = QY(I)
4430 QY(I) = QLY(I)
4440 QLY(I) = CC
4450 NEXT I
4460 QFLG = 0: QMINX = QX(N): QMAXX = QX(J): QMINY = QY(N)
4465 QMAXY = QY(J): QN = J
4470 QYN = B * QX(N) + A
4480 QYJ = B * QX(J) + A
4490 IF B < 0 GOTO 4520
4500 IF QYN < QY(N) THEN QMINY = QYN ELSE QMINY = QY(N)
4510 IF QYJ > QY(J) THEN QMAXY = QYJ ELSE QMAXY = QY(J)
4520 IF B > 0 GOTO 4550
4530 IF QYN > QY(N) THEN QMAXY = QYN ELSE QMAXY = QY(N)
4540 IF QYJ < QY(J) THEN QMINY = QYJ ELSE QMINY = QY(J)
4550 GOSUB 2160
4560 QYN = FNQSC(QYN / QSCLY, QMAXPY, QMINPY, QLNT, QLNB)
4570 QXN = FNQSC(QX(N) / QSCLX, QMAXPX, QMINPX, QLNR, QLNL)
4580 QY2 = FNQSC(QYJ / QSCLY, QMAXPY, QMINPY, QLNT, QLNB)
4590 QX2 = FNQSC(QX(J) / QSCLX, QMAXPX, QMINPX, QLNR, QLNL)
4600 LINE (QXN, QYN)-(QX2, QY2)
4610 FOR I = N TO J
4620 CC = QY(I)
4630 QY(I) = QLY(I)
4640 QLY(I) = CC
4650 NEXT I
4660 QMINX = QX(1): QMAXX = QX(512): QMINY = QY(515)
4665 QMAXY = QY(514): QN = 512
4670 FLLOOP = 1 + FLLOOP
4680 IF FLLOOP > 1 THEN GOTO 4765 ELSE GOSUB 1570
4690 PUT (0, QLNB + 11), BTARY, PSET
4695 LOCATE INT((QLNB / 200) * 25 + 1) + 2, 1
4700 PRINT "INTCPT="; : PRINT USING "###.##^"; A;
4710 PRINT " (STD DEV="; : PRINT USING "###.##^"; GA;
4720 PRINT "( SLOPE="; : PRINT USING "###.##^"; B;
4730 PRINT " (STD DEV="; :PRINT USING "###.##^"; GB;:PRINT ")"
4740 PRINT "R="; R; " E="; EE; " STD DEV PTS="; GP;
4745 REM FOR LLKK = 1 TO 2000:MYBADD0G=LOG(LLKK):NEXT
4750 IF INKEY$ = "" THEN GOTO 4750
4760 FLLOOP = 0
4765 REM GOSUB 1570
4770 RETURN
4780 '***** SAVE *****
4790 CLOSE #1
4800 IF FLDATA > 0 THEN GOTO 4820
4810 PRINT "NO DATA SOURCE. RETURNING TO MENU": GOTO 4910
4820 IF FLDATA = 2 THEN PRINT "DATA PREVIOUSLY SAVED"
4821 INPUT "SAVE AGAIN UNDER ANOTHER NAME? "; RJHANS$

```



```

4822 IF LEFT$(RJHANS$, 1) = "N" THEN GOTO 4900
4823 INPUT "WHICH DRIVE "; DRV$: IF DRV$ = "" THEN DRV$ = "C"
4824 DRV$ = LEFT$(DRV$, 1)
4825 IF DRV$ = "A" OR DRV$ = "B" GOTO 4829
4826 IF DRV$ = "C" OR DRV$ = "D" GOTO 4829
4827 GOTO 4823
4829 DRV$ = DRV$ + ":"
4830 INPUT "FILENAME "; FILENAME$
4840 B$ = DRV$ + LEFT$(FILENAME$, 8)
4850 OPEN "O", #1, B$
4860 SIZE = 518
4870 FOR I = 1 TO SIZE STEP 5
4880 PRINT #1, QY(I), QY(I + 1), QY(I + 2), QY(I + 3), QY(I + 4)
4890 NEXT I
4900 CLOSE #1
4910 OPEN "com1:9600,n,8,1,cs,ds,cd" FOR RANDOM AS #1
4920 FLDATA = 2
4930 RETURN
4940 '***** LOAD *****
4950 CLOSE #1
4951 INPUT "WHICH DRIVE "; DRV$: IF DRV$ = "" THEN DRV$ = "C"
4952 DRV$ = LEFT$(DRV$, 1)
4953 IF DRV$ = "A" OR DRV$ = "B" GOTO 4959
4954 IF DRV$ = "C" OR DRV$ = "D" GOTO 4959
4955 GOTO 4951
4959 DRV$ = DRV$ + ":"
4960 INPUT "FILENAME"; FILENAME$
4970 B$ = DRV$ + LEFT$(FILENAME$, 8)
4980 OPEN "I", #1, B$
4982 ON ERROR GOTO 5230
4990 SIZE = 518
5000 FOR I = 1 TO SIZE STEP 5
5010 INPUT #1, QY(I), QY(I + 1), QY(I + 2), QY(I + 3), QY(I + 4)
5020 NEXT I
5030 PER = QY(513): QMAXY = QY(514): QMINY = QY(515)
5035 V0 = QY(516): VM = QY(517): L = QY(518): EE = QY(519)
5040 PRINT "FILE "; B$; " FOUND."
5050 CLOSE #1
5060 OPEN "com1:9600,n,8,1,cs,ds,cd" FOR RANDOM AS #1
5061 LEFF = 2.303 * L * EE: VFULL = VM - V0
5062 PRINT "V0,VM,VFULL,L,LEFF,E": PRINT V0, VM, VFULL, L; "
    "; LEFF, EE
5063 INPUT "WANT TO CHANGE V0,VM,L,OR E "; ANANS$
5064 IF ANANS$ = "Y" THEN GOSUB 8000
5068 LEFF = 2.303 * L * EE: VFULL = VM - V0
5070 REM FOR ZSAM = 1 TO 5000: ZSAM = LOG(ZSAM): NEXT
5085 FOR I = 1 TO 512
5088 QX(I) = I * PER
5090 CON(I) = -LOG(ABS((QY(I) - V0) / VFULL)) / LEFF
5092 OD(I) = -LOG(ABS((QY(I) - V0) / VFULL)) / 2.303
5095 REM PRINT CON(I)
5100 NEXT I
5110 FLDATA = 2

```

```

5115 RHGRFLAG = 1
5120 RETURN
5130 '***** N'th ORDER *****
5140 PRINT : PRINT "CHOOSE THE ORDER OF THE REACTION": PRINT
5150 PRINT "1) FIRST ORDER           $\ln(C)=\ln(C_0)-K*t$ "
5160 PRINT "2) SECOND ORDER          $(1/C)=(1/C_0)+K*t$ "
5170 PRINT "3) THIRD ORDER           $(1/C)^2=(1/C_0)^2+2*K*t$ "
5180 PRINT "4) ABSORBANCE ONLY       $C=C_0-K*t$ ": PRINT
5190 INPUT "WHICH NUMBER"; ORDER
5200 IF ORDER < 1 OR ORDER > 4 GOTO 5140
5210 RETURN
5220 '***** ERROR *****
5230 'IF(57=ERR)AND(180 > ERL) THEN RESUME 160
5240 IF 57 = ERR THEN PRINT"DP600 OR DISK I/O ERROR":RESUME 140
5250 IF 53 = ERR GOTO 5290
5255 IF 4970 = ERL THEN GOTO 5290
5256 IF 4980 = ERL THEN GOTO 5290
5260 REM PRINT "STOP": PRINT ERR, ERL
5270 REM IF ERR=6 THEN BAD=ERL:GOTO ERL
5280 RESUME NEXT
5290 PRINT "FILE "; B$; " NOT FOUND"
5300 FILENAME$ = ""
5310 CLOSE #1
5320 RESUME 4950
5330 '***** COMPARE *****
5340 INPUT "HOW MANY PLOTS DO YOU WISH TO MAKE (1 TO 3)"; NOPLO
5350 IF NOPLO < 1 OR NOPLO > 3 GOTO 5340
5360 PRINT : PRINT "LOAD FIRST DATA SET FROM DISK": PRINT
5370 GOSUB 4940          'LOAD
5380 GOSUB 1480          'PLOTTER
5390 N1 = N: J1 = J
5400 DIM QY1(515)
5410 FOR I = N TO J
5420 QY1(I) = QLY(I)
5430 NEXT I
5440 IF B < 0 GOTO 5460
5450 QY1(515) = QY1(N): QY1(514) = QY1(J): GOTO 5470
5460 QY1(515) = QY1(J): QY1(514) = QY1(N)
5470 IF NOPLO = 1 GOTO 5750
5480 PRINT : PRINT "LOAD SECOND DATA SET FROM DISK": PRINT
5490 GOSUB 4940          'LOAD
5500 GOSUB 1480          'PLOTTER
5510 N2 = N: J2 = J
5520 DIM QY2(J)
5530 FOR I = N TO J
5540 QY2(I) = QLY(I)
5550 NEXT I
5560 IF B < 0 GOTO 5590
5570 IF QY2(N) < QY1(515) THEN QY1(515) = QY2(N)
5580 IF QY2(J) > QY1(514) THEN QY1(514) = QY2(J)
5585 GOTO 5610
5590 IF QY2(N) > QY1(514) THEN QY1(514) = QY2(N)
5600 IF QY2(J) < QY1(515) THEN QY1(515) = QY2(J)

```

```

5610 IF NOPLO = 2 GOTO 5750
5620 PRINT : PRINT "LOAD THIRD DATA SET FROM DISK": PRINT
5630 GOSUB 4940          'LOAD
5640 GOSUB 1480          'PLOTTER
5650 N3 = N: J3 = J
5660 DIM QY3(J)
5670 FOR I = N TO J
5680 QY3(I) = QLY(I)
5690 NEXT I
5700 IF B < 0 GOTO 5730
5710 IF QY3(N) < QY1(515) THEN QY1(515) = QY3(N)
5720 IF QY3(J) > QY1(514) THEN QY1(514) = QY3(J)
5725 GOTO 5750
5730 IF QY3(N) > QY1(514) THEN QY1(514) = QY3(N)
5740 IF QY3(J) < QY1(515) THEN QY1(515) = QY3(J)
5750 N = N1: J = J1
5760 IF N2 < N1 AND NOPLO > 1 THEN N = N2
5770 IF J2 > J1 AND NOPLO > 1 THEN J = J2
5780 IF N3 < N AND NOPLO > 2 THEN N = N3
5790 IF J3 > J AND NOPLO > 2 THEN J = J3
5800 QFLG = 0: FLORD = 0: QMINX = QX(N): QMAXX = QX(J)
5805 QMINY = QY1(515): QMAXY = QY1(514): QN = J1: N = N1
5810 PRINT : INPUT "WHAT RESOLUTION WOULD YOU LIKE TO GRAPH (1
      TO 10)"; QRES
5820 FOR I = N1 TO J1
5830 QY(I) = QY1(I)
5840 NEXT I
5850 ERASE QY1
5860 FLORD = 0
5870 GOSUB 2170
5880 LOCATE 1, 59
5890 PRINT "
5900 IF NOPLO = 1 GOTO 6040
5910 QFLG = 2: QN = J2: N = N2
5920 FOR I = N2 TO J2
5930 QY(I) = QY2(I)
5940 NEXT I
5950 ERASE QY2
5960 GOSUB 2170
5970 IF NOPLO = 2 GOTO 6040
5980 QN = J3: N = N3
5990 FOR I = N3 TO J3
6000 QY(I) = QY3(I)
6010 NEXT I
6020 GOSUB 2170
6030 ERASE QY3
6040 PUT (0, QLNB + 11), BTARY, PSET: LOCATE INT((QLNB / 200) *
      25 + 1) + 2, 1
6050 PRINT "YOU WILL NEED A NEW DATA SOURCE AFTER RETURNING TO
      MENU"
6060 IF INKEY$ = "" THEN GOTO 6060
6070 PUT (0, QLNB + 11), BTARY, PSET: LOCATE INT((QLNB / 200) *
      25 + 1) + 2, 1

```

```

6080 PRINT "PRESS ANY KEY ONCE TO GET A SCREEN DUMP"
6085 PRINT "TWICE TO RETURN TO MENU";
6090 IF INKEY$ = "" THEN GOTO 6090
6100 PUT (0, QLNB + 11), BTARY, PSET: LOCATE INT((QLNB / 200) *
    25 + 1) + 2, 1
6110 IF INKEY$ = "" THEN GOTO 6110
6120 FLDATA = 0
6130 RETURN
7000 REM SUBROUTINE GET INFO
7040 '
7070 CLS
7080 REM OPEN "com1:9600,n,8,1,cs,ds,cd" AS #1
7100 BOUT$ = B$
7110 PRINT #1, BOUT$
7120 FOR I = 1 TO 1500: QWERT1 = QWERT1 + 1
7140 NEXT I
7150 J = 1
7160 V = LOC(1): IF V < 1 THEN PRINT "NO MESSAGE": GOTO 7350
7170 FOR ZQQZ = 1 TO 500: FF = ZQQZ * ZQQZ: NEXT
7180 AGI$(J) = INPUT$(V, #1)
7190 ON ERROR GOTO 5220
7200 V = LOC(1): IF V < 1 THEN GOTO 7230
7210 J = J + 1
7220 GOTO 7160
7230 FOR HH = 1 TO J
7240 BGI$(HH) = ""
7250 REM PRINT AGI$(HH), VAL(AGI$(HH))
7260 FOR UU = 1 TO LEN(AGI$(HH))
7270 QAQ$ = MID$(AGI$(HH), 1)
7280 ZORP$ = BGI$(HH)
7285 IF ASC(QAQ$) = 45 THEN GOTO 7300
7290 IF ASC(QAQ$) < 48 OR ASC(QAQ$) > 91 THEN GOTO 7330
7300 BGI$(HH) = BGI$(BB) + QAQ$
7310 NEXT UU
7320 NEXT HH
7330 MYINFO = VAL(ZORP$)
7350 RETURN
8000 REM CHANGE V0,VMAX *****
8010 INPUT "DO YOU WANT TO CHECK ACTUAL VOLTAGE VALUES OF
    DATASET"; ANANS$
8020 IF LEFT$(ANANS$, 1) = "N" THEN GOTO 8090
8030 INPUT "FIRST , LAST DATA TO USE "; POINT1, POINT2
8035 TEMPSUM = 0
8040 FOR KZ = POINT1 TO POINT2
8050 TEMPSUM = TEMPSUM + QY(KZ)
8060 NEXT KZ
8070 VNOW = TEMPSUM / (POINT2 - POINT1 + 1)
8080 PRINT "AVERAGE VOLTAGE FOR THAT RANGE IS "; VNOW
8090 INPUT "CHANGE V0 "; ANANS$
8100 IF ANANS$ = "N" THEN GOTO 8200
8110 INPUT "NEW V0"; V0
8200 INPUT "CHECK VOLTAGES AGAIN "; ANANS$
8210 IF LEFT$(ANANS$, 1) = "Y" THEN GOTO 8030

```

```

8240 INPUT "CHANGE VM "; ANANS$
8250 IF ANANS$ = "N" THEN GOTO 8300
8260 INPUT "NEW VMAX "; VM
8270 VFULL = VM - V0
8300 PRINT "L IS NOW "; L: INPUT "CHANGE L "; ANANS$
8320 IF ANANS$ = "N" THEN GOTO 8400
8330 INPUT "NEW L"; L
8400 PRINT "E IS NOW "; EE: INPUT "CHANGE E "; ANANS$
8420 IF ANANS$ = "N" THEN GOTO 8500
8430 INPUT "NEW E "; EE
8500 LEFF = 2.303 * L * EE: VFULL = VM - V0
8510 QY(516) = V0: QY(517) = VM: QY(518) = L: QY(519) = EE
8520 PRINT "V0,VM,VFULL,L,LEFF,E": PRINT V0, VM, VFULL, L; "
    "; LEFF, EE
8515 IF VFULL = 0 OR LEFF = 0 THEN PRINT "BAD CONSTS. ": GOTO
    8010
8530 FOR I = 1 TO 512
8540 QX(I) = I * PER
8550 CON(I) = -LOG(ABS((QY(I) - V0) / VFULL)) / LEFF
8560 REM PRINT CON(I)
8570 NEXT I
8580 FLDATA = 2
8600 RETURN
9800 REM *****DISK DIR*****
9810 CLOSE #1
9820 INPUT "WHICH DRIVE "; DRV$: IF DRV$ = "" THEN DRV$ = "C"
9830 DRV$ = LEFT$(DRV$, 1)
9840 IF DRV$ = "A" OR DRV$ = "B" GOTO 9870
9850 IF DRV$ = "C" OR DRV$ = "D" GOTO 9870
9860 GOTO 9820
9870 MYCALL$ = DRV$ + ":"
9875 FILES MYCALL$
9880 OPEN "com1:9600,n,8,1,cs,ds,cd" FOR RANDOM AS #1
9890 RETURN
9892 INPUT "WHICH DRIVE"; DRV$: IF DRV$ = " " THEN DRV$ = "C"
9894 DRV$ = LEFT$(DRV$, 1)
9896 IF DRV$ = "A" OR DRV$ = "B" GOTO 9905
9898 IF DRV$ = "C" OR DRV$ = "D" GOTO 9905
9900 GOTO 9892
9905 DRV$ = DRV$ + ":"
9910 INPUT "FILE NAME"; FILENAME$
9915 B$ = DRV$ + LEFT$(FILENAME$, 8)
9920 OPEN "O", #1, B$
9925 FOR I = N TO J STEP 5
9930 PRINT #1, QX(I), ",", OD(I), ","
9940 NEXT I
9945 CLOSE #1
9946 GOTO 2106
9999 END

```

## REFERENCES

1. Ramirez, J. E.; Bera, R. K.; Hanrahan, R. J. "Measurement of Kinetic Parameters Relevant to the Operation of an Electron-beam Initiated Atomic Iodine Laser," J. Appl. Phys. 1985, 57(7), 2431.
2. Ramirez, J. E.; Bera, R. K.; Hanrahan, R. J. "Formation of Ground State Ozone on Pulse Radiolysis of Oxygen," Radiat. Phys. Chem. 1984, 23(6), 685.
3. Bera, R. K.; Hanrahan, R. J. "Investigation of OH Dynamics in the Argon Sensitized Pulse Radiolysis of Water Vapor," J. Appl. Phys. 1986, 60(6), 2115.
4. Bera, R. K.; Hanrahan, R. J. "Investigation of OH-H<sub>2</sub> and OH-CO Reactions Using Argon-Sensitized Pulse Radiolysis," J. Appl. Phys. 1987, 62(6), 2523.
5. Bera, R. K.; Hanrahan, R. J. "Investigation of Gas Phase Reactions of OH Radicals with Fluoromethane and Difluoromethane Using Ar-Sensitized Pulse Radiolysis," Radiat. Phys. Chem 1988, 32(3), 579.
6. McCarthy, R. L.; MacLachlan, A. "Transient Benzyl Radical Reactions Produced by High-Energy Radiation," Trans. Faraday Soc. 1960, 56, 1187.
7. Matheson, M. S.; Dorfman, L. M. "Detection of Short-Lived Transients in Radiation Chemistry," J. Chem. Phys. 1960, 32, 1987.
8. Ebert, M.; Keen, J. P.; Swallow, A. J. Pulse Radiolysis, Academic Press: New York, New York, 1965.
9. Matheson, M. S.; Dorfman, L. M. Pulse Radiolysis, The MIT Press: Cambridge, Massachusetts, 1969.
10. Matheson, M. S. "Pulse Radiolysis," in Advances in Radiation Research, Physics and Chemistry, J. F. Duplan and A. Chapiro, eds., Vol. 1, Gordon and Breach Science Publishers: New York, New York, 1973.
11. Tabata, Y., ed. CRC Handbook of Radiation Chemistry, CRC Press: Boca Raton, Florida, 1991; Chapters 2 and 3.

12. Verma, N. C.; Fessenden, R. W. "Time Resolved ESR Spectroscopy. II. The Behavior of H Atom Signals," J. Chem. Phys. 1973, 58(6), 2501.
13. Fessenden, R. W. "Time Resolved ESR Spectroscopy. I. A Kinetic Treatment of Signal Enhancements," J. Chem. Phys. 1973, 58(6), 2489.
14. Trifunac, A. D.; Norris, J. R.; Lawler, R. G. "Nano-second Time-Resolved EPR in Pulse Radiolysis via the Spin Echo Method," J. Chem. Phys. 1979, 71(11), 4380.
15. Maughan, R. L.; Michael, B. D.; Anderson, R. F. "The Application of Wide Band Transformers to the Study of Transient Conductivity in Pulse Irradiated Aqueous Solutions by the D.C. Method," Radiat. Phys. Chem. 1978, 11, 229.
16. Janata, E. "Submicrosecond Pulse Radiolysis Conductivity Measurements in Aqueous Solutions--I," Radiat. Phys. Chem. 1980, 16, 37.
17. Janata, E.; Veltwisch, D.; Asmus, K.-D. "Submicrosecond Pulse Radiolysis Conductivity Measurements in Aqueous Solutions--II," Radiat. Phys. Chem., 1980, 16, 43.
18. Hodgson, B. W.; Keene, J. P.; Land, E. J.; Swallow, A. J. "Light-Induced Fluorescence of Short-Lived Species Produced by a Pulse of Radiation: The Benzophenone Ketyl Radical," J. Chem. Phys. 1975, 63(8), 3671.
19. Dallinger, R. F.; Guanci, J. J.; Woodruff, W. H.; Rodgers, M. A. J. "Vibrational Spectroscopy of the Electronically Excited State: Pulse Radiolysis/Time-Resolved Resonance Raman Study of Triplet (beta)-Carotene," J. Am. Chem. Soc. 1979, 101, 1355.
20. Lee, P. C.; Schmidt, K.; Gordon, S.; Meisel, D. "Resonance Raman of Viologen Radicals," Chem. Phys. Lett. 1981, 80(2), 242.
21. Pagsberg, P.; Wilbrandt, R.; Hansen, K. B.; Weisberg, K. V. "Fast Resonance Raman Spectroscopy of Short-Lived Radicals," Chem. Phys. Lett. 1976, 39(3), 538.
22. Swallow, A. J. Radiation Chemistry: An Introduction, John Wiley & Sons: New York, New York, 1973; Chapters 4 and 7.
23. Hammes, G. G., ed. Techniques of Chemistry, Vol. VIB, Wiley-Interscience: New York, New York, 1974.

24. Bronskill, M. J.; Hunt, J. W. "A Pulse Radiolysis System for the Observation of Short-Lived Transients," J. Phys. Chem. 1968, 72, 3762.
25. Firestone, R. F.; Dorfman, L. M. "Pulse Radiolysis of Gases," in Actions Chimiques et Biologiques des Radiations, M. Haissinsky, ed., Vol. 15, Masson, Paris, 1971.
26. Sauer, M. C., Jr. "Pulse Studies of Gases," in Advances in Radiation Chemistry, M. Burton, J. L. Magee, eds., Vol. 5, John Wiley & Sons: New York, New York, 1976.
27. Adams, G. E.; Fielden, E. M.; Michael, B. D., eds. Fast Processes in Radiation Chemistry and Biology, John Wiley & Sons: New York, New York, 1975.
28. Baxendale, J. H.; Busi, F., eds. The Study of Fast Processes and Transient Species by Electron Pulse Radiolysis, D. Reidel: Dordrecht, Holland, 1982.
29. Paterson, L. K.; Lilie, J. "A Computer-Controlled Pulse Radiolysis System," Int. J. Radiat. Phys. Chem. 1974, 6, 129.
30. Hodgson, B. W.; Keene, J. P. "Some Characteristics of a Pulsed Xenon Lamp for Use as a Light Source in Kinetic Spectrophotometry," Rev. Sci. Instr. 1972, 43(3), 493.
31. Luthjens, L. H. "High Intensity Pulsed Analyzing Light Sources for Nano- and Micro-second Absorption Spectrophotometry," Rev. Sci. Instrum. 1973, 44(11), 1661.
32. Fenger, J. "Intensity Stabilized Pulsed Analyzing Lamp for Ultraviolet Transient Spectrometry," Rev. Sci. Instrum. 1981, 52(12), 1847.
33. Thornton, A. T.; Laurence, G. S. "Computer-Based Systems for the Acquisition and Treatment of Kinetic Data from Flash Photolysis, Laser Photolysis and Pulse Radiolysis Experiments," Radiat. Phys. Chem. 1978, 11, 311.
34. Crumpton, S. C.; Adler, M. S.; Ramirez, J. E.; Hanrahan, R. J. "Microcomputer-Based Data Acquisition System for Fast Chemical Kinetics," in Personal Computers in Chemistry, P. Lykos, ed., John Wiley & Sons: New York, New York, 1981.



35. Foyt, D. C. "Data Acquisition and Analysis in Pulse Radiolysis Part I: Control, Digitization, and Analysis; Part II: Computerization," in J. H. Baxendale and Fabio Busi, eds., The Study of Fast Processes and Transient Species by Electron Pulse Radiolysis, D. Reidel: Dordrecht, Holland, 1982.
36. Allen, A. O. The Radiation Chemistry of Water and Aqueous Solutions, D. Van Nostrand Company, Inc.: Princeton, New Jersey, 1961.
37. Hart, E. J.; Anbar, M. The Hydrated Electron, Wiley-Interscience: New York, New York, 1970.
38. Draganic, I. G.; Draganic, Z. D. The Radiation Chemistry of Water, Academic Press: New York, New York, 1971.
39. Hunt, J. W., in Advances in Chemistry, M. Burton and J. L. Magee, eds., Volume 5, Wiley Interscience: New York, New York, 1976, pp. 185-315.
40. Spinks, J. W. T.; Woods, R. J. An Introduction to Radiation Chemistry, 3rd. ed.; John Wiley & Sons: New York, New York, 1990; Chapters 3, 7, and 8.
41. Benssason, R. V.; Land, E. J.; Truscott, T. G. Flash Photolysis and Pulse Radiolysis Contributions to the Chemistry of Biology and Medicine, Pergamon Press: New York, New York, 1983.
42. Glasstone, S.; Sesonske, A. Nuclear Engineering, 3rd. ed., Van Nostrand Reinhold Co.: New York, New York, 1981; Chapter 7.
43. Buxton, G. V. "Radiation Chemistry of the Liquid State: (1) Water and Homogeneous Aqueous Solutions," in Radiation Chemistry: Principles and Applications, Farhataziz and M. A. J. Rodgers, eds., VCH: New York, New York, 1987.
44. Chatterjee, A.; Magee, J. L. "Track Models and Radiation Chemical Yields," in Radiation Chemistry: Principles and Applications, Farhataziz and M. A. J. Rodgers, eds., VCH: New York, New York, 1987.
45. Magee, J. L.; Chatterjee, A. "Theoretical Aspects of Radiation Chemistry," in Radiation Chemistry: Principles and Applications, Farhataziz and M. A. J. Rodgers, eds., VCH: New York, New York, 1987.

46. Rotblat, J.; Sutton, H. C. "The Effects of High Dose Rates of Ionizing Radiations on Solutions of Iron and Cerium Salts," Proc. Roy. Soc. (London) Ser. A255 1960, 490.
47. Thomas, J. K.; Hart, E. J. "The Radiolysis of Aqueous Solutions at High Intensities," Radiation Research 1962, 17, 408.
48. Thomas, J. K. "The Nature of the Reducing Species in the Radiolysis of Acidic Aqueous Solutions at High Intensities," Int. Journal Appl. Rad. and Isotopes 1965, 16, 451.
49. Anderson, A. R.; Hart, E. J. "Radiation Chemistry of Water with Pulsed High Intensity Electron Beams," J. Phys. Chem. 1962, 66, 70.
50. Buxton, G. V. "Applications of Water Radiolysis in Inorganic Chemistry," in J. H. Baxendale and Fabio Busi, eds., The Study of Fast Processes and Transient Species by Electron Pulse Radiolysis, D. Reidel: Dordrecht, Holland, 1982.
51. Fendler, E. J.; Fendler, J. H., in Progress in Physical Organic Chemistry; A. Streitwieser and R. W. Taft, eds., Volume 7, Interscience: New York, New York, 1970, p. 229.
52. Neta, P., in Advances in Physical Organic Chemistry; V. Gold and D. Bethell, eds., Volume 12, Academic Press: New York, New York, 1976, p. 224.
53. Swallow, A. J. "Reactions of Free Radicals Produced from Organic Compounds in Aqueous Solution by Means of Radiation," Prog. React. Kinet. 1978, 9, 195.
54. Eiben, K.; Fessenden, R. W. "Electron Spin Resonance Studies of Transient Radicals in Aqueous Solutions," J. Phys. Chem. 1971, 75(9), 1186.
55. Dorfman, L. M.; Taub, I. A.; Buhler, R. E. "Pulse Radiolysis Studies. I. Transient Spectra and Reaction-Rate Constants in Irradiated Aqueous Solutions of Benzene," J. Chem. Phys. 1962, 36(11), 3051.
56. Sauer, M. C.; Ward, B. "The Reactions of Hydrogen Atoms with Benzene and Toluene Studied by Pulsed Radiolysis: Reaction Rate Constants and Transient Spectra in the Gas Phase and Aqueous Solution," J. Phys. Chem. 1967, 71, 3971.

57. Studier, M. H.; Hart, E. J. "The Reduction of Benzene by Hydrated Electrons in (gamma)-Ray Irradiated Alkaline Solutions," J. Am. Chem. Soc. 1969, 91, 4068.
58. Marketos, D. G.; Marketou-Mantaka, A.; Stein, G. "Reaction of the Hydrated Electron with Benzene Studied by Pulse Radiolysis," J. Phys. Chem. 1974, 78, 1987.
59. Dorfman, L. M.; Taub, I. A.; Harter, D. A. "Rate Constants for the Reaction of the Hydroxyl Radical with Aromatic Molecules," J. Phys. Chem. 1964, 41, 2954.
60. Marketos, D. G.; Marketou-Mantaka, A.; Stein, G. "Continuous  $\gamma$  and Pulse Radiolysis of Aqueous Benzene Solutions: Some Reactions of the Hydroxycyclohexadienyl Radical," J. Phys. Chem. 1971, 75, 3886.
61. Buxton, G. V.; Langan, J. R.; Lindsay Smith, J. R. "Aromatic Hydroxylation. 8. A Radiation Chemical Study of the Oxidation of Hydroxycyclohexadienyl Radicals," J. Phys. Chem. 1986, 90, 6309.
62. Bhatia, K. "Reactions of the Radiolytically Generated Hydroxycyclohexadienyl Radical in Aqueous Benzene Systems," Radiation Research 1974, 59, 537.
63. Klein, G. W.; Schuler, R. H. "Oxidation of Benzene by Radiolytically Produced OH Radicals," Radiat. Phys. Chem. 1978, 11, 167.
64. Eberhardt, M. K. "Radiation Induced Homolytic Aromatic Substitution. II. Hydroxylation and Phenylation of Benzene," J. Phys. Chem. 1974, 78(18), 1795.
65. Eberhardt, M. K. "Radiation-Induced Homolytic Aromatic Substitution. III. Hydroxylation and Nitration of Benzene," J. Phys. Chem. 1975, 79(11), 1067.
66. Balakrishnan, I.; Reddy, M. P. "Mechanism of Reaction of Hydroxyl Radicals with Benzene in the (gamma) Radiolysis of the Aerated Aqueous Benzene System," J. Phys. Chem. 1970, 74, 850.
67. Srinivasan, T. K. K.; Balakrishnan, I.; Reddy, M. P. "On the Nature of the Products of (gamma) Radiolysis of Aerated Aqueous Solutions of Benzene," J. Phys. Chem. 1969, 73, 2071.
68. Gupta, A. K.; Hanrahan, R. J.; Walker, D. D. "Radiolysis of Sodium and Potassium Tetraphenylborate in Aqueous Systems," J. Phys. Chem. 1991, 95, 3590.

69. Cohen, B. L. "The Disposal of Radioactive Wastes from Fission Reactors," Scientific American, 1977, 236(6), 21.
70. Goldsmith, W. A.; Teichert, W. P.; Allen, D. F.; Ragan, C. C.; Monk, T. H., "Feasibility Study of Alternative Treatment Methods for MVST Supernatant at ORNL," in Analysas Corp., Oak Ridge, TN, CONF-881054 1988, 1988 DOE Model Conference Proceedings. Volume 1, pp 191-202.
71. Bray, L. A.; Elovich, R. J.; Carson, K. J. "Cesium Recovery Using Savannah River Laboratory Resorcinol-Formaldehyde Ion Exchange Resin," PNL-7273 1990, Pacific Northwest Lab., Richland, WA, 17 pp.
72. Glasstone, S.; Jordan, W. H. Nuclear Power and Its Environmental Effects, 3rd. ed.; American Nuclear Society: La Grange Park, Illinois, 1986; Chapters 9 and 10.
73. Lennemann, W. L. "Management of Radioactive Wastes from AEC Fuel-Reprocessing Operations," Nuclear Safety 1973, 14(5), 482.
74. Flaschka, H.; Barnard, A. J., Jr., in Advances in Analytical Chemistry and Instrumentation; Reilley, C. N., ed., Volume 1, Interscience: New York, New York, 1960.
75. Horii, H.; Taniguchi, S. "Oxidation Intermediates of Borohydride and Tetraphenylborate Ions in Aqueous Solutions Obtained by Pulse Radiolysis," J. Chem. Soc., Chem. Commun. 1986, 12, 915.
76. Liu, K. J.; Langan, J. R.; Salmon, G. A.; Holton, D. M.; Edwards, P. P. "Pulse Radiolysis of Solutions of Sodium Tetraphenylborate," J. Phys. Chem. 1988, 92(9), 2449.
77. Beaumond, D.; Rodgers, M. A. J. "Pulse Radiolysis Studies of Ion Association," Trans. Faraday Soc. 1969, 65(11), 2973.
78. Catterall, R.; Slater, J.; Seddon, W. A.; Fletcher, J. W. "Correlation of Optical and Electron Spin Resonance Spectra for Alkali Metal Solutions in Ethylamine and Tetrahydrofuran," Can. J. Chem. 1976, 54(19), 3110.
79. Seddon, W. A.; Fletcher, J. W.; Catterall, R.; Sopchyshyn, F. C. "The Effect of Coordination on the Optical Spectra of Alkali Metal Cation-Electron Pairs in Ethers," Chem. Phys. Lett. 1977, 48(3), 584.

80. Guy, S. C.; Edwards, P. P.; Salmon, G. A. "Solvated Electrons and Electron-Cation Aggregates in N,N-diethylacetamide, N,N-dipropylacetamide, N,N-dimethylpropanamide, Tetramethylurea, and Tetraethylurea," J. Chem. Soc., Chem. Commun. 1982, 21, 1257.
81. Yamamoto, Y.; Nishida, S.; Ma, X. H.; Hayashi, K. "Pulse Radiolysis of Trans-Stilbene in Tetrahydrofuran. Spectral Shift and Decay Kinetics of the Radical Anions in the Presence of Quaternary Ammonium Salts," J. Phys. Chem. 1986, 90(9), 1921.
82. Langan, J. R.; Liu, K. J.; Salmon, G. A.; Edwards, P. P.; Ellaboudy, A.; Holton, D. M. "The Radiation Chemistry of Organic Amides I. A Pulse Radiolysis Study of Solvated Electrons and Alkali-Metal-Electron Species in Cyclic Amides," Proc. R. Soc. London, A 1989, 421(1860), 169.
83. Williams, J. L. R.; Doty, J. C.; Grisdale, P. J.; Regan, T. H.; Borden, D. G. "Boron Photochemistry: 1-Phenyl-1,4-cyclohexadiene from Sodium Tetraphenylborate," Chem. Commun. 1967, 3, 109.
84. Williams, J. L. R.; Doty, J. C.; Grisdale, P. J.; Searle, R.; Regan, T. H.; Happ, G. P.; Maier, D. P. "Boron Photochemistry. I. Irradiation of Sodium Tetraarylborates in Aqueous Solution," J. Am. Chem. Soc. 1967, 89(20), 5153.
85. Williams, J. L. R.; Doty, J. C.; Grisdale, P. J.; Regan, T. H.; Happ, G. P.; Maier, D. P. "Boron Photochemistry. II. Irradiation of Sodium Tetraarylborates in Alcohol Studies," J. Am. Chem. Soc. 1968, 90(1), 53.
86. Eisch, J. J.; Tamao, K.; Wilcsek, R. J. "Rearrangements of Organometallic Compounds. XII. Generation of Boracarbenoid and Boracyclopentene Intermediates from the Photolysis of Tetraorganoborate Salts in Aprotic Media," J. Am. Chem. Soc. 1975, 97(4), 895.
87. Wilkey, J. D.; Schuster, G. B. "Irradiation of Tetraphenylborate Does Not Generate a Borene Anion," J. Org. Chem. 1987, 52(11), 2117.
88. Doty, J. C.; Grisdale, P. J.; Evans, T. R.; Williams, J. L. R. "Boron Photochemistry. VII. Photochemically Induced Electron Transfer from Tetraphenylborate Anion to Singlet Oxygen," J. Organometal. Chem. 1971, 32(2), C35.

89. Sullivan, B. P.; Dressick, W. J.; Meyer, T. J. "Photoelectrochemical Cell Based on the Ion Pair 1,1'-dimethyl-4,4'-bipyridinium," J. Phys. Chem. 1982, 86(8), 1473.
90. Hennig, H.; Walther, D.; Thomas, P. "Photocatalytic Systems. LXII. Photochemical Behavior of Ion-Pair Associates of the Type  $[\text{Co}(\text{NH}_3)_5\text{X}]$ ,  $\text{B}(\text{C}_6\text{H}_5)_4$  During Irradiation in the IPCT [Ion-Pair Charge Transfer] Range," Z. Chem. 1983, 23(12), 446.
91. Clark, S. F.; Watts, R. J.; Dubois, D. L.; Connolly, J. S.; Smart, J. C. "Photochemistry of Electron Donor-Acceptor Complexes of the bis(fulvalene) Dicobalt Mono- and Dications," Coord. Chem. Rev. 1985, 64, 273.
92. Meyerstein, D.; Mulac, W. A. "Reduction of Cobalt(III) Complexes by Monovalent Zinc, Cadmium, and Nickel Ions in Aqueous Solutions," J. Phys. Chem. 1969, 73(4), 1091.
93. Selvarajan, N.; Raghavan, V. "Oxidation of Hexachloroiridate (III) by OH. Evidence of Both Inner and Outer Sphere Electron Transfer Pathways," JCS Chem. Comm. 1980, 336.
94. Buxton, G. V.; Sellers, R. M. "The Radiation Chemistry of Metal Ions in Aqueous Solution," Coord. Chem. Rev. 1977, 22, 195.
95. Meyerstein, D. "Complexes of Cations in Unstable Oxidation States in Aqueous Solutions as Studied by Pulse Radiolysis," Acc. Chem. Res. 1978, 11, 43.
96. Zehavi, D.; Rabani, J. "Pulse Radiolysis of the Aqueous Ferro-Ferricyanide System. I. The Reaction of OH,  $\text{HO}_2$ , and  $\text{O}_2^-$  Radicals," J. Phys. Chem. 1972, 76(25), 3703.
97. Zehavi, D.; Rabani, J. "Pulse Radiolysis of the Aqueous Ferro-Ferricyanide System. II. Reactions of Hydrogen Atoms and  $\text{e}_{\text{aq}}^-$  with Ferrocyanide and Ferricyanide Ions," J. Phys. Chem. 1974, 78(14), 1368.
98. Broszkiewicz, R. K. "Pulse Radiolysis Study on Aquachlorocomplexes of Rh(III)," Radiat. Phys. Chem. 1977, 10, 1.
99. Lilie, J.; Shinohara, N.; Simic, M. G. "The Kinetics of Ligand Detachment from Labile Cobalt(II)-Amine Complexes in Aqueous Solution," J. Am. Chem. Soc. 1976, 98, 6516.

100. Sleight, T. P.; Hare, C. R. "The Photochemistry of Hexachloroiridate (IV)," Inorg. Nucl. Chem. Letters 1968, 4, 165.
101. Waltz, W. L.; Adamson, A. W. "Photochemistry of Complex Ions. VII. Photoelectron Production," J. Phys. Chem. 1963, 73, 4250.
102. Adams, G. E.; Broszkiewicz, R. K.; Michael, B. D. "Pulse Radiolysis Studies of Stable and Transient Complexes of Platinum," Trans. Faraday Soc. 1968, 64, 1256.
103. Broszkiewicz, R. K.; Grodkowski, J. "Pulse Radiolysis Studies on Aqueous Systems  $\text{PtCl}_4^{2-}\text{-Cl}^-$  and  $\text{PtCl}_4^{2-}\text{-Br}^-$ ," Int. J. Radiat. Phys. Chem. 1976, 8, 359.
104. Gupta, A. K.; Hanrahan, R. J.; Parker, R. Z. "Gas-Phase Formation of Hydrogen Chloride by Thermal Chlorine-Steam Reaction," Int. J. Hydrogen Energy 1991, in press.
105. Gray, H. B.; Maverick, A. W. "Solar Chemistry of Metal Complexes," Science 1981, 214, 1201.
106. Moggi, L.; Varani, G.; Manfrin, M. F.; Balzani, V. "Photochemical Reactions of Hexachloroiridate (IV) Ion," Inorg. Chim. Acta 1970, 4(3), 335.
107. Eidem, P. K.; Grey, A. W.; Gray, H. B. "Production of Hydrogen by Irradiation of Metal Complexes in Aqueous Solutions," Inorganic Chim. Acta. 1981, 50, 59.
108. Dainton, F. S.; Rumfeldt, R. "Radical and Molecular Yields in the Radiolysis of Aqueous Solution. Nitrous Oxide Solutions Containing Hexachloro-anions of Iridium and Platinum," Proc. Roy. Soc. (London) A 1967, 298, 239.
109. Mills, G.; Henglein, A. "Radiation Chemical Formation of Colloidal Iridium and Mechanism of Catalysed Hydrogen," Radiat. Phys. Chem. 1985, 26(4), 385.
110. Mills, G.; Henglein, A. "Radiation Chemistry of  $\text{Na}_3\text{IrCl}_6$  Solutions: Catalysed  $\text{H}_2$  Formation by Radicals and Post-Irradiation Reduction of  $\text{IrCl}_6^{3-}$  by Propanol-2," Radiat. Phys. Chem. 1985, 26, 391.
111. Broszkiewicz, R. K. "Pulse Radiolysis Studies on Complexes of Iridium," J. Chem. Soc. Dalton Trans. 1973, 1799.

112. Edwards, J. O. Inorganic Reaction Mechanisms, An Introduction, W. A. Benjamin: New York, New York, 1964.
113. Broszkiewicz, R. K. "Pulse Radiolysis Studies on Chlorocomplexes of Palladium," Int. J. Radiat. Phys. Chem. 1974, 6, 249.
114. Broszkiewicz, R. K. "Redox Reactions of  $\text{OsCl}_5(\text{H}_2\text{O})^-$  and  $\text{OsCl}_6^{2-}$ : A Pulse Radiolysis Study," Radiat. Phys. Chem. 1977, 10, 303.
115. Broszkiewicz, R. K. "Redox Reactions of  $\text{RuCl}_6^{3-}$  and  $\text{RuCl}_6^{2-}$ : A Pulse Radiolysis Study," Radiat. Phys. Chem. 1980, 15, 133.
116. Ram, M. S.; Stanbury, D. M. "Electron Transfer Reactions Involving the Azidyl Radical," J. Phys. Chem. 1986, 90, 3691.
117. West, M. A. "Experimental Methods in Flash Photolysis," in Creation and Detection of the Excited State, W. R. Ware, ed., Vol. 4, Marcel Dekker: New York, New York, 1975.
118. Ingle, J. D., Jr.; Crouch, S. R. Spectrochemical Analysis, Prentice Hall: Englewood Cliffs, New Jersey, 1988; Chapters 1-6 and 13.
119. Hunt, J. W.; Greenstock, C. L.; Bronskill, M. J. "Design Considerations for Nanosecond Pulse Radiolysis Studies Using Kinetic Spectrophotometry," Int. J. Radiat. Phys. Chem. 1972, 4, 87.
120. Vojnovic, B.; Michael, B. D. "Reduction of Electromagnetic Interference from Pulsed Radiation Sources," Radiat. Phys. Chem. 1987, 30(4), 225.
121. Photochemical Research Associates, PRA, London, Ontario, Canada, M301 Power Supply Instruction Manual, 1984/85.
122. Kenney-Wallace, G. A.; Shaede, E. A.; Walker, D. C.; Wallace, S. C. "Nanosecond Pulse Radiolysis Techniques for the Study of Liquids Using a 600 kV Febetron," Int. J. Radiat. Phys. Chem. 1972, 4, 209.
123. Saito, E.; Belloni, J. "All-Silica Cell for Pulse Radiolysis Studies of Liquid Crystals with Low-Energy (600 keV) Electrons," Rev. Sci. Instrum. 1976, 47(5), 629.



124. The Fisher Catalog, Fisher Scientific: Pittsburgh, Pennsylvania, 1991, p. 1072.
125. Hewlett-Packard, McMinnville Division, McMinnville, Oregon, Model 706 System Instruction Manual, 1969.
126. Hewlett-Packard, McMinnville Division, McMinnville, Oregon, Bulletin No. 5952-6730, 1974.
127. Dorfman, L. M. "Pulse Radiolysis," in Techniques of Chemistry, G. G. Hammes, ed., Vol. 6, Pt. 2, John Wiley & Sons: New York, New York, 1974.
128. Ramirez, J. E. "The Pulse Radiolysis of Alkyl Iodides and Oxygen in the Gas Phase," Ph. D. Dissertation, University of Florida, 1981.
129. Belloni, J.; Billiau, F.; Cordier, P.; Delaire, J. A.; Delcourt, M. O. "Primary Processes Studied by Pulse Radiolysis of Liquid Ammonia. 1. Oxidizing Radical Scavenging and Identification of Ultraviolet Transient Absorption Spectrum," J. Phys. Chem. 1978, 82(5), 532.
130. Delaire, J. A.; Delcourt, M. O.; Belloni, J. "Delayed Formation of Solvated Electrons in Basic *n*-Propylamine," Radiat. Phys. Chem. 1980, 15, 255.
131. Mostafavi, M.; Marignier, J. L.; Amblard, J.; Belloni, J. "Nucleation Dynamics of Silver Aggregates Simulation of Photographic Development Processes," Radiat. Phys. Chem. 1989, 34(4), 605.
132. Gascoigne, J., of the Atomic and Molecular Physics Laboratories, Australia National University (ANU), Canberra, Australia. "Febetron Discharge Tube Modification," 1989.
133. Charbonnier, F. M.; Barbour, J. P.; Brewster, J. L. "A New High Intensity Nanosecond Electron Source for Pulse Radiolysis," in Fast Processes in Radiation Chemistry and Biology, G. E. Adams, E. M. Fielden, and B. D. Michael, eds., John Wiley & Sons: New York, New York, 1975.
134. Data Precision, Division of Analogic Corporation, Boston, Massachusetts, Operating Instructions for DATA 6000 Universal Waveform Analyzer, 1982.
135. Data Precision, Division of Analogic Corporation, Boston, Massachusetts, DATA 6000 Programming, 1982.

136. Alfassi, Z. B.; Schuler, R. H. "Reaction of Azide Radicals with Aromatic Compounds. Azide as a Selective Oxidant," J. Phys. Chem. 1985, 89, 3359.
137. Von Sontag, C. The Chemical Basis of Radiation Biology, Taylor and Francis: London, 1987.
138. Weeks, J. L.; Rabani, J. "The Pulse Radiolysis of Deaerated Aqueous Carbonate Solutions I. Transient Optical Spectrum and Mechanism; II.  $pK$  for OH Radicals," J. Phys. Chem. 1966, 70, 2100.
139. Gear, C. E. Numerical Initial Value Problems in Ordinary Differential Equations, John Wiley and Sons: New York, New York, 1962.
140. Brown, R. L. "A Computer Program for Solving Systems of Chemical Rate Equations," Report NBSIR 1978, 76-1055.
141. Land, E. J.; Hart, M. "Pulse Radiolysis Studies of Aqueous Phenol," Trans. Faraday Soc. 1967, 63, 1181.
142. Jorgensen, C. K. "Electron Transfer Spectra of Hexahalide Complexes," Molecular Physics 1959, 2, 312.
143. Latimer, W. M. The Oxidation States of the Elements and Their Potentials in Aqueous Solution, 2d ed., Prentice Hall, Englewood Cliffs, NJ, 1952.
144. MacNevin, W. M.; Kriegen, O. H. "(Ethylenedinitrilo)tetraacetic Acid Chelation of Platinum Group Metals, Spectrophotometric Determination of Iridium," Anal. Chem. 1955, 8, 16.
145. Blasius, E.; Preetz, W.; Schmitt, R. "Untersuchung des Verhaltens der Chlorokomplexe der Platinelemente in Losung und an Anionenaustauschern," Inorg. Nucl. Chem. 1961, 19, 132.
146. Van Loon, G.; Page, J. A. "The Chemistry of Iridium in Basic Aqueous Solution, a Polarographic Study," Can. J. Chem. 1966, 41, 515.
147. Fine, D. A. "On the Spontaneous Reduction of Hexachloroiridate (IV) Aqueous Solutions," Inorg. Chem. 1969, 8, 1014.
148. Poulsen, I. A.; Garner, C. S. "A Thermodynamic and Kinetic Study of Hexachloro and Aquopentachloro Complexes of Iridium(III) in Aqueous Solutions," J. Am. Chem. Soc. 1962, 84, 2032.

149. Kravtsov, V. I.; Petrova, G. M. "Kinetics of Aquation of Chloroiridate(III) Ions and the  $\text{IrCl}_6^{2-}/\text{IrCl}_6^{3-}$  Redox Potential," Russ. J. Inorg. Chem. 1964, 9, 552.
150. Sykes, A. G.; Thorneley, R. N. F. "Identification of Inner and Outer-Sphere Paths in the Reaction of Chromium(II) with Hexachloroiridate(IV), and the Kinetics of the Decomposition of the Binuclear Intermediate," J. Chem. Soc. (A) 1970, 232.
151. Fielden, E. M. "Chemical Dosimetry of Pulsed Electron and X-Ray Sources in the 1-20 MeV Range," in J. H. Baxendale and Fabio Busi, eds., The Study of Fast Processes and Transient Species by Electron Pulse Radiolysis, D. Reidel: Dordrecht, Holland, 1982.
152. Boyd, A. W.; Carver, M. B.; Dixon, R. S. "Computed and Experimental Product Concentrations in the Radiolysis of Water," Radiat. Phys. Chem. 1980, 15, 177.
153. Buxton, G. V.; Greenstock, C. L.; Hellman, W. P.; Ross, A. B. "Critical Review of Rate Constants for Reactions of Hydrated Electrons, Hydrogen Atoms and Hydroxyl Radicals ( $\cdot\text{OH}/\cdot\text{O}^-$ ) in Aqueous Solutions," J. of Phys. and Chem. Ref. Data 1988, 17, 513.
154. Burton, M. and Magee, J. L., eds. Advances In Radiation Chemistry, vol. 2, Wiley-Interscience: New York, New York, 1970, p. 177.
155. Behar, D.; Czapski, G.; Duchovny, I. "Carbonate Radical in Flash Photolysis and Pulse Radiolysis of Aqueous Carbonate Solutions," J. Phys. Chem. 1970, 74, 2206.

## BIOGRAPHICAL SKETCH

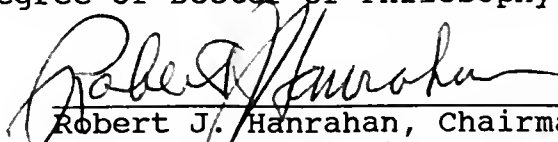
Charles L. Crawford was born in Orlando, Florida on November 24, 1963. He moved with his family to Charlotte, North Carolina in 1966, where he resided until moving to Gainesville, Florida in 1986.

He received the Bachelor of Science degree in Chemistry at the University of North Carolina, Chapel Hill in 1986.

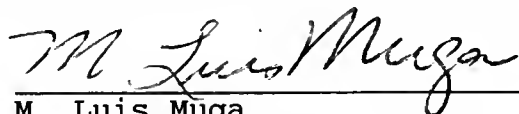
During graduate school at the University of Florida he held graduate teaching and research assistantships in the Department of Chemistry and a graduate research assistantship at Los Alamos National Lab in Los Alamos, New Mexico.

Charles is the youngest son of Nathan and Doris and his older brother is John.

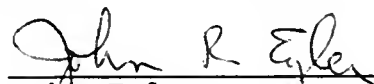
I certify that I have read this study and that in my opinion it conforms to acceptable standards of scholarly presentation and is fully adequate, in scope and quality, as a dissertation for the degree of Doctor of Philosophy.

  
Robert J. Hanrahan, Chairman  
Professor of Chemistry


I certify that I have read this study and that in my opinion it conforms to acceptable standards of scholarly presentation and is fully adequate, in scope and quality, as a dissertation for the degree of Doctor of Philosophy.

  
M. Luis Muga  
Professor of Chemistry

I certify that I have read this study and that in my opinion it conforms to acceptable standards of scholarly presentation and is fully adequate, in scope and quality, as a dissertation for the degree of Doctor of Philosophy.

  
John Eyler  
Professor of Chemistry

I certify that I have read this study and that in my opinion it conforms to acceptable standards of scholarly presentation and is fully adequate, in scope and quality, as a dissertation for the degree of Doctor of Philosophy.

  
Phillip M. Achey  
Professor of Microbiology  
and Cell Science

This dissertation was submitted to the Graduate Faculty of the Department of Chemistry in the College of Liberal Arts and Sciences and to the Graduate School and was accepted as partial fulfillment of the requirements for the degree of Doctor of Philosophy.

December 1991

---

Dean, Graduate School

